

**Transition Metal Complexes of N-heterocyclic Carbenes and
Derivatives Thereof: Synthesis and Reactivity Study**

TIMOTHY G. LAROCQUE

A DISSERTATION SUBMITTED TO
THE FACULTY OF GRADUATE STUDIES
IN PARTIAL FULFILLMENT OF THE REQUIREMENTS
FOR THE DEGREE OF
DOCTOR OF PHILOSOPHY

GRADUATE PROGRAM IN CHEMISTRY
YORK UNIVERSITY
TORONTO, ONTARIO

August 2013

© Timothy G. Larocque, 2013

Abstract

N-heterocyclic carbenes (NHCs) have played a dominant role in organometallic chemistry for decades and revolutionized the field of homogenous catalysis. NHCs have been thoroughly studied, both experimentally and theoretically, and have shown unique reactivity towards transition metals, chalcogens, azides and pnictogens.

This thesis is aimed at utilizing the unique reactivity of *N*-heterocyclic carbenes to develop novel, robust catalysts to mediate organic transformations. The multi-faceted work within this thesis explores the use of NHCs as ancillary ligands on early and late transition metals as potential catalysts for olefin polymerization and ring-closing metathesis, respectively. This work also includes exploring the synthesis and coordination of ancillary ligands derived from the unique reactivity of NHCs towards azides, chalcogens and pnictinidenes.

The reactivity of a novel aryl-substituted acyclic imino-*N*-heterocyclic carbene to early transition metals, cyclooctasulfur and Grubbs-type ruthenium benzylidene complexes was explored. The reactivity of imidazol-2-imide towards Grubbs-type ruthenium benzylidene complexes and the synthesis and coordination of a novel group of ligands bearing an imidazol-2-imine scaffold were also explored. Lastly, this work will include the reactivity of IMes=PPh to Grubbs-type ruthenium benzylidene complexes.

Table of Contents

List of Figures	VII
List of Schemes	IX
List of Tables	XI
Acknowledgments	XII
Abbreviations	XIII
Chapter 1	1
1.1 Introduction	1
1.2 Synthesis of <i>N</i> -Heterocyclic carbenes.....	1
1.3 Reactivity of <i>N</i> -heterocyclic carbenes towards metals.....	5
1.4 Reactivity of <i>N</i> -heterocyclic carbenes towards azides.....	9
1.5 Reactivity of <i>N</i> -heterocyclic carbenes towards chalcogens.....	10
1.6 Reactivity of <i>N</i> -heterocyclic carbenes towards pnictinidenes.....	12
1.7 Scope of thesis work	14
1.8 References	14
Chapter 2	20
2.0 Preface	20
2.1 Introduction	20
2.2. Results and Discussion	23
2.2.1 Coordination of C [^] Imine to early transition metal halides.....	23
2.2.1.1. Coordination of C [^] Imine to titanium.....	23

2.2.1.2. Coordination of free carbene to zirconium and hafnium.....	29
2.2.1.3. Coordination of free carbene to chromium	31
2.2.1.4. Ethylene polymerization catalysis	33
2.2.5. Coordination and reactivity of C [^] Imine to titanium phenoxo complexes ..	34
2.2.5.1 Synthesis of TiCl ₂ (2,6-OC ₆ H ₃ -Me ₂) ₂ (C [^] Imine), 2.7	34
2.2.6. Synthesis of TiCl ₂ (2,6-OC ₆ H ₄ O)(C [^] Imine), 2.9	40
2.2.7. Attempted Synthesis of TiCl ₂ (=N-R)(C [^] Imine)	45
2.2.8. Ethylene polymerization catalysis	46
2.3.1. Synthesis of S [^] Imine	46
2.4.1. Conclusions	49
2.5. Experimental	50
2.5.1 General Considerations	50
2.5.2 Synthesis of TiCl ₄ (C [^] Imine), 2.1	52
2.5.2 Synthesis of TiCl ₃ (C [^] Imine), 2.2	53
2.5.3 Synthesis of ZrCl ₄ (C [^] Imine), 2.3	53
2.5.4 Synthesis of HfCl ₄ (C [^] Imine), 2.4	54
2.5.5 Synthesis of CrCl ₃ (C [^] Imine)(THF), 2.5	55
2.5.6 Synthesis of CrCl ₂ (C [^] Imine)(THF), 2.6	55
2.5.7. Synthesis of TiCl ₂ (2,6-OC ₆ H ₃ -Me ₂) ₂ (C [^] Imine), 2.7	55
2.5.8 Synthesis of TiCl ₂ (2,6-OC ₆ H ₃ -Me ₂) ₂ (1-(2,4,6-trimethylphenyl)imidazole), 2.8	56
2.5.9. Synthesis of TiCl ₂ (1,2-OC ₆ H ₄ O)(C [^] Imine), 2.9	57

2.5.10. Synthesis of S [^] Imine, 2.10	58
2.5.11. General procedure for ethylene polymerization	59
2.5.12. X-ray crystallographic studies	60
2.6. References	61
Chapter 3	67
3.0 Preface	67
3.1 Introduction	67
3.2 Results and Discussion	70
3.3. Conclusions	78
3.4. Experimental	79
3.4.1. General Considerations.....	79
3.4.2. General procedure for the synthesis of 2-(1,3-bis(2,4,6- trimethylphenyl)imidazol-2-imine)-1-(aryl)ethanone hydrochloride salt, IMesN [^] ethanone · HX, 3.1–3.3	80
3.4.2.1. 2-(1,3-bis(2,4,6-trimethylphenyl)imidazol-2-imine)-1-phenylethanone hydrobromide salt, 3.1 :	81
3.4.2.2. 2-(1,3-Bis(2,4,6-trimethylphenyl)imidazol-2-imine)-1-(4- chlorophenyl)ethanone hydrochloride salt, 3.2 :.....	82
3.4.2.3. 2-(1,3-Bis(2,4,6-trimethylphenyl)imidazol-2-imine)-1-(4- nitrophenyl)ethanone hydrobromide salt, 3.3 :	82
3.4.3. 2-(1,3-Bis(2,4,6-trimethylphenyl)imidazol-2-imine)-1-phenylethanone, IMesN [^] ethanone, 3.4 :	83

3.4.4. Sodium 2-(1,3-bis(2,4,6-trimethylphenyl)imidazol-2-imine)-1-phenylethenolate, Na[IMesN ⁺ ethenolate], 3.5 :	84
3.4.5. General procedure for the synthesis of bis(2-(1,3-bis(2,4,6-trimethylphenyl)imidazol-2-imine)-1-(aryl)ethenolate) zirconium dichloride, ZrCl ₂ (IMesN ⁺ ethenolate) ₂ , 3.6 and 3.7 :	85
3.4.5.1. Bis(2-(1,3-bis(2,4,6-trimethylphenyl)imidazol-2-imine)-1-phenylethenolate) zirconium dichloride, 3.6 :	85
3.4.5.2. Bis(2-(1,3-bis(2,4,6-trimethylphenyl)imidazol-2-imine)-1-(4-chlorophenyl)ethenolate) zirconium dichloride, 3.7 :	86
3.4.6. General procedure for the synthesis of cyclopentadienyl (2-(1,3-bis(2,4,6-trimethylphenyl)imidazol-2-imine)-1-(aryl)ethenolate) zirconium dichloride, CpZrCl ₂ (IMesN ⁺ ethenolate), 3.8 and 3.9 :	86
3.4.6.1 Cyclopentadienyl (2-(1,3-bis(2,4,6-trimethylphenyl)imidazol-2-imine)-1-phenylethenolate) zirconium dichloride, 3.8 :	87
3.4.6.2 Cyclopentadienyl (2-(1,3-bis(2,4,6-trimethylphenyl)imidazol-2-imine)-1-(4-chlorophenyl)ethenolate) zirconium dichloride, 3.9 :	87
3.4.7. General procedure for the synthesis of cyclopentadienyl (2-(1,3-bis(2,4,6-trimethylphenyl)imidazol-2-imine)-1-(aryl)ethenolate) titanium dichloride CpTiCl ₂ (IMesN ⁺ ethenolate), 3.10 and 3.11 :	88
3.4.7.1. Cyclopentadienyl (2-(1,3-bis(2,4,6-trimethylphenyl)imidazol-2-imine)-1-phenylethenolate) titanium dichloride, 3.10 :	88

3.4.7.2. Cyclopentadienyl (2-(1,3-bis(2,4,6-trimethylphenyl)imidazol-2-imine)-1-(4-chlorophenyl)ethenolate) titanium dichloride, 3.11 :	89
3.4.8. General procedure for ethylene polymerization.	89
3.4.9. Computational details.	90
3.4.10. X-ray crystallography.	90
References	91
Chapter 4	95
4.1 Introduction	95
4.1.1 Metathesis	95
4.1.2 Evolution of ruthenium metathesis catalysts	98
4.2 Results and Discussion	100
4.2.1. Synthesis and chemistry of cationic ruthenium benzylidene complex....	100
4.2.2. Synthesis and chemistry of ruthenium benzylidene complexes bearing imidazol-2-imine ligand.....	106
4.2.3. Synthesis and chemistry of ruthenium benzylidene complexes bearing NHC-phosphinidene ligands.....	111
4.3 Conclusions and Future Considerations	119
4.4 Experimental	120
4.4.1 General Considerations	120
4.4.2 Synthesis of $[\text{Ru}(\text{C}^{\wedge}\text{Imine})(\text{MeCN})_4(\text{CHPh})][\text{PF}_6]_2$, 4.2	121
4.4.6 Attempted synthesis of $\text{RuCl}(\text{IMes}=\text{N})(\text{PCy}_3)_2(\text{CHPh})$	122
4.4.7 Attempted synthesis of $\text{RuCl}(\text{IMes}=\text{N})(\text{IMes})\text{py}(\text{CHPh})$	122

4.4.8 Attempted synthesis of RuCl(I ^t Bu=N)(PCy ₃) ₂ (CHPh).....	123
4.4.9 Attempted synthesis of Ru(I ^t Bu=N)(PCy ₃) ₂ (CPh)	123
4.4.10 Synthesis of RuCl(IMes)(I ^t Bu=N)py ₂ (CHPh), 4.3	124
4.4.11 Attempted Synthesis of RuCl ₂ (IMes=PPh)(PCy ₃)(CHPh), 4.4	124
4.4.12 Synthesis of RuCl ₂ (IMes=PPh)(PPh ₃)(CHPh), 4.5	125
Decomposition Product, 4.5a	125
4.4.14 Ring-closing metathesis	126
4.5 References	126
Chapter 5	132
5.1 Conclusions and Future Work	132
Supplementary Material	137

List of Figures

Figure 1.2.1 Examples of five-membered NHCs with varying heteroatoms.....	2
Figure 1.3.1. General representation of the three most common methods to coordinating NHCs to metal centres.....	6
Figure 1.3.1. Molecular orbital diagram representing NHC-metal interactions.....	7
Figure 1.4.2. The mesomeric structures for imidazol-2-imide	10
Figure 1.5.1. General reaction of imidazole-2-ylidene and chalcogens	11
Figure 1.5.2. The mesomeric structures for carbene-chalcogen adducts	11
Figure 1.6.1. General synthesis of carbene-pnictinidene adducts	12
Figure 1.6.2. The mesomeric structures for carbene-pnictinidene adducts	13
Figure 2.1. General representation of the imidazolium salts A and B	21
Figure 2.2. General representation of the iminocarbene ligand	23
Figure 2.3. ORTEP plot (50% probability) of 2.1	25
Figure 2.4. ORTEP plot (50% probability) of 2.4	28
Figure 2.5. ORTEP plot (50% probability) of 2.3	30
Figure 2.6. ORTEP plot (50% probability) of 2.5	32
Figure 2.6. ORTEP plot (50% probability) of 2.7	36
Figure 2.7. ORTEP plot (50% probability) of 2.8	40
Figure 2.8. ORTEP plot (50% probability) of 2.9	41
Figure 2.9. Selected regions of the ¹ H NMR spectra of 2.9 at temperatures ranging from 21 to 50 °C.	44
Figure 2.10: ORTEP plot (30% probability) of S [^] imine, 2.10	49

Figure 3.1. Mesomeric structures of substituted imidazole-2-iminate.	68
Figure 3.2. Neutral (A) and anionic (B) bidentate ligands with an imidazol-2-imine fragment	68
Figure 3.3. Early and late transition metal complexes of the salicylaldimine ligand system.	70
Figure 3.4. ORTEP plot (50% probability) of 3.9	75
Figure 4.1. Common types of metathesis reactions	96
Figure 4.2. General accepted metathesis mechanism	97
Figure 4.3. Grubbs' first-generation (GI) catalyst	98
Figure 4.4. Examples of modifications to Grubbs-type ruthenium metathesis catalysts.....	99
Figure 4.5. ORTEP plot (50% probability) of 4.2	104
Figure 4.6. ORTEP plot (30% probability level) of 4.4	113
Figure 4.7. Proposed decomposition pathway of $\text{RuCl}_2(\text{IMes}=\text{PPh})(\text{PCy}_3)(\text{CHPh})$	115
Figure 4.8. ORTEP plot (30% probability level) of 4.5	117

List of Schemes

Scheme 1.2.1. Common synthetic strategies to forming stable free NHCs	3
Scheme 1.2.2. General scheme to forming free carbenes	3
Scheme 2.1. Synthesis of group 4 and 6 metal halide complexes of C [^] Imine....	24
Scheme 1.4.1. General synthesis of <i>N</i> -silylated 2-iminoimidazoline and imidazol-2-imine.....	9
Scheme 2.2. Synthesis of titanium complexes 2.7 and 2.9 from free carbene, C [^] Imine.	35
Scheme 2.3: Synthetic strategy to forming compound, 2.10	47
Scheme 3.1. Synthesis of 2-(1,3-Bis(2,4,6-trimethylphenyl)imidazol-2-imino)-1-arylethanone hydrochloride (3.1–3.3).....	70
Scheme 3.2. Sequential deprotonation of 3.1 to generate a tautomeric mixture of 2-(1,3-Bis(2,4,6-trimethylphenyl)imidazol-2-imine)-1-phenylethanone (3.4₁ and 3.4₂) and the corresponding ethenolate (3.5).....	71
Scheme 3.3. Synthesis of titanium and zirconium complexes of the bis(imine ethenolate) ligand.....	72
Scheme 4.1. Reaction of RuCl ₂ (C [^] Imine)(CHPh) with AgPF ₆ in MeCN.....	102
Scheme 4.2. Proposed synthetic strategy for forming RuCl(X)(PCy ₃) ₂ (CHPh) .	106
Scheme 4.3. Possible formation of a ruthenium alkylidyne complex	107
Scheme 4.4. Dehydrohalogenation of Grubbs first generation catalyst ³¹	107
Scheme 4.5. Aryloxide selectivity based on metal precursor	108
Scheme 4.6. Synthetic scheme to forming compound 4.3	108

Scheme 4.6. Proposed synthetic route to forming	
RuCl ₂ (IMes=PPh)(PCy ₃)(CHPh).....	112
Scheme 4.7. Synthetic strategy for RuCl ₂ (IMes=PPh)(PPh ₃)(CHPh), 4.5	115

List of Tables

Table 1.1. IR values for the CO stretching frequencies of Ni(CO) ₃ (L) complexes	8
Table 2.1. Selected bond lengths and angles for compounds C [^] Imine, 2.1 , 2.2 , 2.3 and 2.5	27
Table 2.2. Selected bond lengths and angles for compounds TiCl ₄ (C [^] Imine), 2.7 and 2.9	39
Table 3.1. Selected bond lengths and bond angles for compound 3.9	76
Table 4.1. Selected bond lengths and bond angles for compound 4.2	105
Table 4.2: Catalytic activity of ruthenium metathesis catalysts in CDCl ₃	110
Table 4.3. Selected bond lengths and bond angles for compound 4.4	113

Acknowledgements

First, I would like to take this opportunity to express my gratitude towards my supervisor, Professor Gino Lavoie. His valuable knowledge and guidance throughout my time at York University allowed me to become a better researcher and leader, and for this I am truly grateful.

I would also like to thank past co-workers Anna Badaj, Jameel Al-Thagfi, Delwar Hossain, Barbara Skrela, Edwin Alvarado, Sarim Dastgir, Mike Harkness and Richard Morris for their support, suggestions and conversations throughout the years.

In addition, I would like to thank Dr. Howard Hunter for his knowledge and guidance in NMR spectroscopy. His humor and kindness was a breath of fresh air.

I will be forever thankful to my family and friends for their support during my post-secondary education. Their love and support helped me achieve my dream. I will be forever indebted to them.

Lastly, I would like to express my deepest appreciation to the love of my life. Shawna stood behind me with undying patience and support, and knew I would succeed. Her kindness, patience and laughter offered a shelter for the storm. For that, I owe her a lifetime of love.

Abbreviations

Ar	Aryl
Cy	Cyclohexyl, - C ₆ H ₁₁
Cat.	Catalyst
DFT	Density functional theory
DMP	Dimethylphenyl
Equiv	Equivalents
EA	Elemental analysis
Hz	Hertz
HMBC	Heteronuclear multiple-bond correlation
HSQC	Heteronuclear single-quantum coherence
IMes	<i>N,N</i> -bis-(2,4,6-trimethylphenyl)imidazol-2-ylidene
Me	Methyl, -CH ₃
Mes	Mesityl, 2,4,6-trimethylphenyl
NMR	Nuclear magnetic resonance
Ph	Phenyl, -C ₆ H ₅
ppm	Parts per million
py	Pyridine, C ₅ H ₅ N
ORTEP	Oak Ridge Thermal Ellipsoid Plot program
RCM	Ring-closing metathesis
SIMes	<i>N,N</i> -bis-(2,4,6-trimethylphenyl)imidazolin-2-ylidene

^t Bu	Tert-butyl, -CMe ₃
THF	Tetrahydrofuran
TMEDA	Tetramethylethylenediamine
TMS	Tetramethylsilane, SiMe ₄
-TMS	Trimethylsilyl, -SiMe ₃
TOF	Turnover frequency
TON	Turnover number
UV	Ultra violet
Vis	Visible
VT	Variable temperature

Chapter 1

1.1 Introduction

A critical element of organometallic chemistry is the drive towards developing compounds for catalytic applications. In recent decades, there has been a great deal of emphasis on developing metal-based catalysts for industrial applications, polymerization and for the synthesis of fine chemicals. The activity of homogeneous catalysts is largely dependent on the ligand-metal combination. A wide variety of ligand classes have thus been explored. However, certain types of ligands have played a more significant role than others in organometallic chemistry. One class of ligands that has received considerable attention in recent years is the *N*-heterocyclic carbene (NHC) ligand.¹ Since the first isolation by Arduengo in 1991,² various synthetic methodologies of symmetrical and non-symmetrical five-membered, two-electron-donating imidazol-2-ylidene ligands have been developed and are now well established.^{1,3}

1.2 Synthesis of *N*-Heterocyclic carbenes

There are numerous examples of saturated and unsaturated, symmetrical and unsymmetrical five-membered heterocycles with a variety of heteroatoms (Figure 1.2.1).

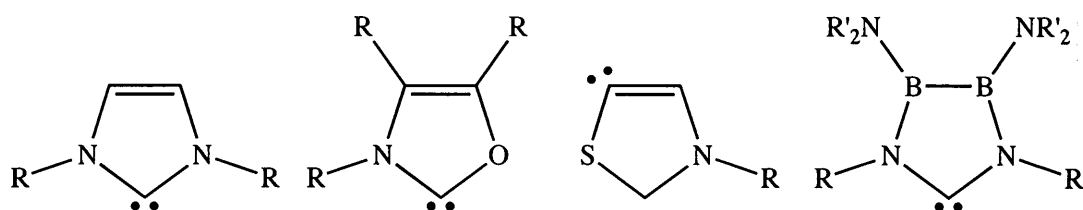
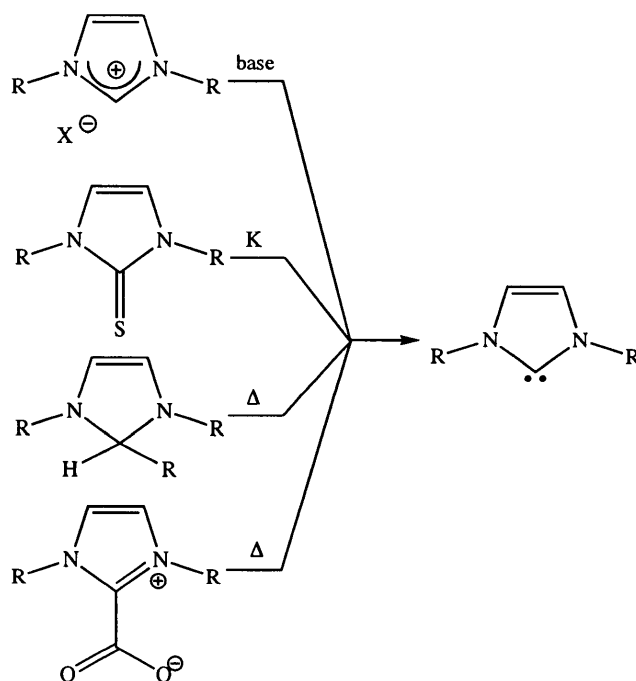
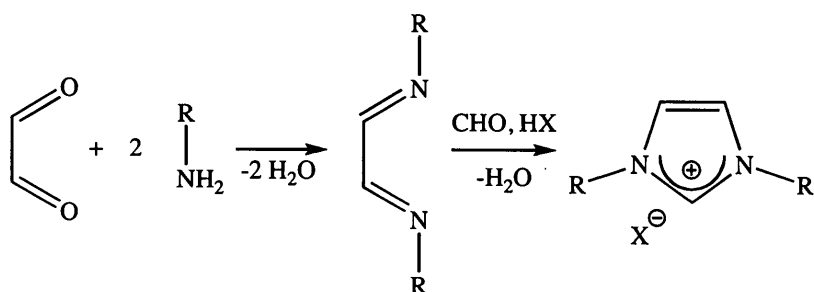


Figure 1.2.1 Examples of five-membered NHCs with varying heteroatoms.

Despite the structural diversity of five-membered NHCs, the largest and most notable group of NHCs is the five-membered imidazole and imidazolidine-based ligands. There are numerous routes to forming stable free carbenes, including deprotonation of the corresponding imidazolium salt, reductive desulfurization and thermal elimination of the appropriate NHC precursor (Scheme 1.2.1).¹⁻⁴ In most cases, the formation of free carbenes is formed by deprotonation of the corresponding imidazolium salt. The general synthesis of symmetrical unsaturated imidazolium salts involves the cyclization of a diimine with formaldehyde and a Brønsted acid, where the diimine starting material is a product of the condensation reaction between a primary amine and glyoxal (Scheme 1.2.2).^{3a,5}



Scheme 1.2.1. Common synthetic strategies to forming stable free NHCs



Scheme 1.2.2. General scheme to forming free carbenes

The readily available precursors and facile synthesis of imidazolium salts has led to a wide range of NHC ligands with varying steric and electronic influences.⁶

There are three areas of the NHC ligand scaffold that offer easy modification that can lead to steric and electronic tailoring. These main areas of

the ligand include the C₄ and C₅ substituents, N,N'-substituents and the degree of saturation of the heterocycle. In the case of C₄ and C₅ substituents, incorporating various electron-donating and/or -withdrawing groups has a significant contribution to the overall electronic properties of the NHC ligand.^{6c} In addition, incorporating aryl, alkyl or other cycles to modify the steric demand and, in some cases, halogenated alkyl or aryl groups, can also affect the electronic properties as well as the sterics. The effect of steric by modifying the substituents at the C₄ and C₅ positions can be represented by the percent buried volume (% V_{Bur}). The percent buried volume is the fraction of the first coordination sphere that a given ligand occupies about the metal centre.⁷ An in depth study by Poater explored quantum mechanically optimized structures of IrCl(CO)₂(NHC) to compile the % V_{Bur} of a variety of NHC ligands.⁷ Likewise, the ability to modify the substituents at the N,N' positions offers tailoring of steric and electronic properties allowing for designed ligand-metal interactions, thus affecting activity, productivity, selectivity and scope of substrates. Although the degree of saturation of the ligand scaffold seems trivial, there are a number of examples in which this has played a role in organometallic catalysis.⁸ It has been shown that the % V_{Bur} for the saturated ring is greater than the unsaturated ring.⁷ As a result, we see a vast and continuously growing library of saturated and unsaturated, symmetrical and unsymmetrical five-membered NHC ligands with a broad range of steric and electronic properties.

1.3 Reactivity of *N*-Heterocyclic Carbenes towards Metals

In the years following the discovery of stable NHC ligands, NHCs were considered simple tertiary phosphine-like ligands. Since that time, considerable theoretical and experimental research has been conducted in deducing that NHCs are unique in their own right.⁹ The coordination of NHC ligands often involves one of three routes of synthesis. The first approach to coordination of NHC ligands is the direct reaction of a free carbene with the metal precursor.^{5,10} This reaction is a simple ligand substitution, with the NHC displacing a neutral Lewis base on the metal centre, for example, a coordinated solvent molecule like THF, MeCN or a phosphine ligand. Transmetalation has also been a very successful synthetic method of coordination of NHC ligands. The most common carbene transmetalating agents are silver-based complexes,¹¹ but recently copper and nickel-carbene complexes have been used for transmetalation to other metals.^{12,12d} The last of the three main methods of coordination involves the in situ deprotonation of the salt, in the presence of the metal precursor (Figure 1.3.1).^{5,12c} The in situ deprotonation is utilized when the isolation of the free carbene is not possible and when the synthesis of the silver transmetalating reagent proves difficult or unachievable.

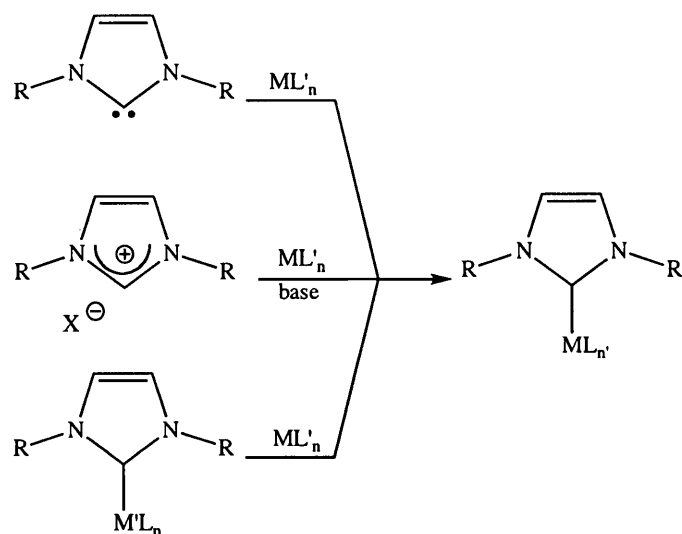


Figure 1.3.1. General representation of the three most common methods to coordinate NHCs to metal centres

NHC ligands are considered to be electron-deficient, strong σ -donating, weak π -accepting ligands. The strong σ -donating capabilities of NHCs arise from the lone pair of electrons in the high-energy σ orbital. Thus, the basicity of NHCs is higher than that of phosphines (I)^{5,9,13} (Figure 1.3.1). The weak π -accepting character of NHCs arises from their ability to accept electron density from filled d orbitals of a metal to an empty low energy π^* orbital (II). Lastly, NHCs are known to contribute electron density to electron-deficient metals via π -d donation (III) (Figure 1.3.1).^{1b,11a,13-14}

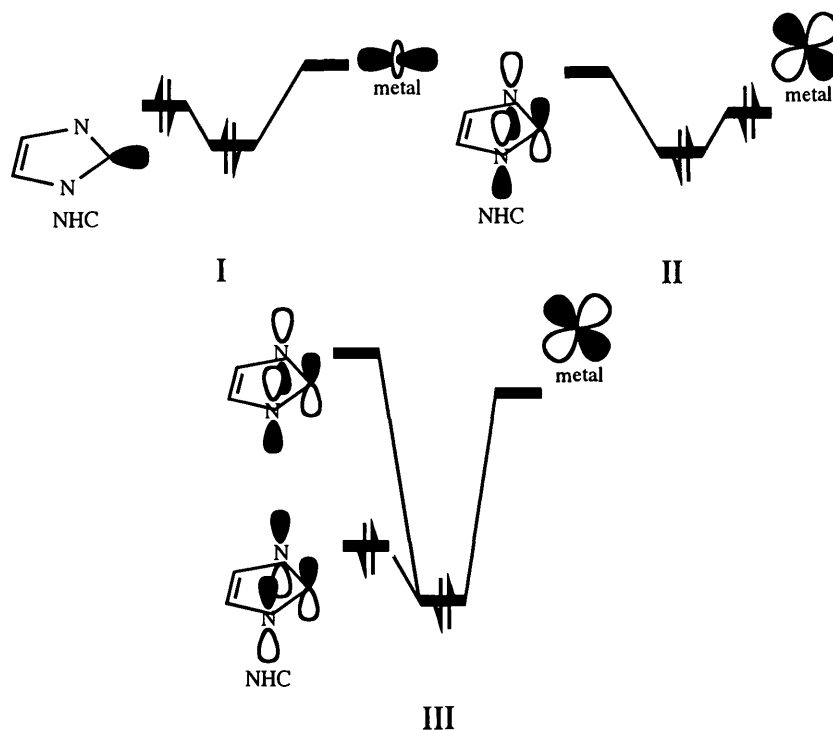


Figure 1.3.1. Molecular orbital diagram representing NHC-metal interactions

The strong ligand-to-metal interaction of NHCs can be illustrated using different techniques, both experimental¹⁵ and computational.^{6c,14,16} There are a number of reports in which the electron-donating capacities of phosphines and NHCs are compared using metal carbonyl complexes. Analyzing the stretching frequencies of metal-bound carbonyls allows for a general assessment of the degree of back-donation and thus, the electron-richness of the metal centre, and ultimately suggesting the relative donating ability of the ancillary ligands.^{6a,6c,17} It is important to note that this method evaluates the overall electron-donating properties of NHCs and does not provide details into the σ -donating and π -

accepting properties of the ligands. Considering the results of Ni(CO)₃(L) complexes^{6a}, where L is either an NHC or a phosphine, the lower-energy stretching frequencies of NHC-bearing metal carbonyls suggests that NHC are stronger donating ligands than phosphines (Table 1.1).

Table 1.1. IR values for the CO stretching frequencies of Ni(CO)₃(L) complexes^{6a}

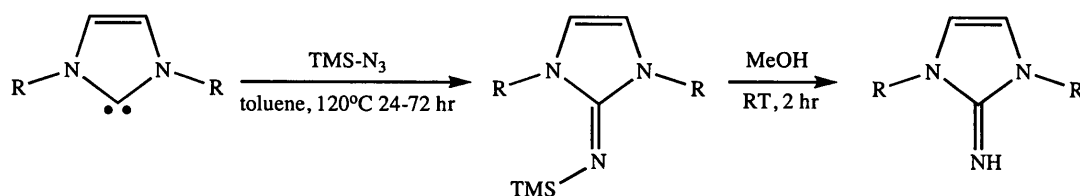
Ligand (L)	ν_{CO} (A ₁)	ν_{CO} (E)
IMes	2050.7	1969
SIMes	2051.5	1970
IPr	2051.5	1070
P ^t Bu ₃	2056.1	1971
PCy ₃	2056.4	1973
PPh ₃	2068.4	1990

Along with experimental evidence of the strong NHC-metal bond, there are numerous computational reports further supporting this trend. Considerable work has been reported using the bond dissociation energies (BDE) of various ligands and metals, and the trend that NHCs are stronger electron-donating ligands than phosphines is observed.^{6a,13,17-18}

The combination of strong σ -donating, weak π -accepting ligands forming robust ligand-metal interactions, and the ability of the ligands to be tuned sterically and electronically has resulted in the widespread use of NHCs in transition metal chemistry.^{1a,1c-e,3a,b,8b,11b,13-14,19} The dynamic role of NHCs as ancillary ligands can be illustrated by the seemingly endless examples of NHC-coordination to almost all transition metals. NHC-bearing metal complexes have been known to facilitate a vast range of organic transformations and have played an integral part of homogenous catalysis for decades.

1.4 Reactivity of *N*-heterocyclic carbenes toward azides

As previously mentioned, *N*-heterocyclic carbenes have been coordinated to a variety of metals and have played a dominant role in the evolution of ligand design in organometallic catalysis. In addition to their coordination to transition metals, the reactivity of NHCs towards main group elements has garnered much attention. Over the last decade, the reactivity of NHCs towards azides has been explored and resulted in a new family of ligands, imidazol-2-imide.²⁰ These monoanionic ligands have garnered considerable attention because of their 2σ , 4π -electron-donor capability, thus making them isoelectronic analogues of cyclopentadienyl and aryloxy ligands. In addition to the successful coordination of the imidazol-2-imide ligands to a variety of transition metals, the imidazol-2-imine form of this novel class of ligand has been used as a ligand scaffold for developing neutral and anionic multidentate ligands.²¹ Tamm first reported the successful reaction between an NHC and trimethylsilyl azide to generate an *N*-silylated 2-iminoimidazoline.^{20b,22}



Scheme 1.4.1. General synthesis of *N*-silylated 2-iminoimidazoline and imidazol-2-imine

The previously reported synthesis of imidazol-2-imide ligands involved 2-imino-1,3-dimethylimidazoline, which was generated using a lengthy synthetic protocol

from 2-aminoimidazole.^{20a,23} The synthetic strategy of treating NHCs with azides was inspired by the facile synthesis of silylated phosphoraneimines.²⁴ Thus, the synthesis of *N*-silylated 2-iminoimidazoline involves treating the free imidazolin-2-ylidene ligand with trimethylsilyl azide in boiling toluene for 24-72 h, depending on the carbene being used.^{20b,22} Two mesomeric structures can be drawn for the imidazol-2-imide ligand, where the imidazolium ring can stabilize a positive charge, thus leading to an increased negative charge on the nitrogen atom, creating a stronger electron-donating ligand (Figure 1.4.2).

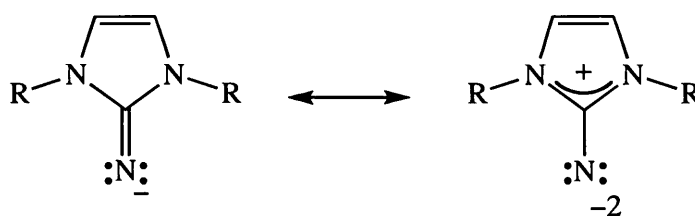


Figure 1.4.2. The mesomeric structures for imidazol-2-imide

The solid-state X-ray structure of *N*-silylated 1,3-di-*tert*-butylimidazolin-2-imine suggests electron delocalization. The exocyclic C–N bond length of 1.275(3) Å for the ligand is shorter than a C–N single bond and longer than a C=N double bond, suggesting the ylidic mesomeric structure.^{20b,22} These ligands have been used as monoanionic ancillary ligands for the synthesis of metal complexes for homogenous catalysis.²⁵

1.5 Reactivity of *N*-heterocyclic carbenes towards chalcogens

Imidazole-2-thiones have been known for many years and have been used as an ancillary ligand for transition metal catalysis.²⁶ One convenient route

to forming imidazole-2-thiones involves reacting imidazole-2-ylidenes with elemental cyclooctasulfur to form the desired thione adduct.^{26a,27} This synthetic methodology can be extended to include other chalcogens (Figure 1.5.1).¹⁹

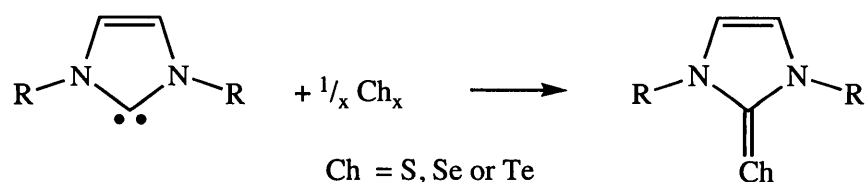


Figure 1.5.1. General reaction of imidazole-2-ylidene and chalcogens

Carbene-chalcogen adducts can be drawn using two mesomeric structures where the imidazolium ring can stabilize a positive charge, thus leading to an ylidic-type structure and creating a stronger electron-donating ligand (Figure 1.5.2).

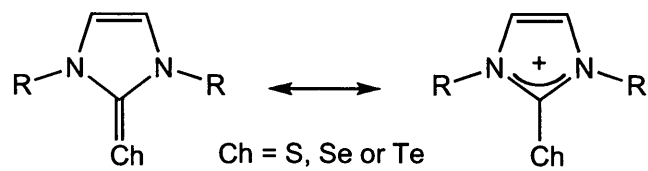


Figure 1.5.2. The mesomeric structures for carbene-chalcogen adducts

The solid-state X-ray structure of IMes=S offers some insight into nature of the carbon-sulfur bond. The carbon-sulfur bond for IMes=S is 1.6756(18) Å is longer than a C=S bond (1.61 Å) and shorter than a C–S bond (1.81 Å), thus indicating it is not true double bond character.²⁷⁻²⁸ In the cases of Se and Te carbene adducts, a similar trend is observed for the X-ray structures where the C–Ch bond is longer than the corresponding C=Ch double bond. The longer C–Ch

bond is a result of electron delocalization from the imidazole ring to the chalcogen atom, resulting in a polarized compound. The presence of electron delocalization is further supported by ^{125}Te and ^{77}Se solution NMR data. High-field ^{125}Te and ^{77}Se resonances for the corresponding compounds compared to other selenium and tellurium species suggests a higher degree of shielding.¹⁹⁻²⁰ This delocalization of electron density illustrates the usefulness of these compounds as strong electron-donating ancillary ligands.

1.6 Reactivity of *N*-heterocyclic carbenes towards pnictinidenes

Despite the overwhelming success and usefulness of carbene-chalcogens, specifically imidazole-2-thiones, there has been little interest in utilizing carbene-pnictinidenes as potential ligands.²⁹ Inspired by the synthesis of imidazole-2-thiones, Arduengo decided to react nucleophilic imidazol-2-ylidenes with cycloarylpnictinidenes to form carbene-pnictinidene adducts (Figure 1.6.1).^{29a}

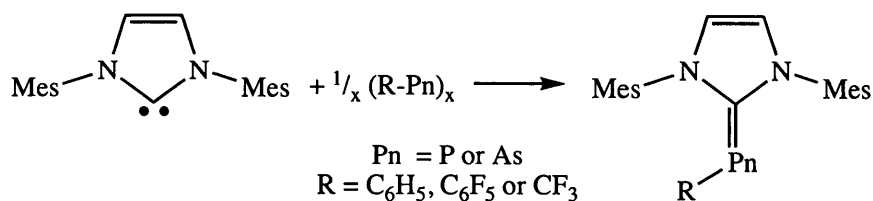


Figure 1.6.1. General synthesis of carbene-pnictinidene adducts

Similar to imidazol-2-imides and carbene-chalcogens, carbene-pnictinidenes can be drawn using two mesomeric structures. Within these structures, the imidazolium ring can stabilize a positive charge leading to an increased negative charge on the phosphorus or arsenic atom, creating a stronger electron-donating

ligand (Figure 1.6.2).

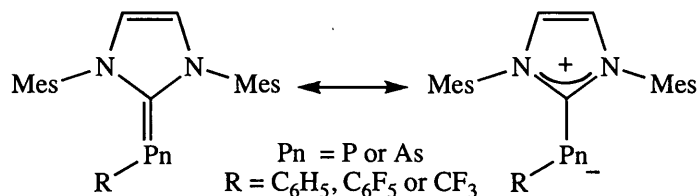


Figure 1.6.2. The mesomeric structures for carbene-pnictinidene adducts

The strongly polarized nature of the carbene-phosphinidene is apparent with the high-field ^{31}P chemical shifts. Typical ^{31}P nuclei in phosphalkenes resonate downfield of δ 200 ppm, whereas the $\text{IMes}=\text{PPh}$ carbene-phosphinidene resonates at δ -23 ppm.^{29a,30} This upfield ^{31}P chemical shift is due to a highly shielded phosphorus atom, a result of π -donation from the imidazole ring. The presence of π -donation from the imidazole ring is further supported by the difference in ^{31}P chemical shifts between the $\text{IMes}=\text{PPh}$ (δ -23 ppm) and $\text{SIMes}=\text{PPh}$ (δ -12 ppm). The difference in ^{31}P chemical shifts between the unsaturated and saturated ring illustrates the effectiveness of the unsaturated imidazole ring at stabilizing a positive charge, resulting in a greater charge polarization. The solid-state X-ray structure of $\text{IMes}=\text{PPh}$, the P–C bond (1.763 Å)^{29a} of the azole is slightly shorter than a P–C single bond (1.843 Å)^{28b}, but longer than the P–C double bonds of phosphalkenes (166).^{28a} Once again, this single-bond character is likely a result of electron delocalization from the imidazole ring to the phosphorus atom. Solution-NMR spectroscopy and solid-state X-ray analysis show a strongly polarized carbene-phosphinidene, which

yields a promising strong electron-donating ancillary ligand for transition metal chemistry.

1.7 Scope of the thesis work

The work included in this thesis is aimed at utilizing the unique reactivity of *N*-heterocyclic carbenes to develop novel, robust catalysts to mediate organic transformations. The multi-faceted work within this thesis explores the use of NHCs as ancillary ligands on early and late transition metals as potential catalysts for olefin polymerization and ring-closing metathesis, respectively. This work also includes exploring the synthesis and coordination of ancillary ligands derived from the unique reactivity of NHCs towards azides, chalcogens and pnictinidenes. The reactivity of a novel aryl-substituted acyclic imino-*N*-heterocyclic carbene to early transition metals, cyclooctasulfur and Grubbs-type ruthenium benzylidene complexes was explored. The reactivity of imidazol-2-imide towards Grubbs-type ruthenium benzylidene complexes and the synthesis and coordination of a novel group of ligands bearing an imidazol-2-imine scaffold were also explored. Lastly, this work will include the reactivity of IMes=PPh to Grubbs-type ruthenium benzylidene complexes.

1.8 References

1 a) P. L. Arnold and I. J. Casely, *Chem. Rev.* **2009**, *109*, 3599; b) D. Bourissou, O. Guerret, F. P. Gabbaï and G. Bertrand, *Chem. Rev.* **2000**, *100*, 39; c) S. Díez-González, N. Marion and S. P. Nolan, *Chem. Rev.* **2009**, *109*, 3612; d) D.

Enders, O. Niemeier and A. Henseler, *Chem. Rev.* **2007**, *107*, 5606; e) G. C. Fortman and S. P. Nolan, *Chem. Soc. Rev.* **2011**, *40*, 5151.

2 A. J. Arduengo, III, R. L. Harlow and M. Kline, *J. Am. Chem. Soc.* **1991**, *113*, 361.

3 a) F. E. Hahn and M. C. Jahnke, *Angew. Chem., Int. Ed.* **2008**, *47*, 3122; b) N. Marion, S. Díez-González and S. P. Nolan, *Angew. Chem., Int. Ed.* **2007**, *46*, 2988; c) M. C. Perry and K. Burgess, *Tetrahedron: Asymmetry* **2003**, *14*, 951.

4 a) T. Dröge and F. Glorius, *Angew. Chem., Int. Ed.* **2010**, *49*, 6940; b) A. M. Voutchkova, L. N. Appelhans, A. R. Chianese and R. H. Crabtree, *J. Am. Chem. Soc.* **2005**, *127*, 17624.

5 W. A. Herrmann, *Angew. Chem., Int. Ed.* **2002**, *41*, 1290.

6 a) R. Dorta, E. D. Stevens, N. M. Scott, C. Costabile, L. Cavallo, C. D. Hoff and S. P. Nolan, *J. Am. Chem. Soc.* **2005**, *127*, 2485; b) R. Dorta, E. D. Stevens, N. M. Scott, C. Costabile, L. Cavallo, C. D. Hoff and S. P. Nolan, *J Am Chem Soc* **2005**, *127*, 2485; c) D. G. Gusev, *Organometallics* **2009**, *28*, 6458.

7 A. Poater, B. Cosenza, A. Correa, S. Giudice, F. Ragone, V. Scarano and L. Cavallo, *Eur. J. Inorg. Chem.* **2009**, 1759.

8 a) R. L. Lord, H. Wang, M. Vieweger and M.-H. Baik, *J. Organomet. Chem.* **2006**, *691*, 5505; b) C. Lujan and S. P. Nolan, *J. Organomet. Chem.* **2011**, *696*, 3935; c) C. A. Urbina-Blanco, X. Bantreil, H. Clavier, A. M. Z. Slawin and S. P. Nolan, *Beilstein J. Org. Chem.* **2010**, *6*, 1120.

9 R. H. Crabtree, *J. Organomet. Chem.* **2005**, *690*, 5451.

- 10 F. E. Hahn and M. C. Jahnke, *Angew. Chem., Int. Ed.* **2008**, *47*, 3122.
- 11 a) J. C. Garrison and W. J. Youngs, *Chem. Rev.* **2005**, *105*, 3978; b) I. J. B. Lin and C. S. Vasam, *Coord. Chem. Rev.* **2007**, *251*, 642.
- 12 a) M. R. L. Furst and C. S. J. Cazin, *Chem. Commun.* **2010**, *46*, 6924; b) A. C. Badaj and G. G. Lavoie, *Organometallics* **2012**, *31*, 1103; c) J. A. Thagfi and G. G. Lavoie, *Organometallics* **2012**, *31*, 7351; d) W. W. N. O, A. J. Lough and R. H. Morris, *Organometallics* **2009**, *28*, 6755.
- 13 H. Jacobsen, A. Correa, A. Poater, C. Costabile and L. Cavallo, *Coord. Chem. Rev.* **2009**, *253*, 687.
- 14 X. Hu, I. Castro-Rodriguez, K. Olsen and K. Meyer, *Organometallics* **2004**, *23*, 755.
- 15 a) S. Díez-González and S. P. Nolan, *Coord. Chem. Rev.* **2007**, *251*, 874; b) W. A. Herrmann, J. Schütz, G. D. Frey and E. Herdtweck, *Organometallics* **2006**, *25*, 2437; c) R. A. Kelly Iii, H. Clavier, S. Giudice, N. M. Scott, E. D. Stevens, J. Bordner, I. Samardjiev, C. D. Hoff, L. Cavallo and S. P. Nolan, *Organometallics* **2007**, *27*, 202; d) S. Fantasia, J. L. Petersen, H. Jacobsen, L. Cavallo and S. P. Nolan, *Organometallics* **2007**, *26*, 5880.
- 16 M. Srebro and A. Michalak, *Inorg. Chem.* **2009**, *48*, 5361.
- 17 R. Dorta, E. D. Stevens, C. D. Hoff and S. P. Nolan, *J. Am. Chem. Soc.* **2003**, *125*, 10490.

- 18 a) L. Cavallo, A. Correa, C. Costabile and H. Jacobsen, *J. Organomet. Chem.* **2005**, 690, 5407; b) N. M. Scott and S. P. Nolan, *Eur. J. Inorg. Chem.* **2005**, 2005, 1815.
- 19 W. A. Herrmann and C. Kocher, *Angew. Chem., Int. Ed.* **1997**, 36, 2162.
- 20 a) N. Kuhn and A. Al-Sheikh, *Coord. Chem. Rev.* **2005**, 249, 829; b) M. Tamm, D. Petrovic, S. Randoll, S. Beer, T. Bannenberg, P. G. Jones and J. Grunenberg, *Org. Biomol. Chem.* **2007**, 5, 523.
- 21 a) S. Dastgir and G. G. Lavoie, *Dalton Trans.* **2010**, 39, 6943; b) S. Dastgir and G. G. Lavoie, *Dalton Trans.* **2012**, 41, 9651; c) M. B. Harkness, E. Alvarado, A. C. Badaj, B. C. Skrela, L. Fan and G. G. Lavoie, *Organometallics* **2013**, 32, 3309; d) T. K. Panda, C. G. Hrib, P. G. Jones, J. Jenter, P. W. Roesky and M. Tamm, *Eur. J. Inorg. Chem.* **2008**, 4270; e) D. Petrovic, T. Bannenberg, S. Randoll, P. G. Jones and M. Tamm, *Dalton Trans.* **2007**, 2812; f) D. Petrovic, T. Gloege, T. Bannenberg, C. G. Hrib, S. Randoll, P. G. Jones and M. Tamm, *Eur. J. Inorg. Chem.* **2007**, 3472.
- 22 M. Tamm, S. Randoll, T. Bannenberg and E. Herdtweck, *Chem. Commun.* **2004**, 876.
- 23 a) N. Kuhn, R. Fawzi, M. Steimann, J. Wiethoff, D. Blaeser and R. Boese, *Z. Naturforsch., B: Chem. Sci.* **1995**, 50, 1779; b) N. Kuhn, M. Grathwohl, M. Steimann and G. Henkel, *Z. Naturforsch., B: Chem. Sci.* **1998**, 53, 997.
- 24 a) K. Dehnicke and F. Weller, *Coord. Chem. Rev.* **1997**, 158, 103; b) D. W. Stephan, J. C. Stewart, F. Guérin, S. Courtenay, J. Kickham, E. Hollink, C.

Beddie, A. Hoskin, T. Graham, P. Wei, R. E. v. H. Spence, W. Xu, L. Koch, X. Gao and D. G. Harrison, *Organometallics* **2003**, *22*, 1937; c) N. L. S. Yue and D. W. Stephan, *Organometallics* **2001**, *20*, 2303.

25 a) W. Apisuk, A. G. Trambitas, B. Kitiyanan, M. Tamm and K. Nomura, *J. Polym. Sci., Part A: Polym. Chem.* **2013**, *51*, 2575; b) S. Beer, K. Brandhorst, J. Grunenberg, C. G. Hrib, P. G. Jones and M. Tamm, *Org Lett* **2008**, *10*, 981; c) S. Beer, K. Brandhorst, C. G. Hrib, X. Wu, B. Haberlag, J. Grunenberg, P. G. Jones and M. Tamm, *Organometallics* **2009**, *28*, 1534; d) S. Beer and M. Tamm, **2007**, pp. INOR; e) A. Gloeckner, T. Bannenberg, C. G. Daniliuc, P. G. Jones and M. Tamm, *Inorg. Chem.* **2012**, *51*, 4368; f) B. Haberlag, X. Wu, K. Brandhorst, J. Grunenberg, C. G. Daniliuc, P. G. Jones and M. Tamm, *Chem. - Eur. J.* **2010**, *16*, 8868; g) S. Lysenko, C. G. Daniliuc, P. G. Jones and M. Tamm, *J. Organomet. Chem.* Ahead of Print; h) K. Nomura, H. Fukuda, W. Apisuk, A. G. Trambitas, B. Kitiyanan and M. Tamm, *J. Mol. Catal. A: Chem.* **2012**, 363-364, 501; i) S. H. Stelzig, M. Tamm and R. M. Waymouth, *J. Polym. Sci., Part A: Polym. Chem.* **2008**, *46*, 6064; j) M. Tamm and S. Randoll, **2006**, pp. INOR; k) M. Tamm, S. Randoll, E. Herdtweck, N. Kleigrewe, G. Kehr, G. Erker and B. Rieger, *Dalton Trans.* **2006**, 459; l) M. Tamm, S. Randoll, E. Herdtweck, N. Kleigrewe, G. Kehr, G. Erker and B. Rieger, *Dalton Trans* **2006**, 459; m) A. G. Trambitas, D. Melcher, L. Hartenstein, P. W. Roesky, C. Daniliuc, P. G. Jones and M. Tamm, *Inorg. Chem.* **2012**, *51*, 6753; n) A. G. Trambitas, T. K. Panda, J. Jenter, P. W. Roesky, C. Daniliuc, C. G. Hrib, P. G. Jones and M. Tamm, *Inorg. Chem.* **2010**,

49, 2435; o) A. G. Trambitas, T. K. Panda, J. Jenter, P. W. Roesky, C. Daniliuc, C. G. Hrib, P. G. Jones and M. Tamm, *Inorg Chem* **2010**, *49*, 2435.

26 a) E. Alvarado, A. C. Badaj, T. G. Larocque and G. G. Lavoie, *Chem. - Eur. J.* **2012**, *18*, 12112; b) Y.-B. Huang, W.-G. Jia and G.-X. Jin, *J. Organomet. Chem.* **2008**, *694*, 86; c) W.-G. Jia, Y.-B. Huang, Y.-J. Lin and G.-X. Jin, *Dalton Trans.* **2008**, 5612; d) W.-G. Jia, Y.-B. Huang, Y.-J. Lin and G.-X. Jin, *Dalton Trans* **2008**, 5612; e) W.-G. Jia, Y.-B. Huang, Y.-J. Lin, G.-L. Wang and G.-X. Jin, *Eur. J. Inorg. Chem.* **2008**, 4063; f) M. Slivarichova, R. Ahmad, Y.-Y. Kuo, J. Nunn, M. F. Haddow, H. Othman and G. R. Owen, *Organometallics* **2011**, *30*, 4779.

27 J. Huang, H.-J. Schanz, E. D. Stevens, S. P. Nolan, K. B. Capps, A. Bauer and C. D. Hoff, *Inorg. Chem.* **2000**, *39*, 1042.

28 a) P. Pyykkö and M. Atsumi, *Chem. Eur. J.* **2009**, *15*, 12770; b) P. Pyykkö and M. Atsumi, *Chem. Eur. J.* **2009**, *15*, 186.

29 a) A. J. Arduengo, III, J. C. Calabrese, A. H. Cowley, H. V. R. Dias, J. R. Goerlich, W. J. Marshall and B. Riegel, *Inorg. Chem.* **1997**, *36*, 2151; b) A. J. Arduengo, III, C. J. Carmalt, J. A. C. Clyburne, A. H. Cowley and R. Pyati, *Chem. Commun.* **1997**, 981; c) O. Back, M. Henry-Ellinger, C. D. Martin, D. Martin and G. Bertrand, *Angew. Chem., Int. Ed.* **2013**, *52*, 2939; d) G. Frison and A. Sevin, *J. Organomet. Chem.* **2002**, 643-644, 105.

30 a) F. Mathey, *Acc. Chem. Res.* **1992**, *25*, 90; b) J. F. Nixon, *Chem. Rev.* **1988**, *88*, 1327.

Chapter 2 Aryl-Substituted Acyclic Imino-*N*-Heterocyclic Carbene:

Coordination to Early Transition Metals

2.0 Preface

This chapter is comprised of three reformatted and slightly modified peer-reviewed journal publications: New Stable Aryl-Substituted Acyclic Imino-*N*-Heterocyclic Carbene: Synthesis, Characterisation and Coordination to Early Transition Metals; T. G. Larocque, A. C. Badaj, S. Dastgir and G. G. Lavoie *Dalton Transactions* 2011, 40(47), 12705–12712; Coordination and Reactivity Study of Titanium Phenoxo Complexes Containing a Bulky Bidentate Imino-*N*-Heterocyclic Carbene Ligand; T. G. Larocque and G. G. Lavoie *J. Organometal. Chem.* 2012, 715, 26–32.; N-Heterocyclic Carbenes and Imidazole-2-thiones as Ligands for the Gold(I)-Catalysed Hydroamination of Phenylacetylene; E. Alvarado, A. C. Badaj, T. G. Larocque and G. G. Lavoie, *Chemistry – A European Journal* 2012, 18, 12112.

2.1 Introduction

As outlined in Chapter 1, NHCs have played an increasingly important role in organometallic chemistry and catalysis.¹ These carbenes, which are excellent σ -donors and poor π -acceptors, impart excellent thermodynamic stability to transition metal complexes.² In many cases, replacement of phosphine ligands with NHCs has resulted in enhanced thermal stability and catalytic activities.³ This observation has led to widespread applications of NHCs in transition metal complex-mediated organic transformations. However,

despite the large number of various catalysts that have been developed for the polymerization of olefins,^{4,5,6,7} very little work has been reported on the use of NHCs in such catalysts.⁸ Included in previously reported NHC-based catalysts are mono and dianionic, multidentate ligand systems.⁸ Of these previously reported catalysts, some show exception catalytic activity towards oligomerization of ethylene.⁹

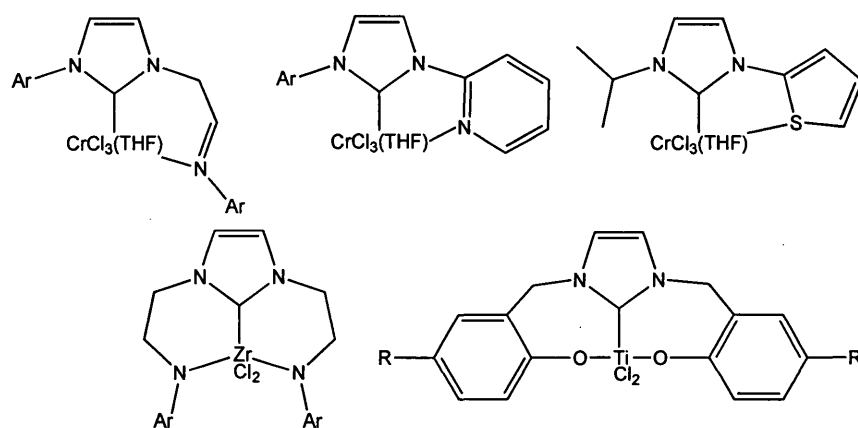


Figure 2.1. General representation of multidentate NHC-based ligands on early transition metals

The Lavoie group became interested in preparing and studying NHC analogues of the bulky α -diimines and 2,6-diiminopyridines to address the poor thermal stability of these systems.^{10,11} Although these late transition metal complexes produce high-molecular-weight polyethylene in good rates, their performance decreases dramatically at temperatures greater than 50 °C due to thermal decomposition.¹² Introduction of the NHC fragment in the ligand scaffold thus offers the potential to mitigate this important shortcoming of these systems.

We have previously described the synthesis and full characterization of the imidazolium salts **A** and **B**, and the corresponding Ag(I) and Cu(I) complexes.^{13,14}

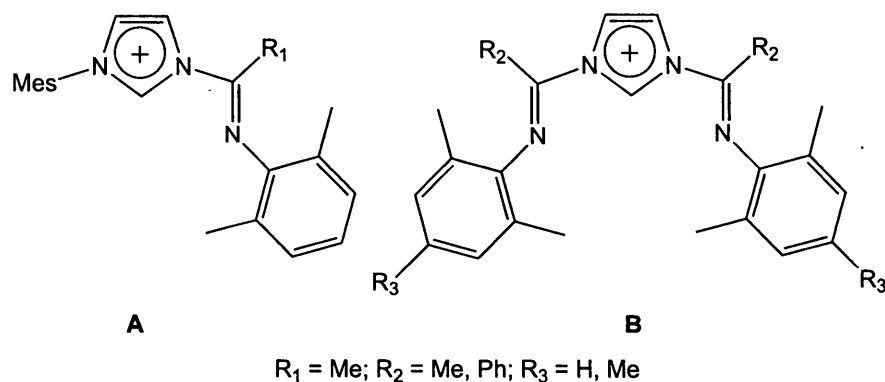


Figure 2.1. General representation of imidazolium salts A and B

Salts similar to **A**, where either aryl ring is replaced by an alkyl group have been reported by other groups and used to prepare late transition metal complexes for studying various catalytic reactions, including Suzuki-Miyaura cross-coupling and cyclopropanation.¹⁵ However, considering the significance of steric bulk in the α -diimine system to achieve high-molecular weight polymers,¹⁰ we decided to investigate the effect of having two aryl rings close to the coordination site in ligand scaffold (Figure 2.2).

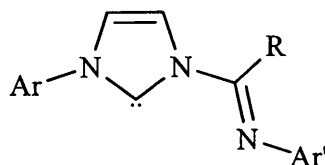


Figure 2.2. General representation of the iminocarbene ligand

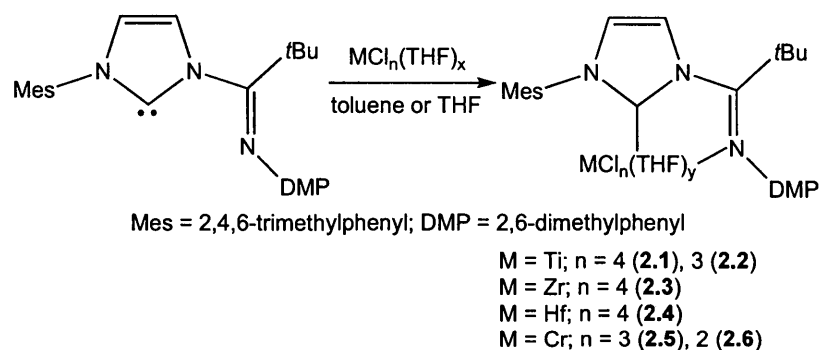
Considering the ubiquity of early transition metal catalysts in olefin polymerization,^{4,7,16,17,18} in this chapter, I describe the synthesis and structural characterization studies with free carbene, C[^]Imine, focused on Group 4 and 6 metals in their common oxidation states. As such, I describe the synthesis and isolation of the corresponding titanium, zirconium, hafnium and chromium metal halides. I also describe the synthesis and isolation of the corresponding titanium aryloxo complexes and the attempted synthesis of titanium imido complexes in hopes of generating five- and six-coordinate metal dichloride complexes that are commonly used as olefin oligomerisation and polymerization catalysts.^{4,6,7,15,16,19}

2.2. Results and Discussion

2.2.1 Coordination of C[^]Imine to Early Transition Metal Halides

2.2.1.1. Coordination of C[^]Imine to titanium

Addition of one equivalent of C[^]Imine to TiCl₄(THF)₂ in THF afforded TiCl₄(C[^]Imine) (**2.1**) as a spectroscopically pure yellow powder in excellent yield (91%).



Scheme 2.1. Synthesis of group 4 and 6 metal halide complexes of C^NImine.

The NMR spectrum is consistent with the desired product. A decrease in the C=N stretching frequency ($\nu_{\text{C=N}} 1609 \text{ cm}^{-1}$) compared to the free ligand ($\nu_{\text{C=N}} 1662 \text{ cm}^{-1}$) is observed, suggesting coordination of the imine nitrogen to the metal centre. Compound **2.1** crystallises in the $P2_1/n$ space group, with the ligand coordinated in a bidentate fashion through the central imidazol-2-ylidene carbon and the imine nitrogen, forming a distorted octahedral complex (Figure 2.3).

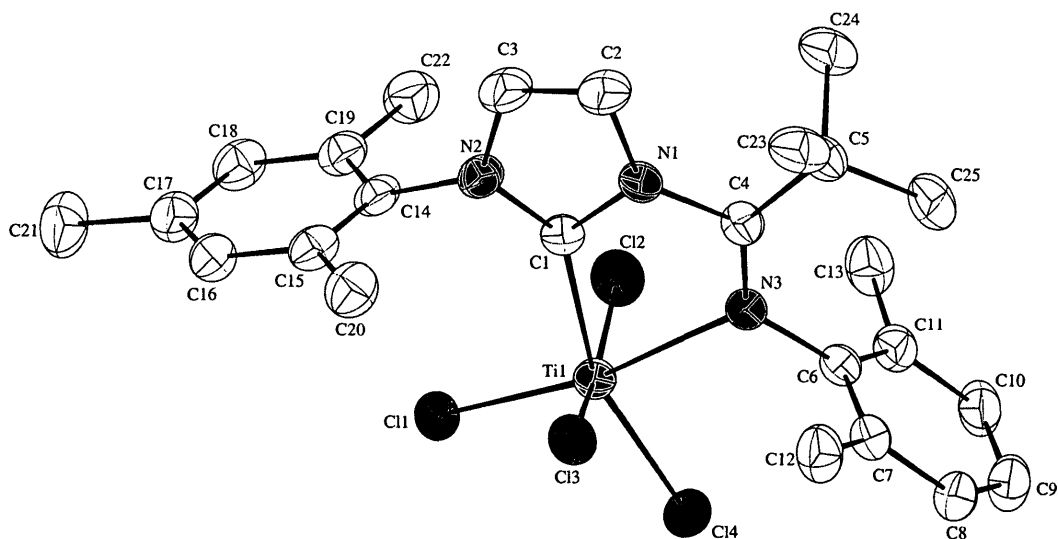


Figure 2.3. ORTEP plot (50% probability level) of 2.1.

Hydrogen atoms and dichloromethane omitted for clarity.

The observed increase in the imine bond length upon coordination from 1.266(3) to 1.287(6) Å is in agreement with the corresponding decrease in IR stretching frequency. The equatorial plane formed by Ti1, C1, N3, Cl1 and Cl4 atoms is almost perfectly orthogonal to the plane formed by Ti1, Cl2 and Cl3, and by those formed by the xylyl and mesityl rings, with respective angles of 89.47°, 88.77° and 89.09°. Other atoms such as N1, N2, C2, C3, C4, C5, C6, and C14 also lie on the equatorial plane defined above. The Cl2–Ti1–Cl3 bond angle is 165.21(7)° with both chlorine atoms bent towards C1 at an average angle of 82.75° and with chloride–carbenic carbon distances of 2.921 and 2.967 Å, considerably shorter than the sum of the van der Waals radii for both atoms (3.45 Å).²⁰ This could possibly arise from intermolecular interactions between the formally vacant p orbital on C1 and the lone pairs of

the adjacent chlorides.²¹ Alternatively, the bending of Cl2 and Cl3 towards the carbene centre may be the result of repulsions between lone pairs on the other two adjacent chlorine atoms, as proposed by Arnold for a comparable highly congested d^0 system.²² The trans effect of the strong carbene σ -donor is manifested by the longer Ti1–Cl4 (2.2808(16) Å), compared to Ti1–Cl1 (2.2370(16) Å). Selected bond lengths and angles for **2.1** and other compounds are listed in Table 2.1.

The corresponding Ti(III) complex **2.2** was prepared by a synthetic route similar to that used for **2.1** and was isolated as a purple solid. The solution magnetic susceptibility of **2.2** was determined to be $\mu_{\text{eff}} = 1.65 \mu_{\text{B}}$ using the Evans method,²³ consistent with the predicted value ($\mu_{\text{eff}}(\text{spin only}) = 1.73$) for one unpaired electron. X-ray quality crystals were obtained from vapour diffusion of pentane into a saturated THF solution (Figure 2.4). $\text{TiCl}_3(\text{C}^{\wedge}\text{Imine})$ (**2.2**) crystallised as a THF adduct in the $I 4_1/a$ space group with an elongated C4–N3 bond length of 1.280(3) Å, in agreement with the corresponding C=N stretching frequency of 1607 cm^{-1} .

Table 2.1. Selected bond lengths and angles for compounds C[^]Imine, 2.1, 2.2, 2.3 and 2.5

	C [^] Imine	2.1	2.2	2.3	2.5
bond length (Å)					
M–C1	–	2.167(5)	2.178(3)	2.297(17)	2.041(4)
M–N3	–	2.358(4)	2.282(2)	2.479(14)	2.156(3)
M–Cl1	–	2.2370(16)	2.3139(9)	2.385(5)	2.2954(13)
M–Cl2	–	2.2930(18)	2.4202(9)	2.419(5)	2.3596(12)
M–Cl3	–	2.2775(18)	2.3595(9)	2.401(5)	2.2985(12)
M–Cl4		2.2808(16)	–	–	–
N1–C1	1.380(3)	1.373(6)	1.374(3)	1.42(2)	1.380(5)
N2–C1	1.354(3)	1.344(6)	1.336(3)	1.38(2)	1.345(5)
N1–C4	1.444(3)	1.448(6)	1.431(3)	1.35(2)	1.424(5)
N3–C4	1.266(3)	1.287(6)	1.280(3)	1.38(2)	1.287(5)
C2–C3	1.338(3)	1.329(8)	1.347(4)	1.19(3)	1.340(6)
bond angle (deg)					
C1–M–N3	–	70.42(16)	71.37(9)	67.0(5)	75.50(14)
N1–C4–N3	122.38(18)	112.3(4)	113.3(2)	112.8(15)	112.3(3)
N1–C1–N2	101.48(19)	104.7(4)	104.9(2)	105.1(14)	105.0(3)
C1–M–Cl1	–	97.18(14)	97.65(8)	100.1(4)	97.53(11)
C1–M–Cl2	–	83.34(15)	81.58(7)	82.85(13)	82.82(11)
C1–M–Cl3	–	82.16(15)	98.61(8)	155.0(4)	94.86(11)
Cl1–M–Cl3	–	92.49(6)	92.96(3)	104.9(2)	91.48(5)
C1–M–Cl4	–	158.65(14)	–	–	–
Cl2–M–Cl3	–	165.21(7)	171.63(4)	96.48(12)	175.77(5)

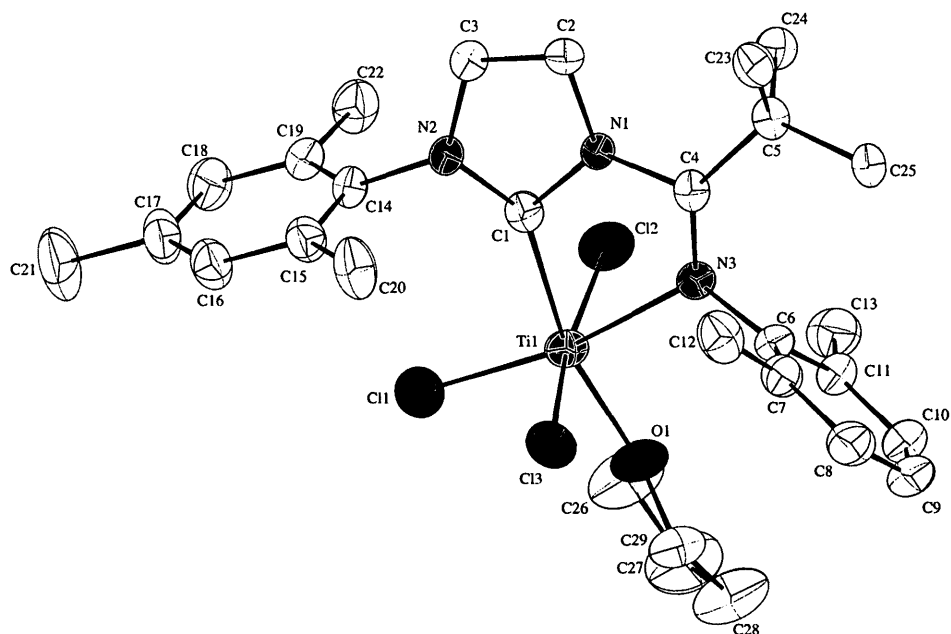


Figure 2.4. ORTEP plot (50% probability level) of 2.2.

Hydrogen atoms omitted for clarity.

The complex has a highly distorted octahedral geometry. The Ti1–C1 bond length of 2.178(3) Å is within expected values and comparable to that observed in **2.1**. Interestingly, the vector formed by that bond is 11.5° off the plane of the imidazole ring. Moreover, the N1–C4–N3–C6 torsion angle is 163.95°, about 16° off the expected 180° value. The added bulk coming from the coordinated THF is likely contributing to these peculiar values. We believe that this increased steric bulk significantly influences other atom positions. In fact, the C1–Ti1–Cl3 bond angle is obtuse with a value of 98.61(8)°. Although the bond angle for C1–Ti1–Cl2 is 81.58(7)° and comparable to the corresponding values observed in **2.1**, both Cl2 and Cl3 point directly towards

N3, further supporting that the bending of the trans chlorine atoms in **2.1** towards C1 may be strictly due to steric reasons and not electronic ones, as also previously proposed by Arnold.²² As expected, all metal-chloride bonds in **2.2** are longer than in the corresponding more electropositive and less sterically-congested Ti(IV) complex **2.1**. Other bond lengths and angles are within normal range.

2.2.1.2. Coordination of free carbene to zirconium and hafnium

The zirconium (**2.3**) and hafnium (**2.4**) complexes were prepared in an analogous manner and isolated as white powders in yields of 67% and 73%, respectively. The NMR spectroscopic data for both complexes were consistent with the desired products and are similar to those for the titanium homologue **2.1**. The C=N stretching frequency for **2.3** and **2.4** were observed at 1606 cm⁻¹ and 1604 cm⁻¹, respectively, indicating a bidentate coordination motif. Coordination of the ligand through the carbene and the imine nitrogen was further corroborated for **2.3** through its X-ray structure (Figure 2.5).

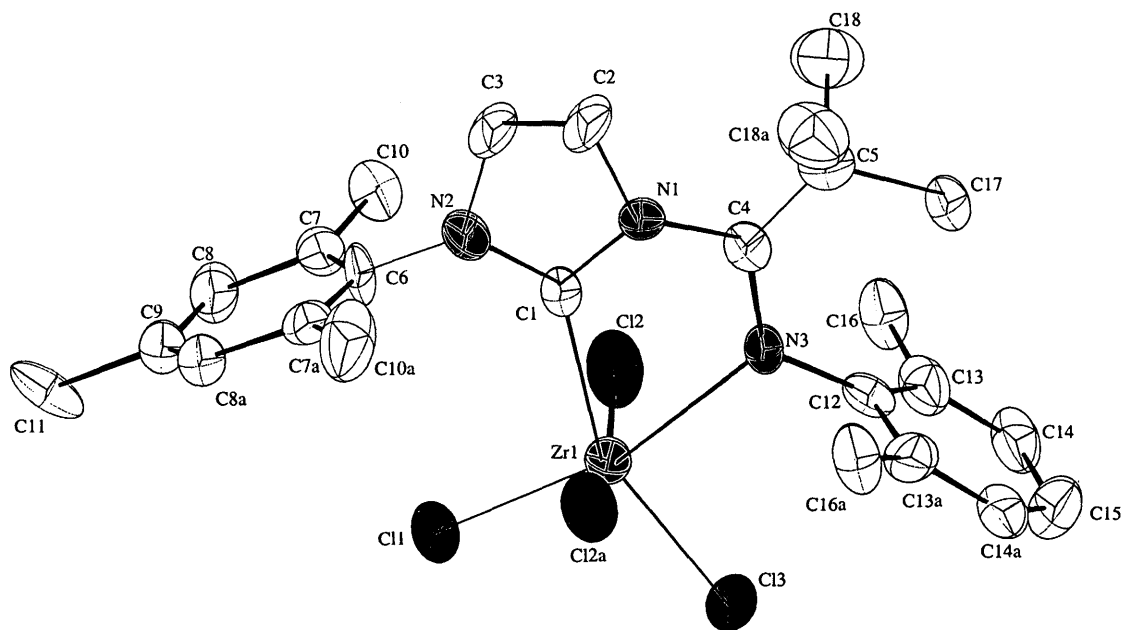


Figure 2.5. ORTEP plot (50% probability level) of 2.3.

Hydrogen atoms omitted for clarity.

Compound **2.3** exhibits a distorted octahedral coordination geometry. In contrast to **2.1**, it crystallises in the *Pnma* space group, with the molecule lying on the crystallographic mirror plane orthogonal to the xylyl and to the mesityl rings, and passing through the imidazol-2-ylidene ring, as well as through C4, C5, C17, N3, Zr1, Cl1 and Cl3. All bond lengths involving the Zr(IV) metal centre are on average 0.13 Å longer than those observed in the corresponding Ti(IV) complex **2.1**, in agreement with difference in covalent radii of both metals reported by Alvarez and Pyykkö.²⁴ The Zr1–C1 and Zr1–N3 bond lengths are 2.319(7) Å and 2.483(5) Å, respectively, with the zirconium–carbene bond length similar to previously reported zirconium NHC complexes.^{25,26} As expected, the metal-chlorine bond trans to the strong

carbene σ -donor is slightly longer (2.407(2)Å) than the one trans to the imine (2.384(2)Å). Cl2 and its crystallographically-equivalent Cl2a are bent towards C1 at an 82.85(13)° angle, similar to that observed for **2.1**, with a carbon-chlorine distance of 3.136 Å, possibly simply due to sterics considerations based on our previous observations for both Ti(III) (**2.1**) and Ti(IV) (**2.2**) compounds.

2.2.1.3. Coordination of free carbene to chromium

The Cr(III) (**2.5**) and Cr(II) (**2.6**) complexes were prepared from the corresponding THF adduct metal halide precursors in 89% yield. In both cases, the complexes were purified by recrystallisation from THF under N₂ at -35 °C. Complexes **2.5** and **2.6** are both paramagnetic with a solution magnetic susceptibility of 3.81 and 2.90 μ_B (Evans Method), respectively, consistent with the predicted values for systems with three ($\mu_{\text{eff}}(\text{spin only}) = 3.87 \mu_B$) and two (2.83 μ_B) unpaired electrons.

X-ray quality crystals were obtained for the trivalent chromium complex **2.5** (Figure 2.6). The complex crystallised in the $I 4_1/a$ space group as a THF adduct and is isostructural with the analogous Ti(III) complex **2.2**.

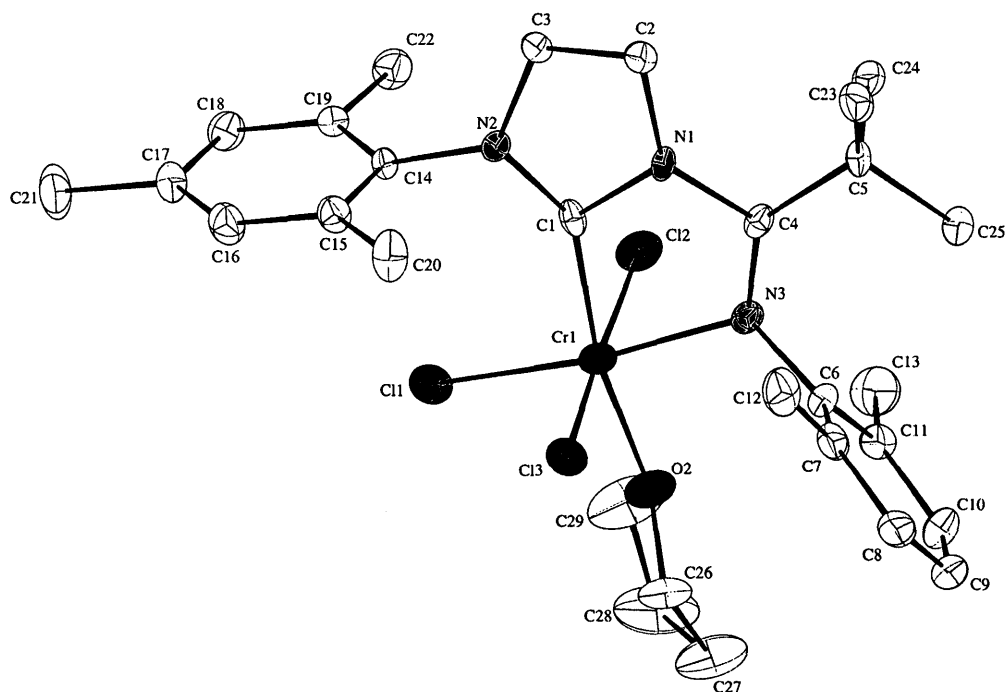


Figure 2.6. ORTEP plot (50% probability level) of 2.5.

Hydrogen atoms and dichloromethane omitted for clarity.

The $\nu_{\text{C=N}}$ stretching frequency of 1604 cm^{-1} is in good agreement with the observed C4–N3 bond length of $1.287(5) \text{ \AA}$ and comparable to the values observed for **2.2**. All other C–C and C–N bond lengths of the C[^]Imine ligand in **2.5** are within experimental error of those observed in **2.2**. In contrast, bond lengths between the metal centre and all six coordinating atoms are shorter than in the corresponding Ti(III) complex. The observed Cr1–C1 and Cr1–N3 bond lengths are in excellent agreement with the expected values based on the difference between the covalent radii of chromium (1.39 \AA) and titanium (1.60 \AA).²⁴ This is in contrast to the observed values for Cr–Cl and Cr–O bonds that are on average only 0.06 \AA shorter than the corresponding bonds

in **2.2**, presumably because of greater repulsive interaction between the π -electrons on the main elements and those in the metal d_{π} -orbitals. Interestingly, as observed for **2.2**, the vector formed by Cr1 and C1 is also off the plane of the imidazole ring by 10.7° and the N1–C4–N3–C6 torsion angle is 163.67° . Moreover, Cl2 and Cl3 are also leaning more towards N3 than C1. All other bond lengths and angles are within expected range and comparable to those observed in the analogous Ti(III) complex **2.2**.

2.2.1.4. Ethylene polymerization catalysis

The catalytic activities of compounds **2.1–2.6** towards ethylene polymerization in toluene were studied at atmospheric pressure and room temperature in the presence of 1000 equivalents of methylaluminoxane (MAO) as cocatalyst. $\text{ZrCl}_4(\text{C}^{\wedge}\text{Imine})$ (**2.3**) was found to be the most active of all three complexes tested with a productivity of $140 \text{ kg PE} \cdot \text{mol M}^{-1} \cdot \text{h}^{-1}$, followed by the Ti(IV) homologue **2.1** at $40 \text{ kg PE} \cdot \text{mol M}^{-1} \cdot \text{h}^{-1}$. Those productivities are three and two times greater than those observed in respective control experiments using $\text{ZrCl}_4(\text{THF})_2$ and $\text{TiCl}_4(\text{THF})_2$. Furthermore, they are only one to two orders of magnitude lower than those observed using zirconocene dichloride as the benchmark catalyst. Reaction with the other complexes reported herein did not lead to any significant amount of solid polymer. In all cases, no soluble waxes or low molecular weight oligomers were generated. The maximum melting endotherms for the polyethylene produced by **2.1** and **2.3** were determined by differential scanning calorimetry and found to be

135.9 and 134.0 °C, respectively, indicative of linear polyethylene.

These preliminary results were promising and suggested that further development of the catalysts should focus on both titanium and zirconium.

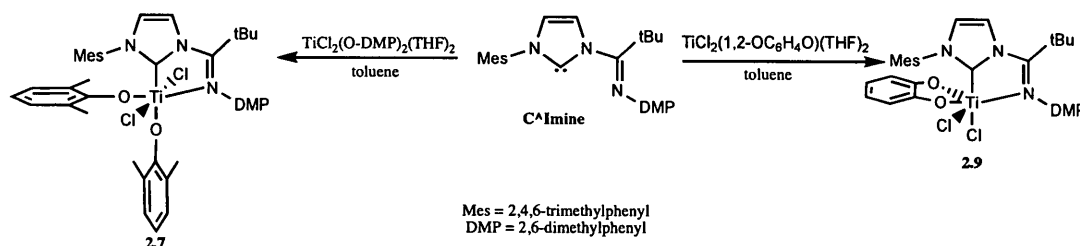
2.2.5. Coordination and reactivity of C[^]Imine to titanium phenoxo complexes

2.2.5.1 Synthesis of TiCl₂(2,6-OC₆H₃-Me₂)₂(C[^]Imine) (2.7)

The early transition metal halide systems bearing C[^]Imine are ideally suited for further tailoring of the activity by incorporation of alkoxide (RO⁻), aryloxo (ArO⁻), amide (R₂N⁻) or even imido (RN²⁻) ligands to form five- and six-coordinate metal dihalide complexes. Such strategies of fine-tuning the performance of the catalyst by incorporating one of these ancillary ligands while retaining two chlorides for subsequent activation has been used to develop other highly active catalytic systems.²⁷ In view of the success of catalysts bearing aryloxo and imido ancillary ligands for α -olefin polymerization,^{5c,19a,27a,28} we chose to prepare titanium complexes of 1-(1-(2,6-dimethylphenylimino)-2,2-dimethylpropyl)-3-(2,4,6-trimethylphenyl)imidazol-2-ylidene carbene (C[^]Imine) containing aryloxo or imido groups as ancillary ligands in an attempt to develop structure–property relationships for ethylene polymerization.

Attempts to treat TiCl₄(C[^]Imine) with two equivalents of Na(2,6-OC₆H₃-Me₂) under a variety of reaction conditions led to a mixture of reaction products. As a result, the TiCl₂(2,6-OC₆H₃-Me₂)₂(THF)₂ metal precursor was prepared and treated with one equivalent of C[^]Imine in toluene to give compound **2.7** as an

orange powder in good yield (82%). The solution ^1H NMR spectrum was consistent with the desired product. The presence of two ortho methyl resonances for the 2,6-dimethylphenoxide ligands at δ 2.58 and 2.41 is a strong indication of the cis arrangement of these ligands. A decrease in the C=N stretching frequency from 1662 cm^{-1} for the free ligand to 1609 cm^{-1} for **2.7** suggests coordination of the ligand to the metal centre in a bidentate mode through both the carbenoid carbon and the imine nitrogen atoms. A comparable decrease in stretching frequency was also observed in $\text{TiCl}_4(\text{C}^{\wedge}\text{Imine})$ and other related early transition metal complexes.²⁹



Scheme 2.2. Synthesis of titanium complexes 2.7 and 2.9 from free carbene, $\text{C}^{\wedge}\text{Imine}$.

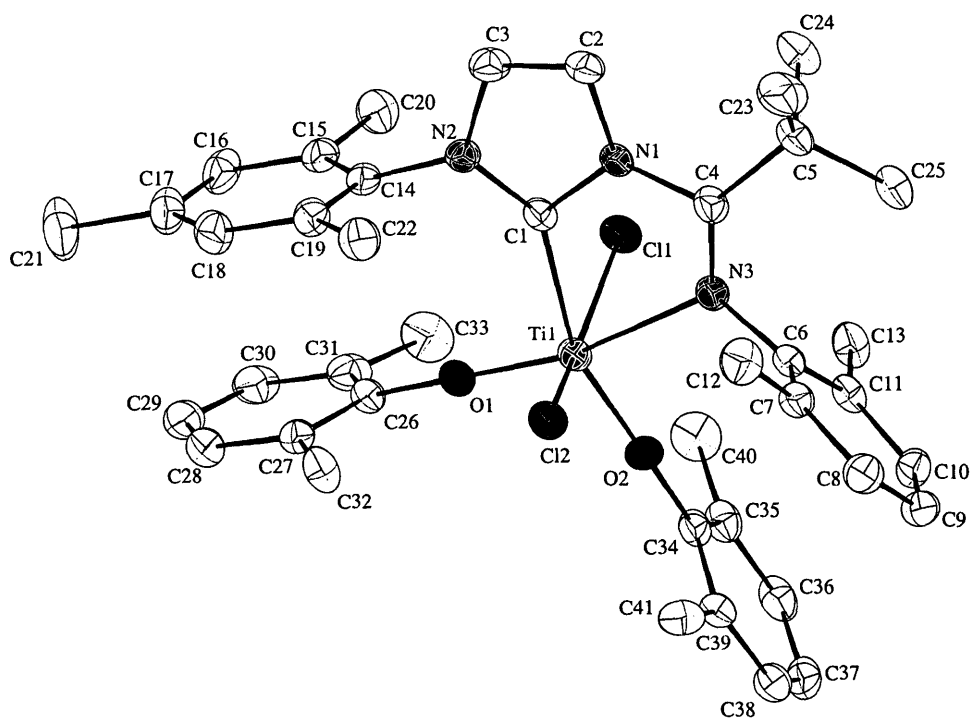


Figure 2.6 ORTEP plot (50% probability) of 2.7.

Hydrogen atoms and a CH₂Cl₂ solvent molecule are omitted for clarity.

In order to confirm the proposed structure of **2.7**, we attempted to isolate single crystals suitable for X-ray crystallographic studies. Crystals of the desired product were successfully grown at $-35\text{ }^{\circ}\text{C}$ under nitrogen by slow liquid diffusion of pentane into a saturated CH₂Cl₂ solution. Analysis of the X-ray diffraction data confirmed the coordination of the ligand through the carbenoid carbon of the carbene and the imine nitrogen, with a C1–Ti1–N3 bite angle of $68.77(10)^{\circ}$, slightly smaller than that observed in TiCl₄(C[^]Imine)²⁹ (Figure 2.6). The structure shows both chloride atoms trans to each other. As expected, the titanium centre of **2.7** exhibits a pseudo-octahedral coordination geometry, commonly observed

in $\text{TiCl}_2(\text{OAr})_2\text{L}_2$ complexes.^{30,31} Angles about the metal centre range from 76.25(8) to 100.80(10)° (Table 2.2).

Upon coordination of C^Imine to titanium in **2.7**, the C=N bond length increases slightly from 1.266(3) to 1.270(4) Å, consistent with the observed decrease in the corresponding IR stretching frequency. The strong σ -donating ability of the carbene gives rise to the trans influence and is illustrated by the longer Ti–O2 bond trans to the carbene (1.821(2) Å), compared to that for Ti–O1 cis to the carbene (1.795(2) Å). The Ti1–C1 and Ti1–N3 bond distances were determined to be 2.226(3) and 2.379(2) Å, respectively. Both values are slightly greater than those observed in the tetrachloride complex $\text{TiCl}_4(\text{C}^{\text{Imine}})^{29}$, possibly due to the larger sterics of the phenoxide ligands or to its stronger trans influence compared to that of chlorides.³² Interestingly, both the Ti1–O1–C26 and the Ti1–O2–C34 bond angles are equivalent at 179.1(2)°.

As expected, we see significant multiple bond character between the metal and the oxygen with the Ti1–O1 (1.795(2) Å) and Ti1–O2 (1.821(2) Å) lengths closer to the expected bond distance of a Ti=O double bond (1.74 Å) than of a Ti–O single bond (1.99 Å).^{24a,33} The steric constraint imposed by the formation for the metallacycle leads to a yaw distortion of 10.0°, slightly higher than that observed in $\text{TiCl}_4(\text{C}^{\text{Imine}})$ (9.1°)²⁹ but considerably smaller than in square planar nickel complexes of C^Imine (14.5–15.7°)³⁴, further illustrating the effect of having a six-coordinate metal centre and sterically-demanding phenoxide ligands.

The xyllyl and mesityl rings of C[^]Imine are almost orthogonal to the best plane formed by the imidazol-2-ylidene ring, at 82.40° and 89.26°, respectively. The phenoxide ring cis to the carbene is almost perfectly aligned with the mesityl ring, with a N2–C1–Ti1–O1 torsion angle of 0.7(3)°. These two rings are also approximately coplanar, as evidenced by the small angle (3.4°) between the mean planes formed by each ring. In contrast, the phenoxide ring trans to the carbene is neither well aligned nor coplanar with the xyllyl ring of C[^]Imine, with a C6–N3–Ti1–O2 torsion angle of 25.1(2)° and an angle between the planes formed by each ring of 15.9°.

Interestingly, previous attempts to grow crystals of **2.7** from slow liquid diffusion of pentane into a saturated THF solution at –35 °C resulted in the decomposition product **2.8**, with two coordinated mesitylimidazole fragments bound to titanium cis to each other (Figure 2.7). Nucleophilic attack of adventitious water on the iminic carbon of the bidentate ligand, which has become a better electrophile through replacement of two chlorides in TiCl₄(C[^]Imine) with the more electronegative phenoxide ligands, likely accounts for its decomposition to mesityl imidazole and *N*-(2,6-dimethylphenyl)pivaloylamide. Interestingly, such cleavage of the N1–C4 bond has not been reported for more electron-rich late transition metal analogues.³⁴ Compound **2.8** was independently synthesized by reacting two equivalents of 1-(2,4,6-trimethylphenyl)imidazole with TiCl₂(2,6-OC₆H₃-Me₂)₂(THF)₂.

Table 2.2. Selected bond lengths and angles for compounds TiCl₄(C^Imine), 2.7 and 2.9.

	TiCl ₄ (C^Imine) ²⁹	2.7	2.9
<i>Bond lengths (Å)</i>			
Ti–C1	2.167(5)	2.226(3)	2.186(3)
Ti–N3	2.358(4)	2.379(2)	2.336(3)
Ti–Cl1	2.2370(16)	2.3844(9)	2.3427(9)
Ti–Cl2	2.2930(18)	2.3245(9)	2.3064(10)
Ti–Cl3	2.2775(18)	–	–
Ti–Cl4	2.2808(16)	–	–
Ti–O1	–	1.795(2)	1.892(2)
Ti–O2	–	1.821(2)	1.854(2)
N1–C1	1.373(6)	1.375(4)	1.376(4)
N2–C1	1.344(6)	1.344(4)	1.338(4)
N1–C4	1.448(6)	1.431(4)	1.441(4)
N3–C4	1.288(6)	1.270(4)	1.288(4)
C2–C3	1.329(8)	1.329(4)	1.326(5)
<i>Bond angles (deg)</i>			
C1–Ti–N3	70.42(16)	68.77(10)	70.20(10)
N1–C4–N3	112.3(4)	113.3(3)	112.9(3)
N1–C1–N2	104.7(4)	104.8(2)	105.0(3)
C1–Ti–Cl1	97.18(14)	76.25(8)	82.07(8)
Cl–Ti–Cl2	83.34(15)	83.47(8)	157.71(8)
C1–Ti–Cl3	82.16(15)	–	–
Cl1–Ti–Cl3	83.32(15)	–	–
C1–Ti–Cl4	158.65(15)	–	–
Cl2–Ti–Cl3	165.21(7)	–	–
C1–Ti–O1	–	97.73(10)	88.97(10)
C1–Ti–O2	–	160.54(10)	99.83(10)
O1–Ti–O2	–	100.80(10)	81.26(9)
Cl1–Ti–O1	–	97.17(7)	169.24(8)
Cl1–Ti–O2	–	95.49(7)	94.34(7)

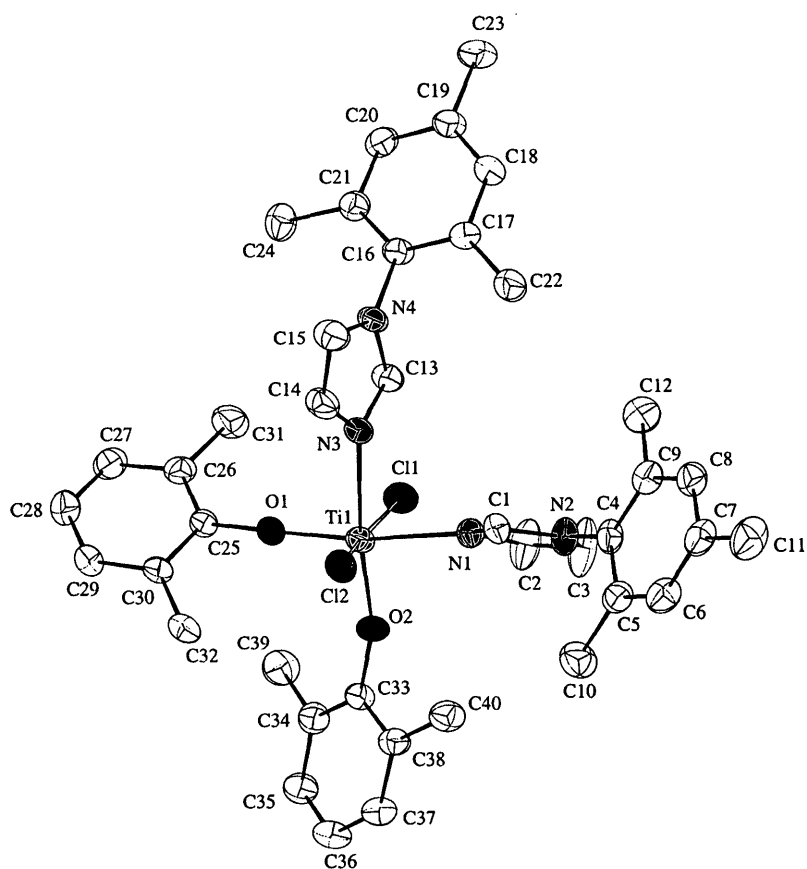


Figure 2.7. ORTEP plot (50% probability) of 2.8.

Hydrogen atoms are omitted for clarity.

2.2.6. Synthesis of $\text{TiCl}_2(2,6\text{-OC}_6\text{H}_4\text{O})(\text{C}^{\wedge}\text{Imine})$ (2.9)

Considering that the cis arrangement of chloride ligands is critical in the formation of active olefin polymerization catalysts, we decided to prepare the catecholate titanium complex, with the expectation that the desired cis-chloride isomer would be produced. Similar to our observations with compound **2.7**, attempts to treat $\text{TiCl}_4(\text{C}^{\wedge}\text{Imine})$ with one equivalent of $\text{Li}_2(2,6\text{-OC}_6\text{H}_4\text{O})$ under a variety of reaction conditions led to a mixture of reaction products. The $\text{TiCl}_2(2,6\text{-}$

OC₆H₄O)(THF)₂ metal precursor was thus prepared³⁵ and treated with one equivalent of C[^]Imine in toluene to give compound **2.9** in good yield (84%) as a dark red powder (Scheme 2). Compound **2.9**, like compound **2.7**, has a lower C=N stretching frequency ($\nu_{\text{C=N}}$ 1610 cm⁻¹) than that of the free carbene, suggesting that the ligand is also coordinating through the imine nitrogen.

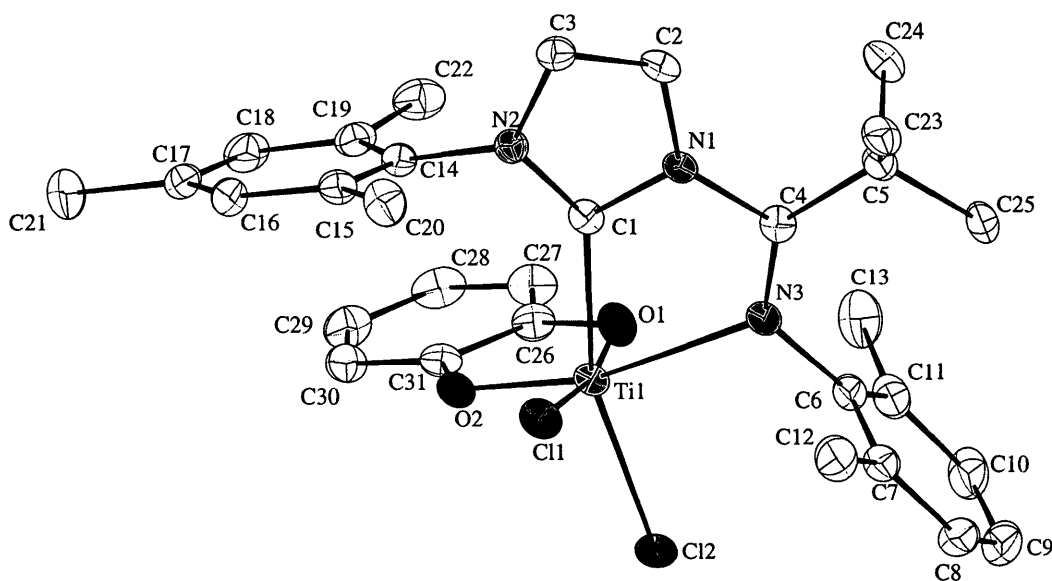


Figure 2.8. ORTEP plot (50% probability) of 2.9.

Hydrogen atoms and a pentane solvent molecule were omitted for clarity.

Crystals of **2.9** suitable for single crystal X-ray diffraction were successfully grown at -35 °C under nitrogen by slow liquid diffusion of pentane into a saturated CH₂Cl₂ solution. X-ray crystallographic analysis confirmed the coordination of the ligand through both the central imidazol-2-ylidene carbon and the imine nitrogen, with a slightly larger C1–Ti1–N3 bite angle (70.20(10)°) than that observed in **2.7**, a result of replacing two 2,6-dimethylphenoxide ligands with

the smaller bidentate 2,6-catecholate (Figure 2.8). This allows for the C[^]Imine ligand to be closer to the metal centre, resulting in shorter Ti1–C1 and Ti1–N3 bonds compared to those observed in **2.7**. As expected, the titanium centre adopts a pseudo-octahedral coordination geometry with bond angles about the metal centre ranging from 70.20(10) to 99.83(10)° (Table 1).

As observed for compound **2.7**, coordination of C[^]Imine results in an increase in the C=N bond length from 1.266(3) to 1.288(4) Å, which is in agreement with the related decrease in the C=N bond IR stretching frequency. The formation of the metallacycle leads to a yaw distortion of 9.0°. To our surprise, we did not see elongation of the Ti1–Cl2 bond from the trans influence of the strong σ -donating carbene. The Ti1–Cl1 and the Ti1–Cl2 bond lengths were determined to be 2.3427(9) and 2.3064(10) Å, respectively and the longer Ti1–Cl1 bond length could be a result of steric crowding of the catecholate ligand. The 2,6-dimethylphenyl and 2,4,6-trimethylphenyl rings are twisted 88.87° and 80.97° off the imidazol-2-ylidene ring, respectively. The catecholate and mesityl rings are approximately coplanar with C14 lying over O2, with an angle between the best planes formed by each ring of 7.94° and a C14–O2 distance of 3.388 Å. Lastly, the ipso carbon (C6) of the xylyl ring is in closer proximity to both Cl2 and C25, at 3.169 and 2.840 Å, respectively.

The solution ¹H NMR spectrum for compound **2.9** at room temperature was surprisingly more complicated than that of compound **2.7**. Broad resonances in the aromatic region at δ 6.41, 5.88 and 5.40 and in the benzylic region at δ

2.47 and 1.58, each respectively integrating to 3, 1, 1, 9 and 3 protons were observed. The broad resonance at δ 6.41 corresponds to the overlapping para and meta protons of the xylyl ring, while those at δ 5.88 and 5.40 are the inequivalent meta protons of the mesityl ring. The resonance at δ 2.47 corresponds to the broad ortho methyl protons of the xylyl ring and to one of the two ortho methyl groups of the mesityl ring, with the second set of inequivalent ortho methyl protons resonating at δ 1.58. The magnetic inequivalence of the protons for both the mesityl and xylyl rings, and the presence of broad resonances suggest restricted rotation for both aryl rings.

This was further supported by variable-temperature NMR experiments (Fig. 5). A ^1H NMR spectrum of **2.9** in CDCl_3 was acquired at 21 °C. The temperature was gradually increased and spectra were recorded at 5 °C intervals up to a final temperature of 50 °C. Both meta proton resonances of the mesityl ring at δ 5.88 and 5.40 coalesced at δ 5.63 at approximately 40 °C, with estimated values for the rate constant and the free energy of activation (ΔG^\ddagger) of 320 s^{-1} and 59 kJ mol^{-1} at coalescence, respectively. The NMR spectrum recorded at 50 °C showed further line sharpening of this resonance and of that assigned to the meta aromatic protons of the xylyl (δ 6.41). Interestingly, in addition to becoming sharper, the relative integration of the resonance at δ 2.47 decreased from the original 9 protons at room temperature to 6 protons at 50 °C, which were assigned to the methyl protons of the xylyl ring. The elevated temperature also resulted in broadening of the ortho methyl resonance from the

mesityl ring at δ 1.58, indicating the beginning of coalescence with the other resonance for the magnetically-inequivalent methyl protons at δ 2.47 (Figure 2.9).

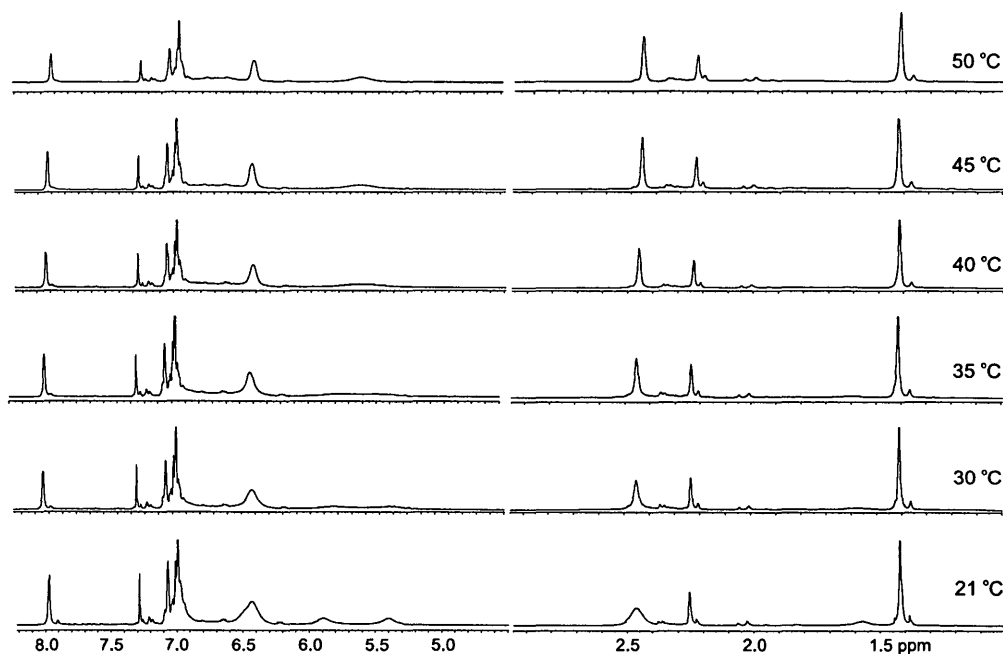


Figure 2.9. Selected regions of the ^1H NMR spectra (CDCl_3 , 300 MHz) of 2.9 at temperatures ranging from 21 to 50 °C.

The restricted rotation likely results from the sterics about the hexacoordinate metal centre introduced by both the ortho-substituted aryl rings, the large *tert*-butyl group and by the rigid bidentate catecholate ligand. While distances of the ipso carbon (C6 and C14) of both aryl rings to nearby atoms (*vide supra*) may suggest a greater energy barrier for rotation of the xylyl ring compared to that of the mesityl ring, our variable-temperature experiments clearly indicate otherwise. This is reasonable considering that the dianionic catecholate ligand produces a stiff chelate with the metal centre and that the

neutral iminic nitrogen atom (N3) forms a weaker and more labile dative bond with the metal centre. Upon restoring the temperature of the solution back to 25 °C, the original spectrum was restored, further supporting restricted rotation of both the xylyl and mesityl rings, and indicating no thermal decomposition.

2.2.7. Attempted Synthesis of $\text{TiCl}_2(=\text{N-R})(\text{C}^{\wedge}\text{Imine})$

In an attempt to further expand the library of potential catalysts, we decided to prepare the titanium imido dichloride complex. Reaction of two equivalents of *tert*-butylamine with $\text{TiCl}_4(\text{C}^{\wedge}\text{Imine})$ led to a mixture of reaction products despite the various reaction conditions and solvents (THF, dichloromethane, chloroform) investigated. Attempts to separate the components of the reaction mixture were unsuccessful. In all cases, the resulting spectra contained a number of unidentified species. All spectra interestingly showed the same two characteristic resonances of equal intensity at δ 8.6 and 8.3 also observed for the decomposition product **2.8**.

As a result, we decided to adopt the same strategy used in the preparation of **2.7** and **2.9** and to attempt simple ligand displacement reactions with titanium imido precursors containing a labile ligand. Thus, $\text{TiCl}_2(\textit{tert}\text{-butylimido})(\text{NHMe}_2)_2$, $\text{TiCl}_2(\textit{tert}\text{-butylimido})(\text{py})_3$, $\text{TiCl}_2(\textit{tert}\text{-butylimido})(\text{TMEDA})$ and $\text{TiCl}_2(\textit{tert}\text{-butylphenylimido})(\text{TMEDA})$ were prepared^{30,36} and each one was treated with one equivalent of $\text{C}^{\wedge}\text{Imine}$ in several solvents (THF, toluene, diethyl ether and chloroform) and at various reaction conditions. In all cases, a complex mixture of unidentified compounds was generated and attempts to isolate the components

were unsuccessful. The ^1H NMR spectra displayed the same distinctive downfield resonances reported above. We believe that upon coordination to the electropositive titanium centre, the C=N bond becomes more electrophilic and more susceptible to nucleophilic attack, thus resulting in decomposition. This decomposition pathway might be mitigated in compounds **2.7** and **2.9** thanks to the bulkier hexacoordinate metal centres and to the greater electron-donating capabilities of two phenoxide ligands, compared to one single imido ligand.

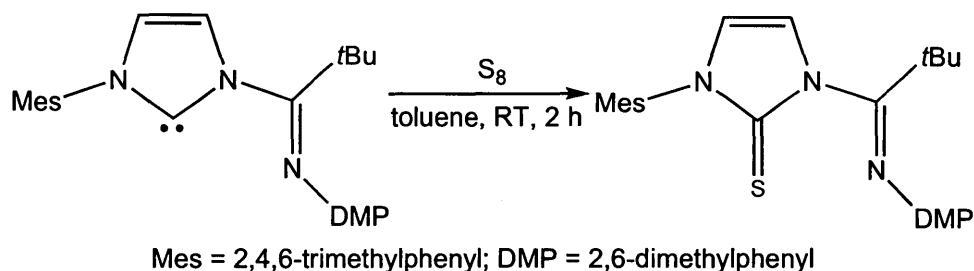
2.2.8. Ethylene polymerization catalysis

The catalytic activities of compounds **2.7** and **2.9** towards ethylene polymerization in toluene were studied at atmospheric pressure and room temperature in the presence of 1000 equivalents methylaluminoxane (MAO) as cocatalyst. In both cases, only trace amounts of polyethylene (PE) was recovered and no soluble waxes or low-molecular-weight oligomers were generated. In contrast, the parent $\text{TiCl}_4(\text{C}^{\wedge}\text{Imine})$ complex showed productivities of $40 \text{ kg PE} \cdot \text{mol M}^{-1} \cdot \text{h}^{-1}$.²⁹ Coordination of the iminic nitrogen (N3) to the more Lewis-acidic metal centre enhances the electrophilicity of the iminic carbon (C4) in compounds **2.7** and **2.9**, making it more susceptible to nucleophilic attack and to decomposition into complexes such as compound **2.8**, which was itself also found to be inactive in ethylene polymerization under comparable conditions.

2.3.1. Synthesis of S[^]Imine

In an attempt to gain further insight into the chemistry involving the aryl-substituted acyclic imino-*N*-heterocyclic carbene ligand, and possibly develop a

hard-soft, nitrogen-sulphur donor ligand, it was decided that synthetic investigations would be extended to prepare compound **2.10**. Treating C[^]imine with sulphur in a toluene solution afforded a spectroscopically pure, beige powder of compound **2.10** in good yield (85%) (Scheme 2.3).



Scheme 2.3: Synthetic strategy to forming compound **2.10**

The NMR spectroscopic analysis revealed an interesting ¹H NMR spectrum. It contained signals ranging from 6.83 ppm to 1.58 ppm. The resonances of the backbone hydrogens of the imidazol-2-ylidene appeared at 6.00 ppm and 5.63 ppm. The broad para methyl protons of mesityl (2.67 ppm) and the non-equivalence of the ortho methyl protons of mesityl ring (1.99 ppm and 1.61 ppm) suggest restricted rotation about the nitrogen-carbon bond of the imidazol-2-ylidene and the mesityl ring. The plausible scenario of restricted rotation was further reinforced by variable temperature NMR experiments. An NMR spectrum of **2.10** in C₆D₆ was acquired at 20 °C. The temperature was gradually increased to obtain spectra at 30 °C, 40 °C, 50 °C, 60 °C and 65 °C (Figure 4). Most noticeably, the mesityl ortho and para methyl signals began to broaden into the baseline at 30 °C and continued to broaden at 40 °C. Once the sample reached 50 °C, the para methyl proton signal began to reappear at 2.43

ppm and continued to sharpen at 60 °C and 65 °C. At 60 °C, the ortho methyl proton resonance begins to reappear as a broad singlet at 1.80 ppm and continued to sharpen at 65°C. As a result, the coalescence temperature was determined to be 60°C. The original spectrum was obtained once the temperature was restored to 20°C. The ¹³C NMR spectrum contained signals ranging from 163.4 ppm to 17.7 ppm. The central carbon of the imidazol-2-ylidene and imine carbon signals appeared at 163.4 ppm and 160.4 ppm, respectively.

Crystals suitable for X-ray diffraction analysis were grown at -35 °C under nitrogen by slow diffusion of pentane into a saturated THF solution (Figure 2.10). X-ray diffraction revealed the ligand adopts the Z-configuration in the solid state. The C1-S1 bond length was determined to be 1.6703(18) Å and is similar to previously reported sulphur-NHC compounds.

The S[^]Imine ligand was coordinated to gold(I) and was used to facilitate hydroamination reactions by another student within the Lavoie group.³⁷

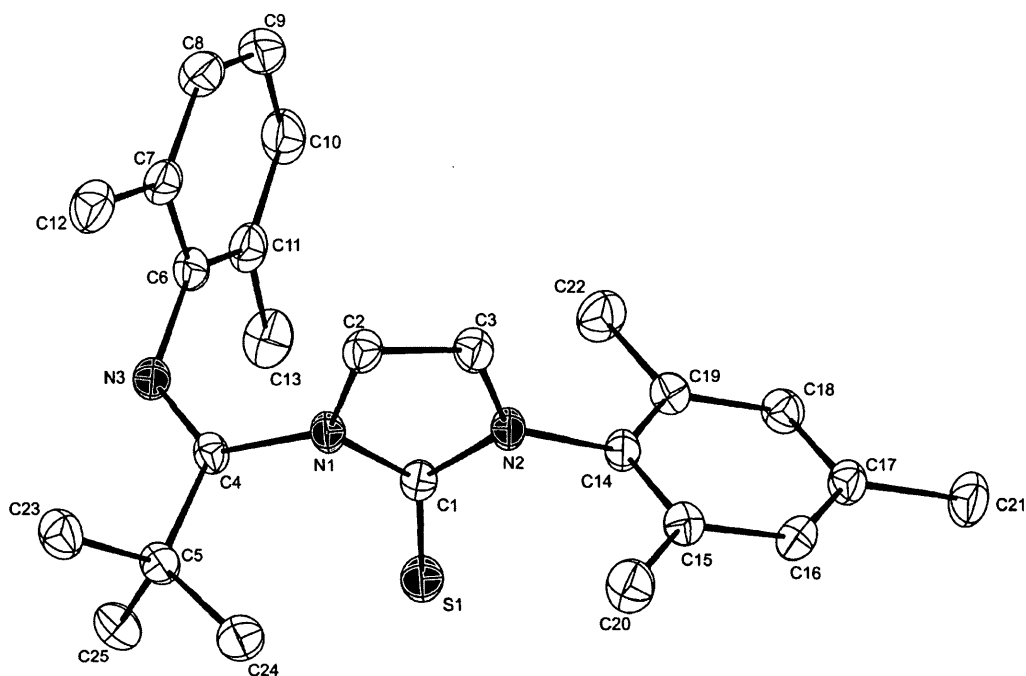


Figure 2.10: ORTEP plot (30% probability) of 2.10.

Hydrogen atoms and CH_2Cl_2 solvate omitted for clarity.

2.4.1. Conclusions

Group 4 and 6 transition metals bearing the aryl-substituted acyclic imino-*N*-heterocyclic carbene were synthesized, isolated and characterized. The catalytic activities during ethylene polymerization of all six complexes were explored. The zirconium and titanium complexes activities showed promise and warranted further tailoring of their coordination sphere. New aryloxo titanium complexes containing a bidentate imino-*N*-heterocyclic carbene were prepared as potential catalysts for olefin polymerization. The metal electronics and sterics about the metal centre were tuned through coordination of either two phenoxide ligands (**2.7**) or one catecholate ligand (**2.9**). NMR experiments revealed

restricted rotation of both aryl rings that are part of the imino-carbene ligand scaffold. The solid-state structure of both complexes was confirmed by X-ray diffraction studies. Attempts to make a related titanium imido complex failed, presumably due to the sensitivity of the imine group towards nucleophilic attack, as evidenced by the formation of the bis(imidazole) decomposition product **2.8**. The catalytic activities of the phenoxide complexes towards ethylene polymerization were assessed and found to be significantly lower than that previously reported for the tetrachloride complex. Compounds **2.7** and **2.9** were more susceptible to nucleophilic attack and to decomposition into complexes such as compound **2.8**, which was itself also found to be inactive in ethylene polymerization under comparable conditions. The reactivity of C[^]Imine towards sulphur was explored and resulted in a new ligand, S[^]Imine. X-ray quality crystals of this new ligand were grown and analyzed. Another student explored the coordination of this ligand with gold and the activity of that complex showed considerable activity towards hydroamination.

2.5. Experimental

2.5.1 General Comments

All manipulations were performed under a dinitrogen atmosphere in a drybox or using standard Schlenk techniques. Solvents used in the preparation of air and/or moisture sensitive compounds were dried using an MBraun Solvent Purification System fitted with alumina columns and stored over molecular sieves under a positive pressure of dinitrogen. Deuterated

solvents were degassed using three freeze-pump-thaw cycles. C₆D₆ and CDCl₃ were vacuum distilled from sodium and CaH₂, respectively, and stored under dinitrogen. NMR spectra were recorded on a Bruker DRX 600 (¹H at 600 MHz, ¹³C at 150.9 MHz), Bruker AV 400 (¹H at 400 MHz, ¹³C at 100 MHz) or Bruker AV 300 (¹H at 300 MHz, ¹³C at 75.5 MHz) spectrometer and are at room temperature unless otherwise stated. The spectra were referenced internally relative to the residual protio-solvent (¹H) and solvent (¹³C) resonances and chemical shifts were reported with respect to $\delta = 0$ for tetramethylsilane. A TA Model 2010 differential scanning calorimeter was used to measure the melting endotherm. The sample was first heated to 160 °C, quenched with liquid nitrogen, and then reheated to 160 °C at a rate of 20 °C/min. Elemental compositions and exact masses were determined by either ANALEST Laboratory of the University of Toronto or by Guelph Chemical Laboratories Inc. located in Guelph, Ontario.

All metal precursors were purchased from either BDH or Sigma-Aldrich. *N*-(2,6-Dimethylphenyl)acetamide was purchased from Sigma-Aldrich or Alfa Aesar and used without further purification. 1-(1-(2,6-Dimethylphenylimino)-2,2-dimethylpropyl)-3-(2,4,6-trimethylphenyl)imidazol-2-ylidene (C[^]Imine)²⁹, TiCl₄(THF)₂³⁸, ZrCl₄(THF)₂³⁸ and HfCl₄(THF)₂³⁸ were prepared using published procedures. TiCl₂(2,6-OC₆H₃-Me₂)₂(THF)₂ and TiCl₂(1,2-OC₆H₄O)(THF)₂ were prepared analogous to the literature procedure. The product was further purified by dissolving it in THF with subsequent precipitation from pentane to

yield the THF adduct^{35,39}. Deuterated NMR solvents were purchased from Cambridge Isotope Laboratories. MAO was graciously donated by Albemarle Corp.

2.5.2 Synthesis of TiCl₄(C[^]Imine) (2.1)

A vial was charged with C[^]Imine (243 mg, 0.650 mmol) and was dissolved in a minimal amount of THF (5 mL) and was added to a THF solution (2 mL) of TiCl₄(THF)₂ (212 mg, 0.634 mmol). The solution immediately darkened to a dark yellowish-brown and was allowed to stir at room temperature for 2.5 hours. Volatiles were removed under reduced pressure to yield a bright yellow solid that was washed with pentane (15 mL) to yield a spectroscopically pure powder (325 mg, 91%). Crystals suitable for X-ray diffraction study were grown at -35 °C under nitrogen by slow liquid diffusion of pentane into a saturated CH₂Cl₂ solution. ¹H NMR (400 MHz, CDCl₃): δ 7.93 (s, 1H, NCHCN_(mesityl)), 7.06 (s, 1H, NCCHN_(mesityl)), 7.03–6.99 (m, 3H, *p*-CH_(2,6-xylyl) + *m*-CH_(2,6-xylyl)), 6.96 (s, 2H, *m*-CH_(mesityl)), 2.50 (s, 6H, *o*-CH_{3(2,6-xylyl)}), 2.31 (s, 3H, *p*-CH_{3(mesityl)}), 2.28 (s, 6H, *o*-CH_{3(mesityl)}), 1.45 (s, 9H, (CH₃)₃C_(imine)); ¹³C{¹H} NMR (100 MHz, CDCl₃): δ 197.4 (NCN), 165.3 (C=N), 146.9 (C_(2,6-xylyl)), 140.2 (*p*-C_(mesityl)), 135.7 (*o*-C_(mesityl)), 134.8 (C_(mesityl)), 131.1 (*o*-C_(2,6-xylyl)), 129.3 (*m*-CH_(mesityl)), 128.3 (*m*-CH_(2,6-xylyl)), 126.7 (*p*-CH_(2,6-xylyl)), 122.9 (NCCN_(mesityl)), 120.0 (NCCN_(mesityl)), 40.9 (C_(imine)), 30.6 ((CH₃)₃C_(imine)), 21.4 (*o*-CH_{3(2,6-xylyl)}), 21.3 (*p*-CH_{3(mesityl)}), 18.9 (*o*-CH_{3(mesityl)}) FTIR (cast film) ν_{C=N} 1609 cm⁻¹. Anal. Calcd. for C₂₅H₃₁Cl₄N₃Ti x 0.5

CH₂Cl₂ (%): C, 53.02; H, 5.52 ; N, 7.40. Found (%): C, 52.68; H, 5.93; N, 7.31.

2.5.2 Synthesis of TiCl₃(C[^]Imine) (2.2)

Compound **2.2** was isolated as a purple solid according to the procedure described for **2.1**, using TiCl₃(THF)₃ as metal precursor and toluene as solvent. Yield: 97%. Crystals suitable for X-ray diffraction study were grown at room temperature under nitrogen by slow vapour diffusion of pentane into a saturated CH₂Cl₂ solution. FTIR (cast film) $\nu_{C=N}$ 1607 cm⁻¹. Anal. Calcd. for C₂₅H₃₁Cl₃N₃Ti · 1.0 THF (%): C, 58.06; H, 6.55; N, 7.00. Found (%): C, 57.77; H, 6.30; N, 6.81.

2.5.3 Synthesis of ZrCl₄(C[^]Imine) (2.3)

Compound **2.3** was isolated as a white solid according to the procedure described for **2.1**, using ZrCl₄(THF)₂ as metal precursor and toluene as solvent. Yield: 67%. Crystals suitable for X-ray diffraction study were grown at -35 °C under nitrogen by slow liquid diffusion of pentane into a saturated THF solution. ¹H NMR (400 MHz, CDCl₃): δ 7.98 (s, 1H, NCHCN_(mesityl)), 7.12 (s, 1H, NCCHN_(mesityl)), 7.06–7.04 (m, 3H, *p*-CH_(2,6-xylyl) + *m*-CH_(2,6-xylyl)), 7.00 (s, 2H, *m*-CH_(mesityl)), 2.50 (s, 6H, *o*-CH_{3(2,6-xylyl)}), 2.33 (s, 3H, *p*-CH_{3(mesityl)}), 2.25 (s, 6H, *o*-CH_{3(mesityl)}), 1.49 (s, 9H, (CH₃)₃C_(imine)); ¹³C{¹H} NMR (100 MHz, CDCl₃): δ 195.3 (NCN), 167.6 (C=N), 144.0 (C_(2,6-xylyl)), 140.6 (*p*-C_(mesityl)), 135.5 (C_(mesityl)), 134.4 (*o*-C_(mesityl)), 131.2 (*o*-CH_(2,6-xylyl)), 129.5 7 (*m*-CH_(mesityl)), 128.7 (*m*-C_(2,6-xylyl)), 127.1 (*p*-CH_(2,6-xylyl)), 123.6 (NCCN_(mesityl)), 121.0 (NCCN_(mesityl)), 41.6 (C_(imine)), 30.9 ((CH₃)₃C_(imine)), 22.6 (*p*-CH_{3(mesityl)}), 21.0 (*o*-

CH₃(*2,6*-xylyl), 18.6 (*o*-CH₃(mesityl)). FTIR (cast film) $\nu_{\text{C=N}}$ 1606 cm⁻¹. Anal. Calcd. for C₂₅H₃₁Cl₄N₃Zr (%): C, 49.50; H, 5.15; N, 6.93. Found (%): C, 47.35; H, 4.91; N, 6.30 (repeated microcombustion analyses of spectroscopically-pure material consistently gave low carbon values). HRMS (AccuTOF™-DART®): Calculated for C₂₅H₃₁Cl₄N₃Zr · C₁₂H₁₄N₂, m/z = 789.1476; Found: 789.1483.

2.5.4 Synthesis of HfCl₄(C[^]Imine) (2.4)

Compound **2.4** was isolated as a white solid according to the procedure described for **2.1**, using HfCl₄(THF)₂ as metal precursor and toluene as solvent. The complex was further purified by recrystallisation at -35 °C under nitrogen by slow liquid diffusion of pentane into a saturated CH₂Cl₂ solution. Yield: 73%. ¹H NMR (400 MHz, CDCl₃): δ 8.01 (s, 1H, NCHCN_(mesityl)), 7.11 (s, 1H, NCCHN_(mesityl)), 7.07–7.03 (m, 3H, *p*-CH_(2,6-xylyl) + *m*-CH_(2,6-xylyl)), 6.98 (s, 2H, *m*-CH_(mesityl)), 2.49 (s, 6H, *o*-CH₃(*2,6*-xylyl)), 2.32 (s, 3H, *p*-CH₃(mesityl)), 2.23 (s, 6H, *o*-CH₃(mesityl)), 1.48 (s, 9H, (CH₃)₃C_(imine)); ¹³C{¹H} NMR (100 MHz, CDCl₃): δ 201.6 (NCN), 168.5 (C=N), 143.7 (C_(2,6-xylyl)), 140.5 (*p*-C_(mesityl)), 135.5 (*o*-C_(mesityl)), 134.3 (C_(mesityl)), 131.5 (*o*-CH_(2,6-xylyl)), 129.4 (*m*-CH_(mesityl)), 128.7 (*m*-C_(2,6-xylyl)), 127.2 (*p*-CH_(2,6-xylyl)), 123.5 (NCCN_(mesityl)), 121.5 (NCCN_(mesityl)), 41.4 (C_(imine)), 30.9 ((CH₃)₃C_(imine)), 21.3 (*p*-CH₃(mesityl)), 21.1 (*o*-CH₃(*2,6*-xylyl)), 18.6 (*o*-CH₃(mesityl)). FTIR (cast film) $\nu_{\text{C=N}}$ 1604 cm⁻¹. Anal. Calcd. for C₂₅H₃₁Cl₄N₃Hf (%): C, 43.28; H, 4.50; N, 6.06. Found (%): C, 42.94; H, 4.71; N, 5.87.

2.5.5 Synthesis of CrCl₃(C[^]Imine)(THF) (2.5)

Compound **2.5** was isolated as a deep dark blue solid according to the procedure described for **2.1**, using CrCl₃(THF)₃ as metal precursor and THF as solvent. Yield: 89%. Crystals suitable for X-ray diffraction study were grown at room temperature under nitrogen by slow vapour diffusion of pentane into a saturated CH₂Cl₂ solution. FTIR (cast film) $\nu_{\text{C=N}}$ 1604 cm⁻¹. Anal. Calcd. for C₂₅H₃₁Cl₃N₃Cr · 1.0 THF (%): C, 57.67; H, 6.51; N, 6.96. Found (%): C, 57.39; H, 6.41; N, 7.20.

2.5.6 Synthesis of CrCl₂(C[^]Imine)(THF) (2.6)

Compound **2.6** was isolated as a blue solid according to the procedure described for **2.1**, using CrCl₂(THF)₃ as metal precursor and THF as solvent. The complex was further purified by recrystallisation at -35 °C under nitrogen by slow liquid diffusion of pentane into a saturated CH₂Cl₂ solution. Yield: 89%. FTIR (cast film) $\nu_{\text{C=N}}$ 1604 cm⁻¹. Anal. Calcd. for C₂₅H₃₁Cl₂N₃Cr · 1.0 THF (%): C, 61.26; H, 6.91; N, 7.39. Found (%): C, 60.89; H, 7.11; N, 7.58.

2.5.7. Synthesis of TiCl₂(2,6-OC₆H₃-Me₂)₂(C[^]Imine) (2.7)

A solution of C[^]Imine (107 mg, 0.287 mmol) dissolved in toluene (5 mL) was added to a toluene solution of TiCl₂(2,6-OC₆H₃-Me₂)₂(THF)₂ (145 mg, 0.287 mmol) and the dark red solution was stirred at room temperature for 4 h. Volatiles were removed under reduced pressure and the product was washed with pentane (15 mL) to yield a bright orange-red powder. A spectroscopically-pure product was acquired by recrystallisation from CH₂Cl₂ and pentane (172 mg,

82%). Crystals suitable for X-ray diffraction study were grown at $-35\text{ }^{\circ}\text{C}$ under nitrogen by slow liquid diffusion of pentane into a saturated CH_2Cl_2 solution. ^1H NMR (400 MHz, C_6D_6): δ 6.93 (d, $J = 2.0$, 1H, $\text{NCHCN}_{(\text{mesityl})}$), 6.77–6.49 (m, 9H, $p\text{-CH}_{(2,6\text{-xylyl})} + p\text{-CH}_{(\text{phenoxide})} + p\text{-CH}_{(\text{phenoxide})} + m\text{-CH}_{(2,6\text{-xylyl})} + m\text{-CH}_{(\text{phenoxide})} + m\text{-CH}_{(\text{phenoxide})}$), 6.47 (s, 2H, $m\text{-CH}_{(\text{mesityl})}$), 5.94 (d, $J = 2.0$, 1H, $\text{NCCHN}_{(\text{mesityl})}$), 2.58 (s, 6H, $o\text{-CH}_3_{(\text{phenoxide})}$), 2.55 (s, 6H, $o\text{-CH}_3_{(2,6\text{-xylyl})}$), 2.43 (s, 6H, $o\text{-CH}_3_{(\text{mesityl})}$), 2.41 (s, 6H, $o\text{-CH}_3_{(\text{phenoxide})}$), 1.84 (s, 3H, $p\text{-CH}_3_{(\text{mesityl})}$), 0.88 (s, 9H, $(\text{CH}_3)_3\text{C}_{(\text{imine})}$); $^{13}\text{C}\{^1\text{H}\}$ NMR (100 MHz, C_6D_6): δ 201.2 (NCN), 167.9 ($\text{C}_{\text{ipso}(\text{phenoxide})}$), 165.7 ($\text{C}_{\text{ipso}(\text{phenoxide})}$), 162.9 (C=N), 146.0 ($\text{C}_{\text{ipso}(2,6\text{-xylyl})}$), 139.8 ($p\text{-C}_{(\text{mesityl})}$), 135.6 ($o\text{-C}_{(\text{mesityl})}$), 131.6 ($o\text{-C}_{(2,6\text{-xylyl})}$), 131.2 ($o\text{-C}_{(\text{phenoxide})}$), 130.5 ($o\text{-C}_{(\text{phenoxide})}$), 129.7 ($m\text{-CH}_{(\text{mesityl})}$), 129.1 ($\text{C}_{\text{ipso}(\text{mesityl})}$), 129.0 ($m\text{-CH}_{(2,6\text{-xylyl})}$), 128.7 ($m\text{-CH}_{(\text{phenoxide})}$), 128.6 ($m\text{-CH}_{(\text{phenoxide})}$), 126.0 ($p\text{-CH}_{(2,6\text{-xylyl})}$), 122.1 ($p\text{-CH}_{(\text{phenoxide})}$), 121.7 ($\text{NCCN}_{(\text{mesityl})}$), 121.3 ($p\text{-CH}_{(\text{phenoxide})}$), 119.6 ($\text{NCCN}_{(\text{mesityl})}$), 40.7 ($(\text{CH}_3)_3\text{C}$), 30.2 ($(\text{CH}_3)_3\text{C}$), 22.0 ($o\text{-CH}_3_{(2,6\text{-xylyl})}$), 21.3 ($p\text{-CH}_3_{(\text{mesityl})}$), 20.5 ($o\text{-CH}_3_{(\text{phenoxide})}$), 19.8 ($o\text{-CH}_3_{(\text{mesityl})}$), 19.2 ($o\text{-CH}_3_{(\text{phenoxide})}$). FTIR (cast film) $\nu_{\text{C=N}}$ 1616 cm^{-1} . Anal. Calcd. for $\text{C}_{41}\text{H}_{49}\text{Cl}_2\text{N}_3\text{O}_2\text{Ti}$ (%): C, 67.03; H, 6.72; N, 5.72; Found (%): C, 66.84; H, 7.01; N, 5.69.

2.5.8 Synthesis of $\text{TiCl}_2(2,6\text{-OC}_6\text{H}_3\text{-Me}_2)_2(1\text{-}(2,4,6\text{-trimethylphenyl)imidazole})_2$ (2.8)

A solution of 1-(2,4,6-trimethylphenyl)imidazole (144 mg, 0.776 mmol) dissolved in toluene (5 mL) was added to a toluene solution of $\text{TiCl}_2(2,6\text{-OC}_6\text{H}_3\text{-Me}_2)_2(\text{THF})_2$ (196 mg, 0.388 mmol) and the dark red solution was stirred at room

temperature for 3 hours. Volatiles were removed under reduced pressure and the product was purified by multiple recrystallisations from CH_2Cl_2 and pentane (201 mg, 70%). ^1H NMR (400 MHz, CDCl_3): δ 8.18 (s, 2H, $\text{NCHN}_{(\text{mesityl})}$), 7.74 (s, 2H, $\text{NCCHN}_{(\text{mesityl})}$), 6.94 (s, 4H, $m\text{-CH}_{(\text{mesityl})}$), 6.87 (d, $J = 7.4$, 4H, $m\text{-CH}_{(\text{phenoxide})}$), 6.77 (s, 2H, $\text{NCHCN}_{(\text{mesityl})}$), 6.70 (t, $J = 7.4$, 2H, $p\text{-CH}_{(\text{phenoxide})}$), 2.33 (s, 18H, $o\text{-CH}_3_{(\text{phenoxide})}$, $p\text{-CH}_3_{(\text{mesityl})}$), 1.95 (s, 12H, $o\text{-CH}_3_{(\text{mesityl})}$); $^{13}\text{C}\{^1\text{H}\}$ NMR (100 MHz, CDCl_3): δ 166.4 ($\text{C}_{\text{ipso}(\text{phenoxide})}$), 141.2 (NCHN), 139.6 ($p\text{-C}_{(\text{mesityl})}$), 134.8 ($o\text{-C}_{(\text{mesityl})}$), 132.4 ($\text{C}_{\text{ipso}(\text{mesityl})}$), 130.8 (NCCN), 129.4 ($o\text{-C}_{(\text{phenoxide})}$), 129.2 ($m\text{-CH}_{(\text{mesityl})}$), 127.9 ($m\text{-CH}_{(\text{phenoxide})}$), 121.7 ($p\text{-CH}_{(\text{phenoxide})}$), 118.8 (NCCN), 21.0 ($p\text{-CH}_3_{(\text{mesityl})}$), 17.5 ($o\text{-CH}_3_{(\text{phenoxide})}$), 17.3 ($o\text{-CH}_3_{(\text{mesityl})}$). Anal. Calcd. for $\text{C}_{40}\text{H}_{46}\text{Cl}_2\text{N}_2\text{O}_2\text{Ti}$ (%): C, 65.49; H, 6.32 ; N, 7.64; Found (%): C, 65.72; H, 6.13; N, 7.77.

2.5.9. Synthesis of $\text{TiCl}_2(1,2\text{-OC}_6\text{H}_4\text{O})(\text{C}^{\wedge}\text{Imine})$ (2.9)

A solution of $\text{C}^{\wedge}\text{Imine}$ (150 mg, 0.401 mmol) dissolved in toluene (2 mL) was added to a toluene solution (5 mL) of $\text{TiCl}_2(1,2\text{-OC}_6\text{H}_4\text{O})(\text{THF})_2$ (149 mg, 0.401 mmol). The dark red solution was allowed to stir for 4 hours. The volume was reduced under reduced pressure and the product was precipitated with pentane. The supernatant was removed and the product was dried *in vacuo* to yield a dark red powder. An analytically-pure product was isolated by recrystallisation from CH_2Cl_2 and pentane (202 mg, 84%). Crystals suitable for X-ray diffraction study were grown at $-35\text{ }^\circ\text{C}$ under nitrogen by slow liquid diffusion of pentane into a saturated CH_2Cl_2 solution. ^1H NMR (400 MHz, CDCl_3): δ 7.93

(d, $J = 2.0$, 1H, $\text{NCHCN}_{(\text{mesityl})}$), 7.07 (d, $J = 2.0$, 1H, $\text{NCCHN}_{(\text{mesityl})}$), 7.03–6.99 (m, 4H, $\text{CH}_{(\text{aryl})}$), 6.41 (br s, 3H, $m\text{-CH}_{(2,6\text{-xylyl})}$, $p\text{-CH}_{(2,6\text{-xylyl})}$), 5.88 (br s, 1H, $m\text{-CH}_{(\text{mesityl})}$), 5.40 (br s, 1H, $m\text{-CH}_{(\text{mesityl})}$), 2.47 (br s, 9H, $o\text{-CH}_3_{(\text{aryl})}$), 2.24 (s, 3H, $p\text{-CH}_3_{(\text{mesityl})}$), 1.58 (br s, 3H, $o\text{-CH}_3_{(\text{aryl})}$), 1.43 (s, 9H, $(\text{CH}_3)_3\text{C}_{(\text{imine})}$); $^{13}\text{C}\{^1\text{H}\}$ NMR (100 MHz, CDCl_3): δ 197.2 (NCN), 166.9 (C=N), 158.7 ($\text{C}_{(\text{aryl})}$), 145.2 ($\text{C}_{(\text{aryl})}$), 139.4 ($p\text{-C}_{(\text{mesityl})}$), 134.8 ($\text{C}_{(\text{aryl})}$), 133.9 ($\text{C}_{(\text{aryl})}$), 129.3 ($m\text{-CH}_{(\text{mesityl})}$), 129.0 ($\text{C}_{(\text{aryl})}$), 128.3 ($m\text{-CH}_{(2,6\text{-xylyl})}$), 126.7 ($p\text{-CH}_{(2,6\text{-xylyl})}$), 123.8 ($\text{NCCN}_{(\text{mesityl})}$), 119.9 ($\text{NCCN}_{(\text{mesityl})}$), 111.2 ($o\text{-C}_{(\text{mesityl})}$), 40.7 ($(\text{CH}_3)_3\text{C}$), 30.4 ($(\text{CH}_3)_3\text{C}$), 21.0 ($p\text{-CH}_3_{(\text{mesityl})}$), 20.0 ($o\text{-CH}_3_{(\text{mesityl})}$), 19.0 ($o\text{-CH}_3_{(2,6\text{-xylyl})}$), 16.6 ($o\text{-CH}_3_{(\text{mesityl})}$). Not all ^{13}C assignments could be made due to poorly defined correlations from the broad resonances. FTIR (cast film) $\nu_{\text{C=N}}$ 1610 cm^{-1} . Anal. Calcd. for $\text{C}_{31}\text{H}_{35}\text{Cl}_2\text{N}_3\text{O}_2\text{Ti}$ (%): C, 62.01; H, 5.88 ; N, 7.00; Found (%): C, 61.78; H, 6.12; N, 6.47.

2.5.10. Synthesis of S^AImine (2.10)

Sulfur (12.7 mg, 0.395 mmol) was added as a solid to a solution (3 mL) of 1 (148 mg, 0.395 mmol) in toluene. The clear, light-yellow solution was allowed to stir for 2.5 h. Volatiles were removed under reduced pressure and the product was washed with pentane (3 x 5 mL) to yield a spectroscopically pure beige powder (136 mg, 0.334 mmol, 85 %). Crystals suitable for study by X-ray diffraction were grown at $-35\text{ }^\circ\text{C}$ under nitrogen by slow liquid diffusion of pentane into a saturated solution in THF. ^1H NMR (400 MHz, C_6D_6): δ 6.87–6.82 (m, 3H; $p\text{-CH}_{(2,6\text{-xylyl})}+m\text{-CH}_{(2,6\text{-xylyl})}$), 6.65 (d, $^3J=3.9\text{Hz}$, 2H; $m\text{-CH}_{(2,6\text{-xylyl})}$),

CH(mesityl)), 6.00 (d, $^3J=2.6\text{Hz}$, 1H; NCHCHN(mesityl)), 5.63 (s, $^3J= 2.6\text{ Hz}$, 1H; NCHCHN(mesityl)), 2.67 (brs, 3H; o-CH₃(2,6-xylyl)), 2.03–1.99 (m, 9H; o-CH₃(2,6-xylyl) + o-CH₃ (mesityl) + p-CH₃ (mesityl)), 1.61 (s, 3H; o-CH₃ (mesityl)), 1.58 ppm (s, 9H; C(CH₃)₃); ^{13}C NMR (100 MHz, CDCl₃): d = 163.4 (NCN), 160.0 (C=N), 145.4 (i-C(2,6-xylyl)), 136.4 (o-C(mesityl)), 135.8 (o- C(mesityl)), 133.6 (i-C(mesityl)), 129.3 (m-CH(mesityl)), 129.1 (m-C(mesityl)), 128.0 (m-CH(2,6-xylyl)), 123.7 (p-CH(2,6-xylyl)), 117.3 (NCCN(mesityl)), 115.0 (NCCN(mesityl)), 41.7 (C(CH₃)₃), 29.8(C(CH₃)₃), 20.9(p-CH₃(mesityl)), 19.5 (br s; o-CH₃(2,6-xylyl)), 17.9 (o-CH₃(mesityl)), 17.3 ppm (o-CH₃(mesityl)); FTIR (cast film): $\nu_{\text{C=N}} = 1660$, $\nu_{\text{C=S}} = 1204\text{ cm}^{-1}$; Elemental analysis calcd (%) for C₂₅H₃₁N₃S: C 74.03, H 7.70, N 10.36; found: C 74.13, H 7.56, N 10.38.

2.5.11. General Procedure for Ethylene Polymerization

Ethylene polymerization was performed at atmospheric pressure and room temperature in a 200-mL Schlenk flask containing a magnetic stir bar. The flask was conditioned in an oven at 160 °C for at least 12 h prior to use. The hot flask was brought to room temperature under dynamic vacuum, and back-filled with ethylene. This cycle was repeated a total of three times. Under an atmosphere of ethylene, the flask was charged with 20 mL of dry toluene and 1000 equivalents of methylaluminoxane (MAO). The solution was stirred for 15 min before a solution of the catalyst in toluene was introduced into the flask via a syringe. The reaction mixture was vigorously stirred for 10 min after the addition of the catalyst, and subsequently quenched with a 50:50 mixture of concentrated

hydrochloric acid and methanol. The resulting mixture was filtered and any solid collected was washed with distilled water. Solids collected were dried under vacuum at approximately 60 °C for several hours.

2.5.12. X-ray crystallographic studies

X-ray crystallographic data were collected at the University of Toronto on a Bruker-Nonius Kappa-CCD diffractometer using monochromated Mo-K α radiation ($\lambda = 0.71073 \text{ \AA}$) at 150 K and were measured using a combination of ϕ scans and ω scans with κ offsets, to fill the Ewald sphere. Intensity data were processed using the Denzo-SMN package⁴⁰. Absorption corrections were carried out using SORTAV.⁴¹ X-ray crystallographic data for compound **3** was collected at McMaster University on a Bruker APEX2 diffractometer using monochromated Mo-K α radiation ($\lambda = 0.71073 \text{ \AA}$) at 100 K and were measured using ϕ and ω scans. Unit cell parameters were determined using at least 50 frames from three different orientations. Data were processed using SAINT, and corrected for absorption with accurate face-indexing as well as redundant data (SADABS), and solved using direct methods and the SHELX program suite. The structures were solved and refined using SHELXTL V6.1⁴² for full-matrix least-squares refinement was based on F^2 . All H atoms were included in calculated positions and allowed to refine in riding-motion approximation with Uiso-tied to the carrier atom. Other crystallographic data (Tables of atomic coordinates with isotropic and anisotropic displacement parameters, bond lengths and angles) are provided as supplementary materials.

2.6. References

- 1 a) A. J. Arduengo, R. L. Harlow and M. Kline, *J. Am. Chem. Soc.* **1991**, *113*, 361; b) P. L. Arnold and I. J. Casely, *Chem. Rev.* **2009**, *109*, 3599; c) D. Bourissou, O. Guerret, F. P. Gabbaï and G. Bertrand, *Chem. Rev.* **1999**, *100*, 39; d) S. Díez-González, N. Marion and S. P. Nolan, *Chem. Rev.* **2009**, *109*, 3612; e) D. Enders, O. Niemeier and A. Henseler, *Chem. Rev.* **2007**, *107*, 5606; f) G. C. Fortman and S. P. Nolan, *Chem. Soc. Rev.* **2011**, *40*, 5151.
- 2 a) R. H. Crabtree, *J. Organomet. Chem.* **2005**, *690*, 5451; b) W. A. Herrmann, *Angew. Chem., Int. Ed.* **2002**, *41*, 1290; c) D. M. Khramov, V. M. Lynch and C. W. Bielawski, *Organometallics* **2007**, *26*, 6042.
- 3 a) E. Despagnet-Ayoub and T. Ritter in *N-Heterocyclic Carbenes as Ligands for Olefin Metathesis Catalysts, Vol. 21* Springer Berlin Heidelberg, **2007**, pp. 193; b) N. Marion and S. P. Nolan, *Acc. Chem. Res.* **2008**, *41*, 1440.
- 4 D. Takeuchi, *Dalton Trans.* **2010**, *39*, 311.
- 5 a) G. J. P. Britovsek, V. C. Gibson and D. F. Wass, *Angew. Chem., Int. Ed.* **1999**, *38*, 428; b) V. C. Gibson, C. Redshaw and G. A. Solan, *Chem. Rev.* **2007**, *107*, 1745; c) V. C. Gibson and S. K. Spitzmesser, *Chem. Rev.* **2003**, *103*, 283; d) W. Kaminsky, A. Funck and H. Hahnsen, *Dalton Trans.* **2009**, *0*, 8803; e) W. Kaminsky and A. Laban, *Appl. Catal., A* **2001**, *222*, 47; f) S. Park, Y. Han, S. K. Kim, J. Lee, H. K. Kim and Y. Do, *J. Organomet. Chem.* **2004**, *689*, 4263; g) D. W. Stephan, *Organometallics* **2005**, *24*, 2548.
- 6 Y. Yoshida, S. Matsui and T. Fujita, *J. Organomet. Chem.* **2005**, *690*, 4382.

- 7 H. Makio and T. Fujita, *Acc. Chem. Res.* **2009**, *42*, 1532.
- 8 a) D. McGuinness, *Dalton Trans.* **2009**, 6915; b) C. Bocchino, M. Napoli, C. Costabile and P. Longo, *J. Polym. Sci., Part A: Polym. Chem.* **2011**, *49*, 862; c) A. A. El-Batta and R. H. Grubbs, **2011**, pp. INOR; d) Y. Hu, G. M. Miyake, B. Wang, D. Cui and E. Y. X. Chen, *Chem. - Eur. J.* **2012**, *18*, 3345; e) I. G. Jung, Y. T. Lee, S. Y. Choi, D. S. Choi, Y. K. Kang and Y. K. Chung, *J. Organomet. Chem.* **2009**, *694*, 297; f) V. Khlebnikov, A. Meduri, H. Mueller-Bunz, B. Milani and M. Albrecht, *New J. Chem.* **2012**, *36*, 1552; g) J. Urbano, A. J. Hormigo, F. P. de, S. P. Nolan, M. M. Diaz-Requejo and P. J. Perez, *Chem. Commun. (Cambridge, U. K.)* **2008**, 759; h) D. Zhang, S. Zhou, Z. Li, Q. Wang and L. Weng, *Dalton Trans.* **2013**, *42*, 12020.
- 9 D. S. McGuinness, V. C. Gibson, D. F. Wass and J. W. Steed, *Journal of the American Chemical Society* **2003**, *125*, 12716.
- 10 L. K. Johnson, C. M. Killian and M. Brookhart, *J. Am. Chem. Soc.* **1995**, *117*, 6414.
- 11 a) G. J. P. Britovsek, V. C. Gibson, S. J. McTavish, G. A. Solan, A. J. P. White, D. J. Williams, G. J. P. Britovsek, B. S. Kimberley and P. J. Maddox, *Chem. Commun.* **1998**, *0*, 849; b) B. L. Small, M. Brookhart and A. M. A. Bennett, *J. Am. Chem. Soc.* **1998**, *120*, 4049.
- 12 a) G. J. P. Britovsek, M. Bruce, V. C. Gibson, B. S. Kimberley, P. J. Maddox, S. Mastroianni, S. J. McTavish, C. Redshaw, G. A. Solan, S. Strömberg, A. J. P. White and D. J. Williams, *J. Am. Chem. Soc.* **1999**, *121*, 8728; b) D. P. Gates, S.

A. Svejda, E. Oñate, C. M. Killian, L. K. Johnson, P. S. White and M. Brookhart, *Macromolecules* **2000**, *33*, 2320; c) S. S. Ivanchev, A. V. Yakimanskii and D. G. Rogozin, *Doklady Physical Chemistry* **2003**, *393*, 334; d) J. Kiesewetter, B. Arikan and W. Kaminsky, *Polymer* **2006**, *47*, 3302; e) S. Mecking, L. K. Johnson, L. Wang and M. Brookhart, *J. Am. Chem. Soc.* **1998**, *120*, 888; f) C. S. Popeney and Z. Guan, *Macromolecules* **2010**, *43*, 4091; g) D. J. Tempel, L. K. Johnson, R. L. Huff, P. S. White and M. Brookhart, *J. Am. Chem. Soc.* **2000**, *122*, 6686.

13 A. C. Badaj, S. Dastgir, A. J. Lough and G. G. Lavoie, *Dalton Trans.* **2010**, *39*, 3361.

14 J. A. Thagfi, S. Dastgir, A. J. Lough and G. G. Lavoie, *Organometallics* **2010**, *29*, 3133.

15 a) K. S. Coleman, S. Dastgir, G. Barnett, M. J. P. Alvite, A. R. Cowley and M. L. H. Green, *J. Organomet. Chem.* **2005**, *690*, 5591; b) S. Dastgir, K. S. Coleman, A. R. Cowley and M. L. H. Green, *Organometallics* **2005**, *25*, 300; c) M. Frøseth, K. A. Netland, C. Rømming and M. Tilset, *J. Organomet. Chem.* **2005**, *690*, 6125; d) K. A. Netland, A. Krivokapic, M. Schröder, K. Boldt, F. Lundvall and M. Tilset, *J. Organomet. Chem.* **2008**, *693*, 3703; e) K. A. Netland, A. Krivokapic and M. Tilset, *J. Coord. Chem.* **2010**, *63*, 2909; f) M. L. Rosenberg, A. Krivokapic and M. Tilset, *Organic Letters* **2008**, *11*, 547; g) M. L. Rosenberg, K. r. Vlašaná, N. S. Gupta, D. Wragg and M. Tilset, *J. Org. Chem.* **2011**, *76*, 2465.

16 T. Agapie, *Coord. Chem. Rev.* **2011**, *255*, 861.

- 17 K. C. Gupta and A. K. Sutar, *Coord. Chem. Rev.* **2008**, 252, 1420.
- 18 D. F. Wass, *Dalton Trans.* **2007**, 0, 816.
- 19 a) P. D. Bolton and P. Mountford, *Adv. Synth. Catal.* **2005**, 347, 355; b) S. Licciulli, I. Thapa, K. Albahily, I. Korobkov, S. Gambarotta, R. Duchateau, R. Chevalier and K. Schuhen, *Angew. Chem., Int. Ed.* **2010**, 49, 9225; c) L. A. MacAdams, G. P. Buffone, C. D. Incarvito, A. L. Rheingold and K. H. Theopold, *J. Am. Chem. Soc.* **2005**, 127, 1082; d) A.-S. Rodrigues and J.-F. Carpentier, *Coord. Chem. Rev.* **2008**, 252, 2137.
- 20 A. Bondi, *J. Phys. Chem.* **1964**, 68, 441.
- 21 a) C. D. Abernethy, G. M. Codd, M. D. Spicer and M. K. Taylor, *J. Am. Chem. Soc.* **2003**, 125, 1128; b) B. M. Gardner, J. McMaster and S. T. Liddle, *Dalton Trans.* **2009**, 6924; c) P. Shukla, J. A. Johnson, D. Vidovic, A. H. Cowley and C. D. Abernethy, *Chem. Commun.* **2004**, 360.
- 22 S. A. Mungur, A. J. Blake, C. Wilson, J. McMaster and P. L. Arnold, *Organometallics* **2006**, 25, 1861.
- 23 a) G. A. Bain and J. F. Berry, *J. Chem. Educ.* **2008**, 85, 532; b) D. F. Evans, *J. Chem. Soc.* **1959**, 2003.
- 24 a) P. Pyykkö and M. Atsumi, *Chem. Eur. J.* **2009**, 15, 186; b) B. Cordero, V. Gomez, A. E. Platero-Prats, M. Reves, J. Echeverria, E. Cremades, F. Barragan and S. Alvarez, *Dalton Trans.* **2008**, 2832.
- 25 S. P. Downing, S. C. Guadano, D. Pugh, A. A. Danopoulos, R. M. Bellabarba, M. Hanton, D. Smith and R. P. Tooze, *Organometallics* **2007**, 26, 3762.

- 26 a) C. Lorber and L. Vendier, *Dalton Trans.* **2009**, 6972; b) D. Zhang, H. Aihara, T. Watanabe, T. Matsuo and H. Kawaguchi, *J. Organomet. Chem.* **2007**, 692, 234.
- 27 a) N. Hazari and P. Mountford, *Acc. Chem. Res.* **2005**, 38, 839; b) K. Nomura, S. Hasumi, M. Fujiki and K. Itagaki, *Dalton Trans.* **2009**, 9052.
- 28 a) N. R. d. S. Basso, P. P. Greco, C. L. P. Carone, P. R. Livotto, L. M. T. Simplicio, R. Z. N. da, G. B. Galland and S. J. H. Z. dos, *J. Mol. Catal. A: Chem.* **2007**, 267, 129; b) J.-B. Cazaux, P. Braunstein, L. Magna, L. Saussine and H. Olivier-Bourbigou, *Eur. J. Inorg. Chem.* **2009**, 2942; c) P. M. Gurubasavaraj and K. Nomura, *Inorg. Chem.* **2009**, 48, 9491; d) K. Itagaki, K. Kakinuki, S. Katao, T. Khamnaen, M. Fujiki, K. Nomura and S. Hasumi, *Organometallics* **2009**, 28, 1942; e) K. Nomura, *Dalton Trans.* **2009**, 8811; f) C. Redshaw, *Dalton Trans.* **2010**, 39, 5595; g) J. A. Suttill, D. S. McGuinness, M. Pichler, M. G. Gardiner, D. H. Morgan and S. J. Evans, *Dalton Trans.* **2012**, 41, 6625.
- 29 T. G. Larocque, A. C. Badaj, S. Dastgir and G. G. Lavoie, *Dalton Trans.* **2011**, 40, 12705.
- 30 A. J. Nielson, C. Shen, P. Schwerdtfeger and J. M. Waters, *Eur. J. Inorg. Chem.* **2005**, 1343.
- 31 H. Yasuda, Y. Nakayama, K. Takei, A. Nakamura, Y. Kai and N. Kanehisa, *J. Organomet. Chem.* **1994**, 473, 105.
- 32 H.-M. Gau, C.-S. Lee, C.-C. Lin, M.-K. Jiang, Y.-C. Ho and C.-N. Kuo, *J. Am. Chem. Soc.* **1996**, 118, 2936.

- 33 P. Pyykkö and M. Atsumi, *Chem. Eur. J.* **2009**, *15*, 12770.
- 34 A. C. Badaj and G. G. Lavoie, *Organometallics* **2012**, *31*, 1103.
- 35 A. Flamini, D. J. Cole-Hamilton and G. Wilkinson, *J. Chem. Soc., Dalton Trans.* **1978**, 454.
- 36 A. J. Blake, P. E. Collier, S. C. Dunn, W.-S. Li, P. Mountford and O. V. Shishkin, *J. Chem. Soc., Dalton Trans.* **1997**, 1549.
- 37 E. Alvarado, A. C. Badaj, T. G. Larocque and G. G. Lavoie, *Chemistry – A European Journal* **2012**, *18*, 12112.
- 38 L. E. Manzer, *Inorg. Synth.* **1982**, *21*, 135.
- 39 S. A. Waratuk, M. G. Thorn, P. E. Fanwick, A. P. Rothwell and I. P. Rothwell, *J. Am. Chem. Soc.* **1999**, *121*, 9111.
- 40 Z. Otwinowski and W. Minor, *Methods Enzymol.* **1997**, *276*, 307.
- 41 R. H. Blessing, *Acta Crystallogr., Sect. A: Found. Crystallogr.* **1995**, *A51*, 33.
- 42 G. M. Sheldrick, *Acta Crystallogr., Sect. A: Found. Crystallogr.* **2008**, *A64*, 112.

Chapter 3 Imidazol-2-imine Ethenolate Ligand: Synthesis and Coordination

3.0 Preface

This chapter is comprised of a reformatted and slightly modified peer-reviewed journal publication. Reproduced with permission from Coordination and reactivity study of titanium and zirconium complexes of the first imidazol-2-imine ethenolate ligand; T. G. Larocque, S. Dastgir, G. G. Lavoie, *Organometallics*, 32 (15), 4314–4320 DOI: 10.1021/om4004708. Copyright 2013 American Chemical Society. All work was performed by myself, excluding the synthesis and characterization of **3.1**, **3.3**, **3.4₁** and **3.4₂** and the computational work.

3.1 Introduction

As discussed in Chapter 1, the reactivity of NHCs towards azides has been explored, generating a new class of anionic imidazol-2-imate ligands that are analogous to the phenoxides.¹ Thanks to the stability of imidazolium salts, these imidazol-2-imates can exist in different mesomeric forms with unexpectedly high electron density located on the exocyclic nitrogen (Figure 3.1). Several groups have recently explored the possibility to utilize imidazol-2-imates either as ancillary monodentate monoanionic ligands,¹ or as neutral fragment incorporated in more complex bidentate and tridentate ligand scaffolds.^{1b,2}

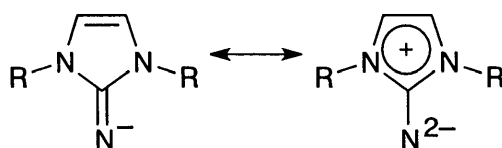
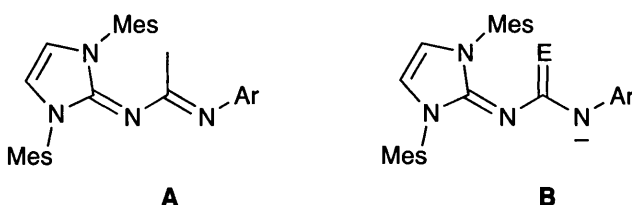


Figure 3.1. Mesomeric structures of substituted imidazole-2-iminate.



Ar = 2,6-dimethylphenyl, Ar' = 4-methylphenyl; E = O, S

Figure 3.2. Neutral (A) and anionic (B) bidentate ligands with an imidazol-2-imine fragment.

Our group has reported the synthesis of neutral imine imidazol-2-imine ligands (**A**, Figure 3.2) and their coordination to titanium(IV) and palladium(II).³ Structure characterization of these complexes showed two different binding modes depending on the metal centre.^{3a} While the ligand coordinates to Ti(IV) in the expected N[^]N chelate, the use of Pd(II) led to the formation of a dimeric structure with monodentate coordination of the ligand to the metal through the terminal imine nitrogen. To enforce coordination of the ligand in a bidentate fashion to both early and late transition metals, we recently reported the related *anionic* ureate and thioureate ligands (**B**, Figure 3.2).⁴

Other bidentate monoanionic systems, and most notably the substituted salicylaldimine ligands, have proven to be extremely versatile and have led to

highly active olefin polymerization catalysts based on both early and late transition metals. Studied by Fujita⁵ and Grubbs,⁶ these salicylaldimine ligands coordinate to the metal through the neutral imine nitrogen and anionic oxygen atoms (Figure 3.3). It is important to note that the salicylaldimine ligands are not the only example of a highly active homogeneous catalysts bearing a bidentate N-O ancillary ligand. In recent decades, Laurel Schafer has shown the usefulness of amidate ligands on transition metals to facilitate hydroamination, hydroaminoalkylation and amidation of aldehydes.⁷

While the new anionic ureate and thioureate ligands **B** coordinated to both early and late transition metals, thereby successfully addressing the shortcomings of the first-generation neutral ligand system **A**, both the desired $N_{p\text{-tolyl}}^{\wedge}N_{\text{imidazol-2-ylidene}}$ and the undesired $N_{p\text{-tolyl}}^{\wedge}E$ ($E = O, S$) chelates, with an uncoordinated imidazol-2-imine fragment, were observed. Inspired by the salicylaldimine system, we decided to design a new ligand scaffold that could bind to the metal centre in a bidentate fashion exclusively through a *neutral* imine nitrogen donor and an *anionic* oxygen donor. As such, the new ligand scaffold combines an imidazol-2-imine fragment, as the neutral nitrogen donor, and an enolate, as the anionic oxygen donor. The synthesis of these new substituted $N^{\wedge}O$ ligands, their coordination to group 4 metals and the potential of the resulting complexes as ethylene polymerization catalysts are reported.

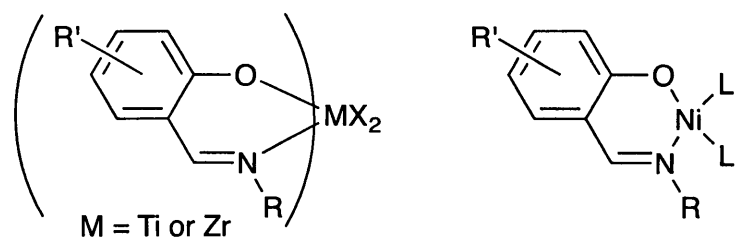
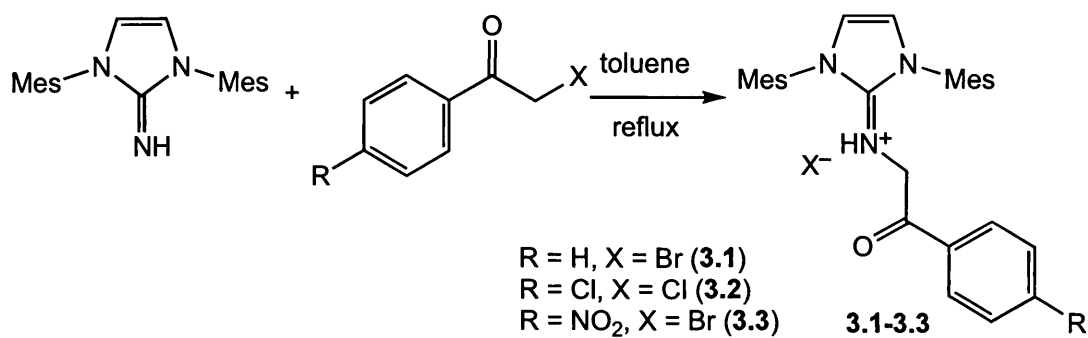


Figure 3.3. Early and late transition metal complexes of the salicylaldimine ligand system.

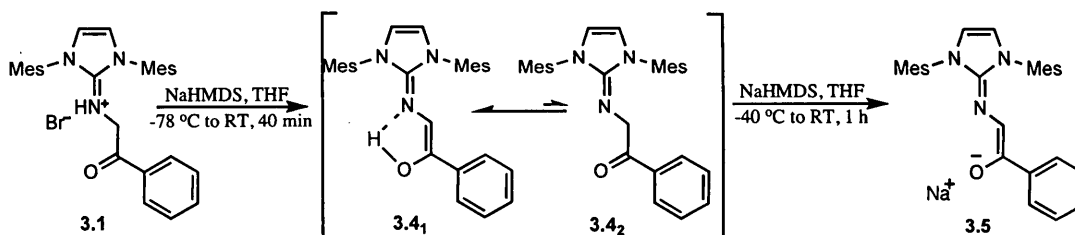
3.2 Results and Discussion



Scheme 3.1. Synthesis of 2-(1,3-Bis(2,4,6-trimethylphenyl)imidazol-2-imino)-1-arylethanone Hydrochloride (3.1–3.3)

The ketone imidazol-2-imine ligand precursors **3.1–3.3** were prepared in good yield (75–89%) by refluxing a toluene solution of 1,3-bis(2,4,6-trimethylphenyl)imidazol-2-imine⁴ with the corresponding 2-halo-1-arylethanone for 12 h (Scheme 3.1). Solution NMR spectra for compounds **3.1–3.3** are

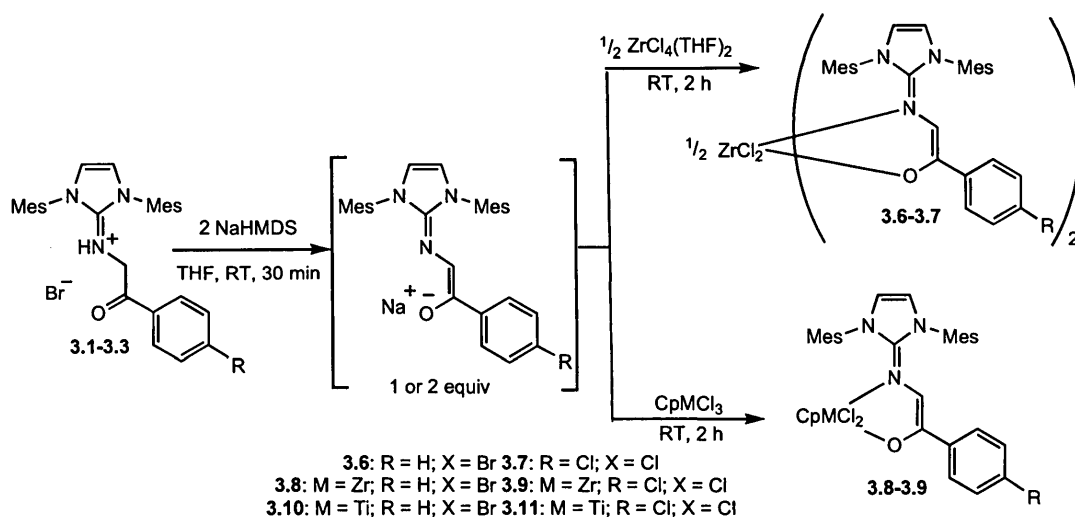
consistent with their expected structure. All ^1H and ^{13}C resonances were assigned using a series of one- and two-dimensional ^1H and ^{13}C NMR experiments, including heteronuclear single quantum correlation (HSQC) and heteronuclear multiple bond correlation (HMBC) techniques. The characteristic iminic proton for **3.1–3.3** appears at δ 7.99, 9.71 and 8.26, respectively, as a triplet, coupled to two vicinal methylene protons ($^3J = 6.4\text{--}6.9$ Hz). These methylene protons and those of the imidazole backbone resonate at approximately δ 4.5 and 6.7, respectively.



Scheme 3.2. Sequential Deprotonation of 3.1 to Generate a Tautomeric Mixture of 2-(1,3-Bis(2,4,6-trimethylphenyl)imidazol-2-imine)-1-phenylethanone (3.4₁ and 3.4₂) and the Corresponding Ethenolate (3.5)

Deprotonation of compound **3.1** with one equivalent of sodium hexamethyldisilazide (NaHMDS) gave a mixture of two tautomers, **3.4₁** and **3.4₂**, in a 3:1 ratio (Scheme 3.2). The major tautomer was identified spectroscopically as the enol (**3.4₁**), with the characteristic vinyl proton and the corresponding carbon nucleus resonating, respectively, at δ 6.39 and 108.6 in chloroform-*d*. The methylene protons of the corresponding minor keto tautomer (**3.4₂**) were observed as a singlet at a lower frequency (δ 4.40), integrating to two protons,

with the α -carbon atom resonating at δ 54.5. Further deprotonation of the tautomeric mixture **3.4** with an additional equivalent of NaHMDS gave **3.5**, as a single molecule, in 87% yield (Scheme 2). The proton on the α -carbon atom resonates downfield at δ 6.21 (C_6D_6), with the carbon nucleus observed in the expected vinyl region of the spectrum at δ 103.8.



Scheme 3.3. Synthesis of Titanium and Zirconium Complexes of the Bis(imine ethenolate) Ligand.

The sodium ethenolate salt **3.5** could also be prepared directly by addition of two equivalents of base to **3.1**, and used with no further purification in the preparation of titanium and zirconium complexes. Thus, addition of two equivalents of NaHMDS at -40 °C to a THF suspension of compound **3.1**, with subsequent warming to room temperature, resulted in an intense yellow solution of **3.5**. Without further purification, the sodium ethenolate solution was added to a THF solution of $ZrCl_4(THF)_2$ in a 2:1 stoichiometric ratio, resulting in the

immediate precipitation of the desired bis(imine ethenolate) zirconium dichloride complex **3.6** as a yellow solid in moderate yield (60%) (Scheme 3.3). Similarly, the *para*-chloro derivative **3.7** could also be prepared from, albeit in slightly lower yield (42%). Attempts to synthesize the *p*-nitrophenyl analogue from **3.3** resulted in a mixture of reaction products that could not be successfully isolated.

Compounds **3.6** and **3.7** were characterized by NMR spectroscopy and combustion analysis. The ^1H NMR spectrum (CDCl_3) of **3.6** contained only one set of resonances, indicating the selective generation of a single isomer with two sets of ligands that are magnetically equivalent. As expected, the NMR spectrum of **3.6** no longer displays the distinctive triplet at δ 7.99 corresponding to the imine proton of **3.1**. A singlet observed at δ 5.91 for the vinylic protons of the ligand, integrating to two protons (one proton for each set of ligand), is consistent with double deprotonation of **3.1** and coordination to zirconium. Theazole ring backbone protons resonate at δ 6.59 as a singlet integrating to four protons (two protons for each set of ligand). As observed for compound **3.6**, the ^1H and ^{13}C NMR spectra of **3.7** show only one set of resonance for the enolate ligands, indicating the generation of a single coordination isomer. Although the structure of neither **3.6** nor **3.7** could be confirmed by X-ray diffraction studies, based on zirconium work using ureate and thioureate ligands⁴ and substituted salicylaldimine ligands,⁸ we would expect the chloride atoms to adopt a *cis* conformation, with both enolate ligands coordinated to the metal with the oxygen atoms *trans* to each other. However, in bis(salicylaldimine) metal complexes

with sterically-demanding substituents on the imine nitrogen, a *trans-N/cis-O/cis-Cl* isomer is in fact preferred.^{8b,9} Considering that our ethenolate ligand bears most of the bulk on the nitrogen atom, we think that complexes **3.6** and **3.7** may also adopt a *trans-N/cis-O/cis-Cl* arrangement. This is supported by DFT (B3LYP/LanL2DZ) calculations on compound **3.6**, which predicts this isomer to be 12.6 kcal/mol more stable than the corresponding *cis-N/trans-O/cis-Cl* isomer. Attempts to prepare the related titanium complexes using the same methodology only led to mixtures of species, possibly coordination isomers, which could not be isolated and characterized.

Cyclopentadienyl (imine ethenolate) complexes of zirconium (**3.8-3.9**) and titanium (**3.10-3.11**) were prepared by adding the ethenolate salt, prepared in situ by double deprotonation of **3.1-3.3** with NaHMDS, to CpMCl₃ (Scheme 3.3). The zirconium complexes **3.8** and **3.9** were isolated as yellow solids in 47 and 59% yield, respectively. The ¹H NMR spectra of both complexes showed characteristic resonances of the ethenolate ligand, with an additional resonance for the cyclopentadienyl protons at δ 6.0 in chloroform-*d*, integrating to five protons.

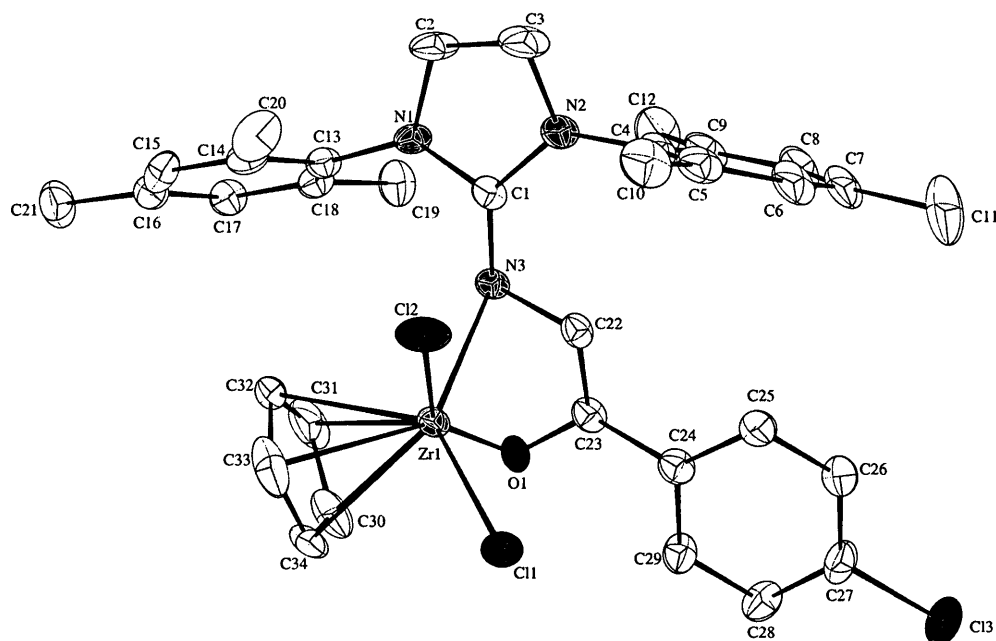


Figure 3.4. ORTEP plot (50% probability) of 3.9. Only one of two independent molecules found in the asymmetric unit cell is drawn. Hydrogen atoms and diethyl ether were omitted for clarity.

Crystals of compound **3.9** suitable for X-ray diffraction studies were grown at $-35\text{ }^{\circ}\text{C}$ under nitrogen by slow liquid diffusion of diethyl ether into a saturated CH_2Cl_2 solution. Compound **3.9** crystallizes in the $P2_1/n$ space group and exhibits a distorted piano stool geometry with the cyclopentadienyl ligand adopting an η^5 hapticity (Figure 3.4; Table 3.1). As expected, the ligand coordinates in a bidentate fashion through the imine nitrogen and ethenolate oxygen atoms. The formation of a 5-membered metallacycle leads to an O1–Zr–N3 bite angle of $75.92(9)^{\circ}$, which is significantly larger than that observed for the 4-membered metallacycle formed in $\text{Ti}(\text{IMesN}^{\wedge}\text{Imine})\text{Cl}_4$ ($60.50(12)^{\circ}$). The cyclopentadienyl

ligand is asymmetrically bound to zirconium, with Zr–C bond lengths ranging from 2.481(4) to 2.534(4) Å, with shorter bonds anti to the chloride atoms and longer ones anti to the imine ethenolate donor atoms. The mesityl rings of ligand are almost orthogonal to the best plane formed by the imidazol-2-imine ring, at 84.36° and 70.21°, respectively.

The *p*-chlorophenyl andazole rings slightly deviate by 9.1° and 17.9°, respectively, from coplanarity with the best plane formed by N3, C22, C23 and O1, possibly indicating little electron delocalization from the imidazole ring to the exocyclic atoms (N3, C22, C23 and O1). However, the C1–N3 bond is only slightly shorter than C1–N1, C1–N2 and C22–N3.

Table 3.1. Selected bond lengths and bond angles for compound 3.9^a

Selected Bond Lengths (Å)		Selected Bond Angles (deg)	
Zr1–Cl1	2.4626(10)	O1–Zr1–N3	75.92(9)
Zr1–Cl2	2.4995(9)	O1–Zr1–Cl1	90.80(7)
Zr1–O1	2.059(2)	N3–Zr1–Cl1	131.58(7)
Zr1–N3	2.276(3)	O1–Zr1–Cl2	145.06(7)
Zr1–C30	2.521(4)	N3–Zr1–Cl2	79.70(7)
Zr1–C31	2.492(4)	Cl1–Zr1–Cl2	86.95(4)
Zr1–C32	2.481(4)	Zr1–N3–C1	141.00(2)
Zr1–C33	2.503(4)	Zr1–N3–C22	83.15(2)
Zr1–C34	2.534(4)	Zr1–O1–C23	92.15(2)
N1–C1	1.363(4)	C1–N3–C22	118.65(3)
N2–C1	1.377(4)	N3–C22–C23	119.25(3)
N3–C1	1.332(4)	C22–C23–O1	117.20(3)
N3–C22	1.413(4)		
C22–C23	1.357(5)		
O1–C23	1.356(4)		

^a Average bond lengths and angles for both molecules present in the asymmetric unit cell

Furthermore, the length of these bonds, as well as those for C22–C23 and O1–C23, are all intermediate to those expected for single and double bonds,¹⁰

indicating significant bond conjugation. Interestingly, despite the relatively long Zr1–C22 and Zr1–C23 distances (2.5 Å), the position of zirconium with respect to the ethenolate ligand in fact resembles that of metal bound to an η^4 -1,4-butadiene ligand, perhaps another manifestation of the double bond character between N3 and C22, and O1 and C23, which would arise from electron delocalization from the imidazole ring through the conjugated system.

While the effect of steric from the bulky imidazole ring cannot be ruled out, the weaker coulombic interactions between the formally charged metal centre and the neutral nitrogen donor, in contrast to the negatively charged oxygen atom, likely accounts for the longer Zr1–N3 bond (2.276(3) Å), compared to Zr1–O1. Furthermore, π -donation of the oxygen atom to the Lewis acidity metal centre leads to a Zr–O1 bond length of 2.059(2), which is intermediate between those for Zr–O single (2.17 Å) and Zr=O double (1.84 Å) bonds.¹⁰

Addition of one equivalent of sodium ethenolate, prepared in situ, to CpTiCl₃ resulted in an immediate color change of the THF solution from yellow to deep blue, indicative of a ligand-to-metal charge transfer, with formation of complexes **3.10** and **3.11** in 74 and 56% yield, respectively. NMR spectra of both complexes are in agreement with their structure, with resonances and chemical shifts similar to those observed for compounds **3.8** and **3.9**. Attempts to prepare the cyclopentadienyl zirconium and titanium complexes of the *p*-nitrophenyl derivative resulted in a mixture of reaction products that could not be successfully isolated.

All titanium and zirconium complexes were evaluated for their activity in ethylene polymerization. Complexes were activated with methylaluminoxane (MAO) as cocatalyst in toluene, at room temperature and at one atmosphere of ethylene. While all four zirconium complexes gave only trace amounts of polyethylene, titanium complex **3.10** gave polymer at a moderate rate of 110 kg PE mol cat⁻¹ h⁻¹. The small electronic perturbation arising from replacing the para hydrogen atom with the more electronegative chlorine atom led to a slight enhancement in catalytic activity for complex **3.11** (170 kg PE mol cat⁻¹ h⁻¹). These activities favorably compare to the best ones reported by Lancaster and Bochmann for a series of titanium and zirconium cyclopentadienyl salicylaldiminate complexes.¹¹ While they are also comparable to those reported for bis(salicylaldiminate)ZrCl₂ complexes that have small alkyl substituents on the phenol ring, these activities are orders of magnitude lower than those of related complexes with larger *tert*-butyl, adamantyl and cumyl groups.¹⁴ The lower activity observed in our complexes may therefore be a result of an unoptimized substitution pattern on the ethenolate ligand. Alternatively, it may also be a result of either the different ligand arrangement (*trans*-N/*cis*-O/*cis*-Cl vs. *cis*-N/*trans*-O/*cis*-Cl) or of a lesser electrophilic metal centre, a result of electron delocalization from the imidazole ring to the exocyclic nitrogen atom.^{1e,3-4}

3.3. Conclusions

The synthesis of a new monoanionic bidentate ligand structure that incorporates the electron-rich imidazol-2-imine fragment was reported for the first

time, and coordinated to zirconium and titanium. Bis(ethenolate) and (cyclopentadienyl)(ethenolate) metal dichloride complexes were successfully prepared and fully characterized. The solid-state structure of the cyclopentadienyl zirconium complex **3.9** confirmed the targeted bidentate coordination of the ligand, resulting in a four-legged piano stool configuration. The synthesis of the bis(imine ethenolate) zirconium dichloride complexes furthermore proved to be very selective, with the formation of one single highly symmetric molecule. While all zirconium complexes tested showed no activity in ethylene polymerization, both titanium complexes **3.10** and **3.11** were effective catalysts at room temperature, with activities up to 170 kg PE mol cat⁻¹ h⁻¹. A decrease in the electron-donating capabilities of the ligand through the inductive effect of a more electronegative chlorine atom led to enhanced catalyst activities. Work on determining the effect of other ligand substitution patterns on catalyst performance will be reported in due course.

3.4. Experimental

3.4.1. General Considerations

All manipulations were performed under a dinitrogen atmosphere in a drybox or using standard Schlenk techniques. Solvents used in the preparation of air and/or moisture sensitive compounds were dried using an MBraun Solvent Purification System fitted with alumina columns and stored over molecular sieves under a positive pressure of argon. Toluene for polymerization was distilled under argon after being dried with the MBraun SPS. Deuterated solvents were

degassed using three freeze-pump-thaw cycles. C_6D_6 and $CDCl_3$ were vacuum distilled from sodium and CaH_2 , respectively, and stored under dinitrogen. NMR spectra were recorded on a Bruker DRX 600 (1H at 600 MHz, ^{13}C at 150.9 MHz), Bruker AV 400 (1H at 400 MHz, ^{13}C at 100 MHz) or Bruker AV 300 (1H at 300 MHz, ^{13}C at 75.5 MHz) spectrometer and are at room temperature unless otherwise stated. The spectra were referenced internally relative to the residual protio-solvent (1H) and solvent (^{13}C) resonances and chemical shifts were reported with respect to $\delta = 0$ for tetramethylsilane. Elemental compositions were determined by Guelph Chemical Laboratories Inc. located in Guelph, Ontario.

All metal precursors were purchased from either BDH or Sigma-Aldrich. All acetophenones and NaHMDS were purchased from Sigma-Aldrich and used as received. Deuterated NMR solvents were purchased from Cambridge Isotope Laboratories. MAO was graciously donated by Albemarle Corp. Lastly, 1,3-bis(2,4,6-trimethylphenyl)imidazol-2-imine^{1c} and $ZrCl_4(THF)_2$ ¹² were prepared using published procedures.

3.4.2. General procedure for the synthesis of 2-(1,3-bis(2,4,6-trimethylphenyl)imidazol-2-imine)-1-(aryl)ethanone hydrochloride salt, IMesN⁺ethanone · HX, 3.1–3.3.

In a typical procedure, the substituted 2-halo-1-(4-substituted phenyl)ethanone (3.65 mmol) was added as a solid to a toluene (20 mL) solution of 1,3-bis(2,4,6-trimethylphenyl)imidazol-2-imine (3.28 mmol). The solution was refluxed for a few hours, resulting in the formation of a precipitate. The reaction

mixture was then cooled to room temperature and filtered. The solid was washed with pentane (2 × 15 mL) and dried in vacuo to yield the product as a powder.

3.4.2.1. 2-(1,3-bis(2,4,6-trimethylphenyl)imidazol-2-imine)-1-phenylethanone hydrobromide salt, 3.1:

89% yield. ^1H NMR (400 MHz, CDCl_3): *major isomer (keto form, 82%)* δ 7.99 (t, 1H, $J = 6.9$ Hz, NH), 7.49 (t, 1H, $J = 7.8$ Hz, $p\text{-CH}_{(\text{phenyl})}$), 7.46 (d, 1H, $J = 7.8$ Hz, $o\text{-CH}_{(\text{phenyl})}$), 7.30 (t, 1H, $J = 7.8$ Hz, $m\text{-CH}_{(\text{phenyl})}$), 6.89 (s, 4H, $m\text{-CH}_{(\text{mesityl})}$), 6.77 (s, 2H, -NCHCHN-), 4.48 (d, 2H, $J = 6.9$ Hz, $\text{=NH-CH}_2\text{-C-}$), 2.23 (s, 12H, $o\text{-CH}_3(\text{mesityl})$), 2.21 (s, 6H, $p\text{-CH}_3(\text{mesityl})$); *minor isomer (enol form, 18%; some resonances are missing due to accidental overlap with those of the major isomer)* δ 7.06 (s, 4H, $m\text{-CH}_{(\text{mesityl})}$), 6.83 (s, 2H, -NCHCHN-), 6.69 (s + br, 2H, =NH-CH=CPh-), 4.97 (s + br, 1H, -C(Ph)OH), 2.35 (s, 6H, $p\text{-CH}_3(\text{mesityl})$), 2.16 (s, 12H, $o\text{-CH}_3(\text{mesityl})$). $^{13}\text{C}\{^1\text{H}\}$ NMR (100 MHz, CDCl_3): *major isomer* δ 192.2 (O=C), 144.8 (-NCN-), 141.4 (ipso- $\text{C}_{(\text{mesityl})}$), 136.0 ($o\text{-C}_{(\text{mesityl})}$), 133.7 ($p\text{-C}_{(\text{phenyl})}$), 130.0 ($p\text{-C}_{(\text{mesityl})}$), 128.4 ($o\text{-C}_{(\text{phenyl})}$), 127.5 ($m\text{-C}_{(\text{phenyl})}$), 117.7 (-NCHCHN-), 48.6 ($\text{=NH-CH}_2\text{-C-}$), 21.1 ($p\text{-CH}_3(\text{mesityl})$), 17.8 ($p\text{-CH}_3(\text{mesityl})$); *minor isomer (some resonances are missing due to accidental overlap with those of the major isomer)* δ 145.2 (-NCN-), 141.4 ($o\text{-C}_{(\text{mesityl})}$), 135.6 ($\text{C}_{(\text{mesityl})}$), 130.4 ($p\text{-C}_{(\text{mesityl})}$), 117.2 (-NCHCHN-), 21.2 ($p\text{-CH}_3(\text{mesityl})$), 17.6 ($p\text{-CH}_3(\text{mesityl})$). Anal. Calcd. for $\text{C}_{29}\text{H}_{32}\text{BrN}_3\text{O}$ (%): C, 67.18; H, 6.22; N, 8.10; Found (%): C, 67.20; H, 6.31; N, 8.35.

3.4.2.2. 2-(1,3-Bis(2,4,6-trimethylphenyl)imidazol-2-imine)-1-(4-chlorophenyl)ethanone hydrochloride salt, 3.2:

81% yield. ^1H NMR (400 MHz, CDCl_3): δ 9.71 (t, 1H, $J = 6.4$ Hz, NH), 7.42 (d, 2H, $J = 8.7$ Hz, $o\text{-CH}_{(\text{phenyl})}$), 7.28 (d, 2H, $J = 8.7$ Hz, $m\text{-CH}_{(\text{phenyl})}$), 6.91 (s, 4H, $m\text{-CH}_{(\text{mesityl})}$), 6.67 (s, 2H, -NCHCHN-), 4.47 (d, 2H, $J = 6.4$ Hz, $\text{=NH-CH}_2\text{-C-}$), 2.22 (s, 18H, $p\text{-CH}_3(\text{mesityl}) + o\text{-CH}_3(\text{mesityl})$). $^{13}\text{C}\{^1\text{H}\}$ NMR (100 MHz, CDCl_3): δ 191.4 (O=C), 145.2 (-NCN-), 141.3 ($p\text{-C}_{(\text{mesityl})}$), 140.0 (ipso- $\text{C}_{(\text{phenyl})}$), 132.2 ($p\text{-CH}_{(\text{phenyl})}$), 130.4 ($o\text{-C}_{(\text{mesityl})}$), 130.1 ($m\text{-CH}_{(\text{mesityl})}$), 128.9 (ipso- $\text{C}_{(\text{mesityl})}$), 128.8 ($o\text{-CH}_{(\text{phenyl})}$), 128.7 ($m\text{-CH}_{(\text{phenyl})}$), 117.3 (-NCHCHN-), 48.5 ($\text{=NH-CH}_2\text{-C-}$), 21.1 ($p\text{-CH}_3(\text{mesityl})$), 17.7 ($o\text{-CH}_3(\text{mesityl})$). Anal. Calcd. for $\text{C}_{29}\text{H}_{31}\text{Cl}_2\text{N}_3\text{O}$ (%): C, 68.50; H, 6.14; N, 8.26; Found (%): C, 68.66; H, 5.95; N, 8.44.

3.4.2.3. 2-(1,3-Bis(2,4,6-trimethylphenyl)imidazol-2-imine)-1-(4-nitrophenyl)ethanone hydrobromide salt, 3.3:

75% yield. ^1H NMR (400 MHz, CDCl_3): δ 8.26 (t, 1H, $J = 6.4$ Hz, NH), 8.16 (d, 2H, $J = 8.7$ Hz, $m\text{-CH}_{(\text{nitrophenyl})}$), 7.68 (d, 2H, $J = 8.7$ Hz, $o\text{-CH}_{(\text{nitrophenyl})}$), 6.93 (s, 4H, $m\text{-CH}_{(\text{mesityl})}$), 6.74 (s, 2H, NCHCHN), 4.60 (d, 2H, $J = 6.4$ Hz, $\text{=NH-CH}_2\text{-C-}$), 2.22 (s, 12H, $p\text{-CH}_3(\text{mesityl})$) 2.16 (s, 6H, $o\text{-CH}_3(\text{mesityl})$). $^{13}\text{C}\{^1\text{H}\}$ NMR (100 MHz, CDCl_3): δ 191.6 (O=C), 144.8 (-NCN-), 150.5 ($p\text{-C}_{(\text{nitrophenyl})}$), 138.3 (ipso- $\text{C}_{(\text{nitrophenyl})}$), 136.0 (ipso- $\text{C}_{(\text{mesityl})}$), 135.6 ($p\text{-C}_{(\text{mesityl})}$), 130.2 ($o\text{-C}_{(\text{mesityl})}$), 128.6 ($o\text{-CH}_{(\text{nitrophenyl})}$), 123.5 ($m\text{-CH}_{(\text{nitrophenyl})}$), 117.6 (-NCHCHN-), 49.0 ($\text{=NH-CH}_2\text{=C-}$), 17.7 ($o\text{-CH}_3(\text{mesityl})$), 17.6 ($p\text{-CH}_3(\text{mesityl})$). Anal. Calcd. For $\text{C}_{29}\text{H}_{31}\text{BrN}_4\text{O}_3$ (%): C, 61.81; H, 5.55; N, 9.94; Found (%): C, 61.85; H, 5.38; N, 10.12.

3.4.3. 2-(1,3-Bis(2,4,6-trimethylphenyl)imidazol-2-imine)-1-phenylethanone, IMesN⁺ethanone, 3.4:

Compound **3.1** (2.6 g, 5.0 mmol) was suspended in THF (30 mL) and a solution of NaHMDS (938 mg, 5.11 mmol) in THF (10 mL) was added dropwise at $-78\text{ }^{\circ}\text{C}$. The reaction mixture was stirred for 10 min, subsequently slowly warmed to room temperature and stirred for an additional 30 min. The pale yellow solution was filtered, evaporated to dryness and extracted with pentane (2 \times 30 mL). The off-white solid was dried in vacuo and the pale yellow pentane solution was concentrated to 15 mL and left at $-78\text{ }^{\circ}\text{C}$ for 4 h to collect additional product through precipitation. The precipitated off-white solid was washed with cold ($-78\text{ }^{\circ}\text{C}$) pentane (10 mL) and dried in vacuo. Yield: 1.8 g (82%). ^1H NMR (400 MHz, CDCl_3): *major isomer (enol form 75%)* δ 7.41 (d, 1H, $J = 7.7\text{ Hz}$, $o\text{-CH}_{(\text{phenyl})}$), 7.08 (t, 1H, $J = 7.7\text{ Hz}$, $p\text{-CH}_{(\text{phenyl})}$), 6.94–6.84 (m, 2H, $m\text{-CH}_{(\text{phenyl})}$), 6.71 (s, 4H, $m\text{-CH}_{(\text{mesityl})}$), 6.39 (s, 1H, $=\text{N-CH=C-}$), 5.60 (s, 2H, $-\text{NCHCHN-}$), 2.13 (s, 12H, $o\text{-CH}_3(\text{mesityl})$), 2.11 (s, 6H, $p\text{-CH}_3(\text{mesityl})$); *minor isomer (keto form, 25%)* δ 7.57 (d, 1H, $J = 7.7\text{ Hz}$, $o\text{-CH}_{(\text{phenyl})}$), 7.04–6.84 (m, 2H, $m\text{-CH}_{(\text{phenyl})}$) + 1H, $p\text{-CH}_{(\text{phenyl})}$), 6.62 (s, 4H, $m\text{-CH}_{(\text{mesityl})}$), 5.65 (s, 2H, $-\text{NCHCHN-}$), 4.40 (s, 2H, $=\text{N-CH}_2\text{-C-}$), 2.35 (s, 12H, $o\text{-CH}_3(\text{mesityl})$), 1.98 (s, 6H, $p\text{-CH}_3(\text{mesityl})$). $^{13}\text{C}\{^1\text{H}\}$ NMR (100 MHz, CDCl_3): *major isomer* δ 141.9 ($-\text{NCN-}$), 136.4 ($\text{C}_{(\text{mesityl})}$), 136.2 (O-C), 133.9 ($o\text{-C}_{(\text{mesityl})}$), 128.9 ($p\text{-C}_{(\text{mesityl})}$), 126.1 ($p\text{-C}_{(\text{phenyl})}$), 129.1 ($m\text{-C}_{(\text{phenyl})}$), 123.2 ($o\text{-C}_{(\text{phenyl})}$), 108.6 ($=\text{N-CH=C-}$), 114.7 ($-\text{NCHCHN-}$), 21.6 ($p\text{-CH}_3(\text{mesityl})$), 18.6 ($o\text{-CH}_3(\text{mesityl})$); *minor isomer* δ 196.6 ($\text{C}_{(\text{ketone})}$), 145.5 ($-\text{NCN-}$), 136.7 ($\text{C}_{(\text{mesityl})}$),

136.3 ($C_{(\text{phenyl})}$) 132.7 ($m\text{-}C_{(\text{phenyl})}$), 129.1 ($p\text{-}C_{(\text{mesityl})}$), 128.8 ($o\text{-}C_{(\text{mesityl})}$), 128.7 ($p\text{-}C_{(\text{phenyl})}$), 123.2 ($o\text{-}C_{(\text{phenyl})}$), 114.2 (-NCHCHN-), 54.5 ($\text{=N-CH}_2\text{-C-}$), 21.5 ($p\text{-CH}_3_{(\text{mesityl})}$), 18.9 ($o\text{-CH}_3_{(\text{mesityl})}$). Anal. Calcd. for $\text{C}_{29}\text{H}_{31}\text{N}_3\text{O}$ (%): C, 79.60; H, 7.14; N, 9.60; Found (%): C, 79.35; H, 7.17; N, 9.38.

3.4.4. Sodium 2-(1,3-bis(2,4,6-trimethylphenyl)imidazol-2-imine)-1-phenylethenolate, Na[IMesN[^]ethenolate], 3.5:

To a THF (2 mL) suspension of NaH (11.5 mg, 480 μmol) at -40°C slowly was added a cold (-40°C) solution of **3.4** (150 mg, 343 μmol) in THF (5 mL). The reaction mixture was slowly warmed to room temperature and stirred for 60 min, resulting in the color slowly changing to intense yellow. Pentane (5 mL) was added to precipitate the product, which was filtered, washed with pentane (2×5 mL) and dried in vacuo to yield a yellow solid. Yield: 137 mg (87%). ^1H NMR (400 MHz, C_6D_6): δ 7.26 (t, 2H, $J = 7.4$ Hz, $m\text{-CH}_{(\text{phenyl})}$), 7.08 (t, 1H, $J = 7.4$ Hz, $p\text{-CH}_{(\text{phenyl})}$), 6.98 (s, 1H, $m\text{-CH}_{(\text{mesityl})}$), 6.82 (d, 2H, $J = 7.4$ Hz, $o\text{-CH}_{(\text{phenyl})}$), 6.75 (s, 1H, $m\text{-CH}_{(\text{mesityl})}$), 6.30 (s, 1H, $m\text{-CH}_{(\text{mesityl})}$), 6.21 (s, 1H, =N-CH=C-), 6.08 (s, 1H, $m\text{-CH}_{(\text{mesityl})}$), 5.61 (d, 1H, $J = 2.7$ Hz -NCHCHN-), 5.58 (d, 1H, $J = 2.7$ Hz -NCHCHN-), 2.49 (s, 3H, $\text{CH}_3_{(\text{mesityl})}$), 2.28 (s, 3H, $\text{CH}_3_{(\text{mesityl})}$), 2.16 (s, 3H, $\text{CH}_3_{(\text{mesityl})}$), 2.15 (s, 3H, $\text{CH}_3_{(\text{mesityl})}$), 2.05 (s, 3H, $\text{CH}_3_{(\text{mesityl})}$), 1.89 (s, 3H, $\text{CH}_3_{(\text{mesityl})}$). $^{13}\text{C}\{^1\text{H}\}$ NMR (100.6 MHz, C_6D_6): δ 150.3 (O-C), 146.5 (ipso- $C_{(\text{mesityl})}$), 141.5 (-NCN-), 137.9 (aromatic CH), 137.7 (aromatic CH), 137.4 (aromatic CH), 136.9 (aromatic CH), 135.8 (aromatic CH), 135.5 (aromatic CH), 135.2 (aromatic CH), 133.3 (ipso- $C_{(\text{mesityl})}$), 130.3 (aromatic CH), 129.6 (aromatic

CH), 129.0 (aromatic CH), 128.7 (*m*-CH_(mesityl)), 127.7 (*m*-CH_(phenyl)), 124.5 (*o*-CH_(phenyl)), 122.5 (*p*-CH_(phenyl)), 114.3 (–NCHCHN–), 113.8 (–NCHCHN–), 103.8 (=N–CH=C–), 21.1 (CH_{3(mesityl)}), 20.7 (CH_{3(mesityl)}), 19.3 (CH_{3(mesityl)}), 18.8 (CH_{3(mesityl)}), 18.4 (CH_{3(mesityl)}), 16.9 (CH_{3(mesityl)}). Anal. Calcd. for C₂₉H₃₀N₃NaO (%): C, 75.79; H, 6.58; N, 9.14; Found (%): C, 76.04; H, 6.62; N, 8.87.

3.4.5. General procedure for the synthesis of bis(2-(1,3-bis(2,4,6-trimethylphenyl)imidazol-2-imine)-1-(aryl)ethenolate) zirconium dichloride, ZrCl₂(IMesN[^]ethenolate)₂, 3.6 and 3.7:

NaHMDS (0.773 mmol) was slowly added at room temperature as a solid to a THF (5 mL) suspension of compound **1** (0.386 mmol). The solution immediately turned an bright yellow and the reaction mixture was allowed to stir for 30 min. The solution was then added to a THF (2 mL) solution of ZrCl₂(THF)₂ (0.386 mmol). A white precipitate formed immediately. The yellow solution was stirred for 2 h, subsequently filtered through a pad of Celite and dried under reduced pressure. The product was washed with Et₂O (2 × 5 mL) and dried in vacuo to yield a yellow powder.

3.4.5.1. Bis(2-(1,3-bis(2,4,6-trimethylphenyl)imidazol-2-imine)-1-phenylethenolate) zirconium dichloride, 3.6:

60% yield. ¹H NMR (400 MHz, CDCl₃): δ 6.98 (m, 12H, *m*-CH_(mesityl) + *m*-CH_(phenyl)), 6.88 (d, 2H, *J* = 7.4 Hz, *p*-CH_(phenyl)), 6.74 (d, 4H, *J* = 7.4 Hz, *o*-CH_(phenyl)), 6.58 (s, 4H, –NCHCHN–), 5.93 (s, 2H, =N–CH=C–), 2.30 (s, 12H, *p*-

$CH_{3(\text{mesityl})}$, 2.24 (s, 24H, $o\text{-}CH_{3(\text{mesityl})}$); $^{13}C\{^1H\}$ NMR (100 MHz, $CDCl_3$): δ 145.5 (O–C), 139.2 ($p\text{-}C_{(\text{mesityl})}$), 137.1 (ipso- $C_{(\text{phenyl})}$), 136.3 (ipso- $C_{(\text{mesityl})}$), 132.3 (–NCN–), 129.6 ($m\text{-}CH_{(\text{mesityl})}$), 126.9 ($m\text{-}CH_{(\text{phenyl})}$), 124.3 ($p\text{-}CH_{(\text{phenyl})}$), 123.5 ($o\text{-}CH_{(\text{phenyl})}$), 117.4 (–NCHCHN–), 113.0 (=N–CH=C–), 21.1 ($p\text{-}CH_{3(\text{mesityl})}$), 19.2 ($o\text{-}CH_{3(\text{mesityl})}$). Anal. Calcd. for $C_{58}H_{60}Cl_2N_6O_2Zr$ (%): C, 67.29; H, 5.84; N, 8.12; Found (%): C, 67.48; H, 6.02; N, 7.94.

3.4.5.2. Bis(2-(1,3-bis(2,4,6-trimethylphenyl)imidazol-2-imine)-1-(4-chlorophenyl)ethenolate) zirconium dichloride, 3.7:

42% yield. 1H NMR (400 MHz, C_6D_6): δ 6.96 (s, 8H, $m\text{-}CH_{(\text{mesityl})}$) 6.92 (d, 4H, $J = 8.4$ Hz, $m\text{-}CH_{(\text{chlorophenyl})}$), 6.64 (d, 4H, $J = 8.4$ Hz, $o\text{-}CH_{(\text{chlorophenyl})}$), 6.59 (s, 4H, –NCHCHN–), 5.91 (s, 2H, =N–CH=C–), 2.30 (s, 12H, $p\text{-}CH_{3(\text{mesityl})}$), 2.21 (s, 24H, $o\text{-}CH_{3(\text{mesityl})}$); $^{13}C\{^1H\}$ NMR (100 MHz, $CDCl_3$): δ 144.4 (O–C), 139.3 ($p\text{-}C_{(\text{mesityl})}$), 136.2 (ipso- $C_{(\text{mesityl})}$ + $o\text{-}C_{(\text{mesityl})}$), 135.6 ($p\text{-}C_{(\text{chlorophenyl})}$), 132.2 (–NCN–), 129.6 ($m\text{-}CH_{(\text{mesityl})}$), 129.5 (ipso- $C_{(\text{chlorophenyl})}$), 127.1 ($m\text{-}CH_{(\text{chlorophenyl})}$), 124.5 ($o\text{-}CH_{(\text{chlorophenyl})}$), 117.5 (–NCHCHN–), 113.4 (=N–CH=C–), 21.1 ($p\text{-}CH_{3(\text{mesityl})}$), 19.2 ($o\text{-}CH_{3(\text{mesityl})}$). Anal. Calcd. for $C_{58}H_{58}Cl_4N_6O_2Zr$ (%): C, 63.09; H, 5.29; N, 7.61; Found (%): C, 63.32; H, 5.01; N, 7.43.

3.4.6. General procedure for the synthesis of cyclopentadienyl (2-(1,3-bis(2,4,6-trimethylphenyl)imidazol-2-imine)-1-(aryl)ethenolate) zirconium dichloride, CpZrCl₂(IMesN[^]ethenolate), 3.8 and 3.9:

NaHMDS (0.773 mmol) was slowly added as a solid to a THF (5 mL) suspension of compound 1 (0.386 mmol). The solution immediately turned an

bright yellow and the reaction mixture was allowed to stir for 30 min. The solution was then added to a THF (2 mL) solution of CpZrCl₃ (0.386 mmol). A white precipitate immediately formed and the reaction mixture was allowed to stir for 2 h. The reaction mixture was then filtered through a pad of Celite and dried under reduced pressure. The product was washed with diethyl ether (2 × 5 mL) and dried in vacuo to yield a yellow powder.

3.4.6.1 Cyclopentadienyl (2-(1,3-bis(2,4,6-trimethylphenyl)imidazol-2-imine)-1-phenylethenolate) zirconium dichloride, 3.8:

47% yield. ¹H NMR (400 MHz, CDCl₃): δ 7.13–7.09 (m, 7H, *m*-CH_(mesityl) + *o*-CH_(phenyl) + *p*-CH_(phenyl)), 6.92 (dd, 2H, *J* = 7.2, 6.0 Hz, *m*-CH_(phenyl)), 6.53 (s, 2H, –NCHCHN–), 6.10 (s, 1H, =N–CH=C–), 6.04 (s, 5H, Cp), 2.34 (s, 6H, *p*-CH_{3(mesityl)}), 2.31 (s, 12H, *o*-CH_{3(mesityl)}). ¹³C{¹H} NMR (100 MHz, CDCl₃): δ 147.8 (O–C), 147.4 (–NCN–), 140.5 (*p*-C_(mesityl)), 136.2 (*o*-C_(mesityl)), 132.9 (ipso-C_(phenyl)), 132.7 (ipso-C_(mesityl)), 130.1 (*m*-CH_(mesityl)), 128.3 (*p*-CH_(phenyl)), 127.5 (*o*-CH_(phenyl)), 125.6 (*m*-CH_(phenyl)), 117.7 (–NCHCHN–), 115.8 (Cp), 103.9 (=N–CH=C–), 21.0 (*p*-CH_{3(mesityl)}), 18.7 (*o*-CH_{3(mesityl)}). Anal. Calcd. for C₃₄H₃₅Cl₂N₃OZr (%): C, 61.52; H, 5.31; N, 6.33; Found (%): C, 61.30; H, 5.24; N, 6.10.

3.4.6.2 Cyclopentadienyl (2-(1,3-bis(2,4,6-trimethylphenyl)imidazol-2-imine)-1-(4-chlorophenyl)ethenolate) zirconium dichloride, 3.9:

59% yield. ¹H NMR (400 MHz, CDCl₃): δ 7.08 (s, 4H, *m*-CH_(mesityl)), 7.06 (d, 2H, *J* = 8.5 Hz, *o*-CH_(chlorophenyl)), 6.84 (d, 2H, *J* = 8.5 Hz, *m*-CH_(chlorophenyl)), 6.55 (s, 2H, –NCHCHN–), 6.09 (s, 1H, =N–CH=C–), 6.02 (s, 5H, Cp), 2.34 (s, 6H, *p*-

$CH_{3(mesityl)}$, 2.30 (s, 12H, $o-CH_{3(mesityl)}$). $^{13}C\{^1H\}$ NMR (100 MHz, $CDCl_3$): δ 147.5 ($-NCN-$), 146.6 (O-C), 140.5 ($p-C_{(mesityl)}$), 136.1 ($o-C_{(mesityl)}$), 133.8 ($p-C_{(chlorophenyl)}$), 132.6 (ipso- $C_{(mesityl)}$), 131.6 (ipso- $C_{(chlorophenyl)}$), 130.3 ($m-CH_{(mesityl)}$), 127.7 ($o-CH_{(chlorophenyl)}$), 126.8 ($m-CH_{(chlorophenyl)}$), 117.8 ($-NCHCHN-$), 115.9 (Cp), 104.71 ($=N-CH=C-$), 21.0 ($p-CH_{3(mesityl)}$), 18.7 ($o-CH_{3(mesityl)}$). Anal. Calcd. for $C_{34}H_{34}Cl_3N_3OZr$ (%): C, 58.49; H, 4.91; N, 6.02; Found (%): C, 58.64; H, 4.72; N, 5.76.

3.4.7. General procedure for the synthesis of cyclopentadienyl (2-(1,3-bis(2,4,6-trimethylphenyl)imidazol-2-imine)-1-(aryl)ethenolate) titanium dichloride $CpTiCl_2(ImesN^{\wedge}ethenolate)$, 3.10 and 3.11:

Compounds **3.10** and **3.11** were prepared using the same procedure used for the preparation of compounds **3.8** and **3.9**, with the exception that the $CpTiCl_3$ was used as metal precursor. The product was purified by redissolving it in toluene, filtering the mixture and removing the volatiles in vacuo to yield blue powders. Analytically-pure samples were obtained by recrystallization from THF and pentane at -35 °C.

3.4.7.1. Cyclopentadienyl (2-(1,3-bis(2,4,6-trimethylphenyl)imidazol-2-imine)-1-phenylethenolate) titanium dichloride, 3.10:

74% yield; 1H NMR (400 MHz, C_6D_6): δ 7.19–7.17 (m, 4H, $o-CH_{(phenyl)}$ + $m-CH_{(phenyl)}$), 6.90 (d, 1H, $J = 8.5$ Hz, $p-CH_{(phenyl)}$), 6.78 (s, 1H, $=N-CH=C-$), 6.73 (s, 4H, $m-CH_{(mesityl)}$), 6.12 (s, 5H, Cp), 5.56 (s, 2H, $-NCHCHN-$), 2.12 (s, 12H, $o-CH_{3(mesityl)}$), 2.09 (s, 6H, $p-CH_{3(mesityl)}$). $^{13}C\{^1H\}$ NMR (100 MHz, C_6D_6): δ 156.8

(O–C), 144.8 (–NCN–_(mesityl)), 139.1 (*p*-C_(mesityl)), 137.7 (ipso-C_(phenyl)), 136.5 (*o*-C_(mesityl)), 133.9 (ipso-C_(mesityl)), 129.6 (*m*-CH_(mesityl)), 127.0 (*m*-CH_(phenyl)), 125.4 (*p*-CH_(phenyl)), 124.2 (N–CH=C), 122.3 (*o*-CH_(phenyl)), 120.5 (Cp), 115.0 (–NCHCHN–), 20.9 (*p*-CH_{3(mesityl)}), 18.0 (*o*-CH_{3(mesityl)}). Anal. Calcd. for C₃₄H₃₅Cl₂N₃OTi (%): C, 65.82; H, 5.69; N, 6.77; Found (%): C, 66.10; H, 5.90; N, 7.02.

3.4.7.2. Cyclopentadienyl (2-(1,3-bis(2,4,6-trimethylphenyl)imidazol-2-imine)-1-(4-chlorophenyl)ethenolate) titanium dichloride, 3.11:

56% yield. ¹H NMR (400 MHz, C₆D₆): δ 7.05 (d, 2H, *J* = 8.6 Hz, *m*-CH_(chlorophenyl)), 6.97 (d, 2H, *J* = 8.6 Hz, *o*-CH_(chlorophenyl)), 6.71 (s, 4H, *m*-CH_(mesityl)), 6.68 (s, 1H, =N–CH=C–), 6.05 (s, 5H, Cp), 5.56 (s, 2H, –NCHCHN–), 2.09 (s, 12H, *o*-CH_{3(mesityl)}), 2.06 (s, 6H, *p*-CH_{3(mesityl)}). ¹³C{¹H} NMR (100 MHz, C₆D₆): δ 155.6 (O–C), 144.8 (–NCN–), 139.2 (*p*-C_(mesityl)), 136.4 (*o*-C_(mesityl)), 136.3 (*p*-C_(chlorophenyl)), 133.8 (ipso-C_(mesityl)), 130.7 (ipso-C_(chlorophenyl)), 129.9 (*m*-CH_(mesityl)), 128.6 (*m*-CH_(chlorophenyl)), 124.6 (=N–CH=C–), 123.4 (*o*-CH_(chlorophenyl)), 120.6 (Cp), 115.1 (–NCHCHN–), 20.9 (*p*-CH_{3(mesityl)}), 17.9 (*o*-CH_{3(mesityl)}). Anal. Calcd. for C₃₄H₃₄Cl₃N₃OTi (%): C, 62.36; H, 5.23; N, 6.42; Found (%): C, 62.15; H, 5.09; N, 6.38.

3.4.8. General Procedure for Ethylene Polymerization.

Ethylene polymerization was performed at atmospheric pressure and room temperature in a 200 mL Schlenk flask containing a magnetic stir bar. The flask was conditioned in an oven at 160 °C for at least 12 h prior to use. The hot flask was brought to room temperature under dynamic vacuum, and back-filled

with ethylene. This cycle was repeated a total of three times. Under an atmosphere of ethylene, the flask was charged with 20 mL of dry toluene and 1000 equivalents of methylaluminoxane (MAO). The solution was stirred for 15 min before a solution of the catalyst in toluene was introduced into the flask via a syringe. The reaction mixture was vigorously stirred for 10 min after the addition of the catalyst, and subsequently quenched with a 50:50 mixture of concentrated hydrochloric acid and methanol. The resulting mixture was filtered and any solid collected was washed with distilled water. Solids collected were dried under vacuum at approximately 60 °C for several hours.

3.4.9. Computational Details.

DFT calculations were carried out at the hybrid B3LYP level of theory with LanL2DZ as basis set using Gaussian 9¹³ and GaussView 3¹⁴ for computing and molecular visualization, respectively. These calculations were performed on the Shared Hierarchical Academic Research Computing Network (SHARCNET: www.sharcnet.ca).

3.4.10. X-ray Crystallography.

Detailed crystallographic data for compound **3.9** (Tables of atomic coordinates with isotropic and anisotropic displacement parameters, bond lengths and angles) are provided as supplementary materials. Crystallographic data for **3.9** were collected at the University of Toronto on a Bruker-Nonius Kappa-CCD diffractometer using monochromated Mo-K α radiation ($\lambda = 0.71073$ Å) at 150K and were measured using a combination of ϕ scans and ω scans with

κ offsets, to fill the Ewald sphere. Intensity data were processed using the Denzo-SMN package.¹⁵ Absorption corrections were carried out using SORTAV.¹⁶ The structure was solved with using Superflip¹⁷ and refined using WinGX¹⁸ with SHELXS-97¹⁹ for full-matrix least-squares refinement that was based on F^2 . All H atoms were included in calculated positions and allowed to refine in riding-motion approximation with U_{iso} tied to the carrier atom.

3.5 References

- 1 a) T. K. Panda, A. G. Trambitas, T. Bannenberg, C. G. Hrib, S. Randoll, P. G. Jones and M. Tamm, *Inorg. Chem.* **2009**, *48*, 5462; b) D. Petrovic, T. Bannenberg, S. Randoll, P. G. Jones and M. Tamm, *Dalton Trans.* **2007**, 2812;
- c) M. Tamm, D. Petrovic, S. Randoll, S. Beer, T. Bannenberg, P. G. Jones and J. Grunenberg, *Org. Biomol. Chem.* **2007**, *5*, 523; d) M. Tamm, S. Randoll, T. Bannenberg and E. Herdtweck, *Chem. Commun. (Cambridge, U. K.)* **2004**, 876;
- e) M. Tamm, S. Randoll, E. Herdtweck, N. Kleigrewe, G. Kehr, G. Erker and B. Rieger, *Dalton Trans.* **2006**, 459.
- 2 S. Randoll, P. G. Jones and M. Tamm, *Organometallics* **2008**, *27*, 3232.
- 3 a) S. Dastgir and G. G. Lavoie, *Dalton Trans.* **2010**, *39*, 6943; b) S. Dastgir and G. G. Lavoie, *Dalton Trans.* **2012**, *41*, 9651.
- 4 M. B. Harkness, E. Alvarado, A. C. Badaj, B. C. Skrela, L. Fan and G. G. Lavoie, *Organometallics* **2013**, *32*, 3309.
- 5 S. Matsui, Y. Tohi, M. Mitani, J. Saito, H. Makio, H. Tanaka, M. Nitabaru, T. Nakano and T. Fujita, *Chem. Lett.* **1999**, 1065.

6 C. Wang, S. Friedrich, T. R. Younkin, R. T. Li, R. H. Grubbs, D. A. Bansleben and M. W. Day, *Organometallics* **1998**, *17*, 3149.

7 a) P. Garcia, P. R. Payne, E. Chong, R. L. Webster, B. J. Barron, A. C. Behrle, J. A. R. Schmidt and L. L. Schafer, *Tetrahedron* **2013**, *69*, 5737; b) P. Horrillo-Martinez, B. O. Patrick, L. L. Schafer and M. D. Fryzuk, *Dalton Trans.* **2012**, *41*, 1609; c) D. C. Leitch, R. H. Platel and L. L. Schafer, *J. Am. Chem. Soc.* **2011**, *133*, 15453; d) M. C. Wood, D. C. Leitch, C. S. Yeung, J. A. Kozak and L. L. Schafer, *Angew. Chem., Int. Ed.* **2007**, *46*, 354; e) Z. Zhang and L. L. Schafer, *Org. Lett.* **2003**, *5*, 4733.

8 a) H. Makio and T. Fujita, *Acc. Chem. Res.* **2009**, *42*, 1532; b) H. Makio, H. Terao, A. Iwashita and T. Fujita, *Chem. Rev. (Washington, DC, U. S.)* **2011**, *111*, 2363; c) M. Mitani, R. Furuyama, J. Mohri, J. Saito, S. Ishii, H. Terao, T. Nakano, H. Tanaka and T. Fujita, *J. Am. Chem. Soc.* **2003**, *125*, 4293; d) M. Mitani, J. Mohri, Y. Yoshida, J. Saito, S. Ishii, K. Tsuru, S. Matsui, R. Furuyama, T. Nakano, H. Tanaka, S.-i. Kojoh, T. Matsugi, N. Kashiwa and T. Fujita, *J. Am. Chem. Soc.* **2002**, *124*, 3327; e) J. Sun, Z. Cheng, Y. Nie, H. Schumann and M. Hummert, *Appl. Organomet. Chem.* **2007**, *21*, 268; f) H. Terao, S. Ishii, M. Mitani, H. Tanaka and T. Fujita, *J. Am. Chem. Soc.* **2008**, *130*, 17636; g) G. W. Theaker, C. Morton and P. Scott, *Macromolecules (Washington, DC, U. S.)* **2011**, *44*, 1393; h) J. Strauch, T. H. Warren, G. Erker, R. Frohlich and P. Saarenketo, *Inorg. Chim. Acta* **2000**, *300-302*, 810.

9 A. L. Johnson, M. G. Davidson, M. D. Lunn and M. F. Mahon, *Eur. J. Inorg.*

Chem. **2006**, 3088.

10 a) P. Pyykkö and M. Atsumi, *Chem. Eur. J.* **2009**, *15*, 186; b) P. Pyykkö and M.

Atsumi, *Chem. Eur. J.* **2009**, *15*, 12770.

11 R. K. J. Bott, D. L. Hughes, M. Schormann, M. Bochmann and S. J.

Lancaster, *J. Organomet. Chem.* **2003**, *665*, 135.

12 L. E. Manzer, *Inorg. Synth.* **1982**, *21*, 135.

13 Frisch, M. J.; Trucks, G. W.; Schlegel, H. B.; Scuseria, G. E.; Robb, M. A.;

Cheeseman, J. R.; Scalmani, G.; Barone, V.; Mennucci, B.; Petersson, G. A.;

Nakatsuji, H.; Caricato, M.; Li, X.; Hratchian, H. P.; Izmaylov, A. F.; Bloino, J.;

Zheng, G.; Sonnenberg, J. L.; Hada, M.; Ehara, M.; Toyota, K.; Fukuda, R.;

Hasegawa, J.; Ishida, M.; Nakajima, T.; Honda, Y.; Kitao, O.; Nakai, H.; Vreven,

T.; Montgomery, J., J. A.; Peralta, J. E.; Ogliaro, F.; Bearpark, M.; Heyd, J. J.;

Brothers, E.; Kudin, K. N.; Staroverov, V. N.; Kobayashi, R.; Normand, J.;

Raghavachari, K.; Rendell, A.; Burant, J. C.; Iyengar, S. S.; Tomasi, J.; Cossi,

M.; Rega, N.; Millam, J. M.; Klene, M.; Knox, J. E.; Cross, J. B.; Bakken, V.;

Adamo, C.; Jaramillo, J.; Gomperts, R.; Stratmann, R. E.; Yazyev, O.; Austin, A.

J.; Cammi, R.; Pomelli, C.; Ochterski, J. W.; Martin, R. L.; Morokuma, K.;

Zakrzewski, V. G.; Voth, G. A.; Salvador, P.; Dannenberg, J. J.; Dapprich, S.;

Daniels, A. D.; Farkas, Ö.; Foresman, J. B.; Ortiz, J. V.; Cioslowski, J.; Fox, D. J.

Gaussian 09, Revision C.01; Gaussian, Inc.: Wallingford, CT, 2009;

- 14 Ik, R. D.; Keith, T.; Millam, J.; Eppinnett, K.; Hovell, L. W.; Gilliland, R. *GaussView 3*; Gaussian, Inc.: Carnegie, PA, 2003;
- 15 Otwinowski, Z.; Minor, W. *Processing of x-ray diffraction data collected in oscillation mode.*; Academic Press: London, 1997; **276** (Macromolecular Crystallography, Part A); pp 307–326.
- 16 Blessing, R. H. *Acta Crystallogr., Sect. A: Found. Crystallogr.* **1995**, *A51*, 33–38.
- 17 Palatinus, L.; Chapuis, G. *J. Appl. Crystallogr.* **2007**, *40*, 786–790.
- 18 Farrugia, L. G. *J. App. Cryst.* **1999**, *32*, 837–838.
- 19 G. M. Sheldrick, *Acta Crystallogr., Sect. A: Found Crystallogr.* **2008**, *A64*, 112.

Chapter 4 Grubbs-type Metathesis Catalysts: A Three Pronged Approach

4.1 Introduction

The formation of carbon-carbon bonds is one of the most important transformations in organic chemistry and has propelled the research interest of homogenous organometallic catalysis. As a result, a great deal of emphasis has been placed on developing catalysts with specifically designed ancillary ligands for the syntheses of specific desired products under controlled conditions. One area of transition metal catalysis that has garnered much attention in recent decades is ruthenium-based olefin metathesis.¹ The availability of easily prepared, robust ruthenium metathesis catalysts has led to their tremendous usage in facilitating a wide variety of organic transformations.

4.1.1 Metathesis

There are several metathesis subtypes, which include cross-metathesis (CM)^{1a,b,1e,2}, ring-opening metathesis polymerization (ROMP)^{2g,3}, ring-closing metathesis (RCM)^{1e,2a,2d,2g,4}, acyclic diene metathesis polymerization (ADMET)^{2g,3a,5} and ring-opening cross-metathesis (ROCM)^{2e,2g,6}. In all cases, a metal alkylidene is present to facilitate the carbon-carbon double bond rearrangement.

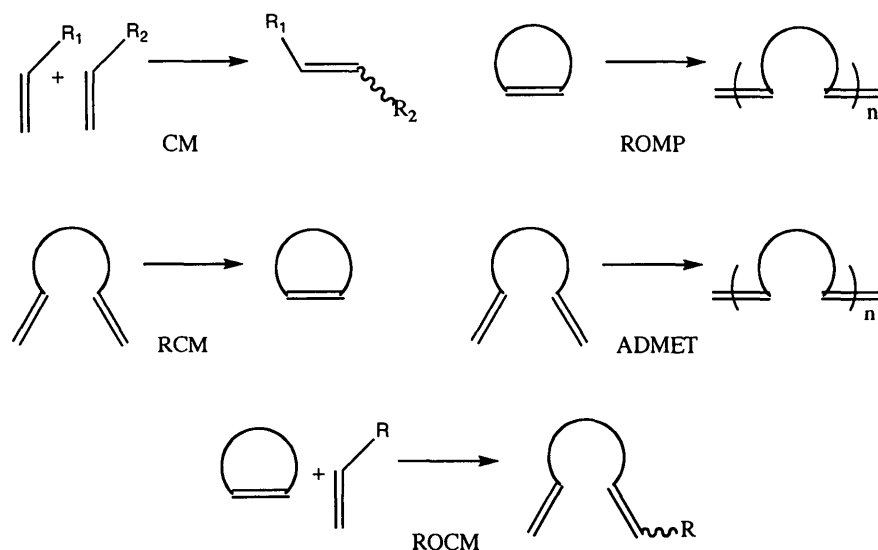


Figure 4.1. Common types of metathesis reactions

The highly studied olefin metathesis reaction mechanism, first proposed by Chauvin⁷, involves a series of alternating [2 + 2]-cycloadditions and cycloreversions, involving a catalytically important metallocyclobutane intermediate (Figure 4.2).⁸

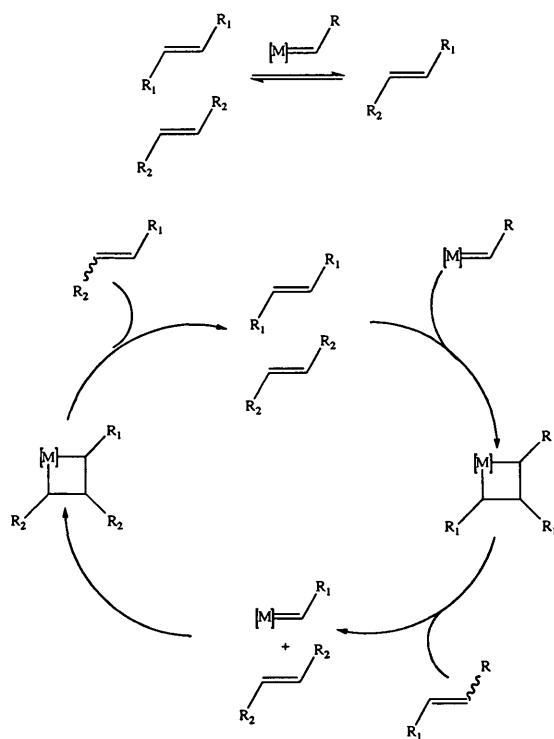


Figure 4.2. General accepted metathesis mechanism

The most notable metathesis catalysts are based on molybdenum^{3h,4b,9}, tungsten^{3h,9c-g} and ruthenium.^{1,2d,3e,4a,b,9a,10} In our case, we were most interested in ruthenium alkylidene metathesis catalysts because of their stability and tolerance towards many different organic functional groups. One of the first, and most notable, ruthenium-based metathesis catalyst is Grubbs first-generation (GI) catalyst (Figure 4.3).¹¹

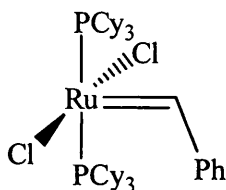


Figure 4.3. Grubbs first-generation (G1) catalyst

4.1.2 Evolution of ruthenium metathesis catalysts

Since the isolation of G1, there has been a great deal of emphasis on improving the productivity of this catalyst. The most notable modification to Grubbs first-generation catalyst was substituting one of the neutral ancillary phosphine ligands with an *N*-heterocyclic carbene (NHC) ligand.^{1b,1d,e,2d,4a,10b,c,12}

As discussed in Chapter 1, NHC ligands are excellent σ -donors and poor π -acceptors and impart excellent thermodynamic stability to transition metal complexes. Substituting one of the tertiary phosphines with an NHC ligand offers enhanced stability of the coordinatively unsaturated intermediate in the metathesis catalytic cycle.^{1b,2d} In addition, certain NHC ligands offer considerably more steric bulk around the metal centre compared to tertiary phosphines, thus promoting dissociation of the phosphine and initiation of the catalytic cycle.^{1b,2d,13} As a result, the combination of a strong electron-donating, non-labile, sterically bulky NHC ligand and a labile ligand resulted in significantly greater metathesis productivity.

Other notable advancements and modifications^{2d,6a,10c,14} to Grubbs-type ruthenium complexes include using more labile ligands, such as PPh_3 ¹⁵ or

pyridine¹⁶, as a replacement for the second phosphine, substituting the chloride ligand(s)¹⁷ and modifying the benzylidene^{11b,14,18} ligand itself (Figure 4.4).

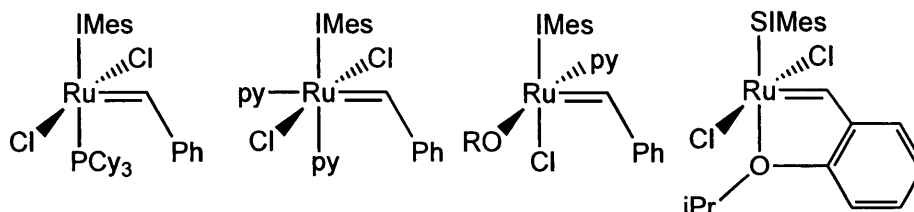


Figure 4.4. Examples of modifications to Grubbs-type ruthenium metathesis catalysts

Despite the extensive research into ruthenium metathesis catalysts over the last few decades, we found a few areas that remained underdeveloped. The use of multidentate ligands, both mono^{19,20} and dianionic,²¹ and chelating benzylidene ligands,²² have been used in the synthesis of Grubbs-type ruthenium complexes, but considerably less attention was given towards incorporating neutral bidentate ligands.²³ As a result, we became interested in developing the area of Grubbs-type ruthenium complexes bearing neutral, bidentate ligands, specifically the aryl-substituted acyclic imino-*N*-heterocyclic carbene.²⁴

The second area of Grubbs-type ruthenium complexes that garnered our attention was the substitution of the chloride ligand(s) with alkyl/aryloxide ligand(s).^{17b,21b,c,25} Fogg has demonstrated that substituting one or two of the halides with an aryloxide can lead to enhanced activity for ring-closing metathesis when compared to other Grubbs-type catalysts (Scheme 1). In one study,^{21b} Fogg demonstrated that the activity of the ruthenium complexes in metathesis decreases as the aryloxide becomes more electron-deficient. This

observed trend provided an opportunity to investigate substituting one or two of the halides of Grubbs first- and second-generation catalysts with the imidazol-2-imide ligand.²⁶

We were also interested in substituting one of the tertiary phosphines of GI with an NHC-phosphinidene.²⁷ As discussed in Chapter 1, NHC-phosphinidene ligands are strong electron-donating ligands with considerable bulk (from the NHC), and the ligands can be easily modified both electronically and sterically. Incorporation of an NHC-phosphinidene ligand would yield a ruthenium complex bearing a strong electron-donating and sterically bulky ligand and a labile tertiary phosphine ligand for dissociation/initiation. We herein report our progress in these research interests.

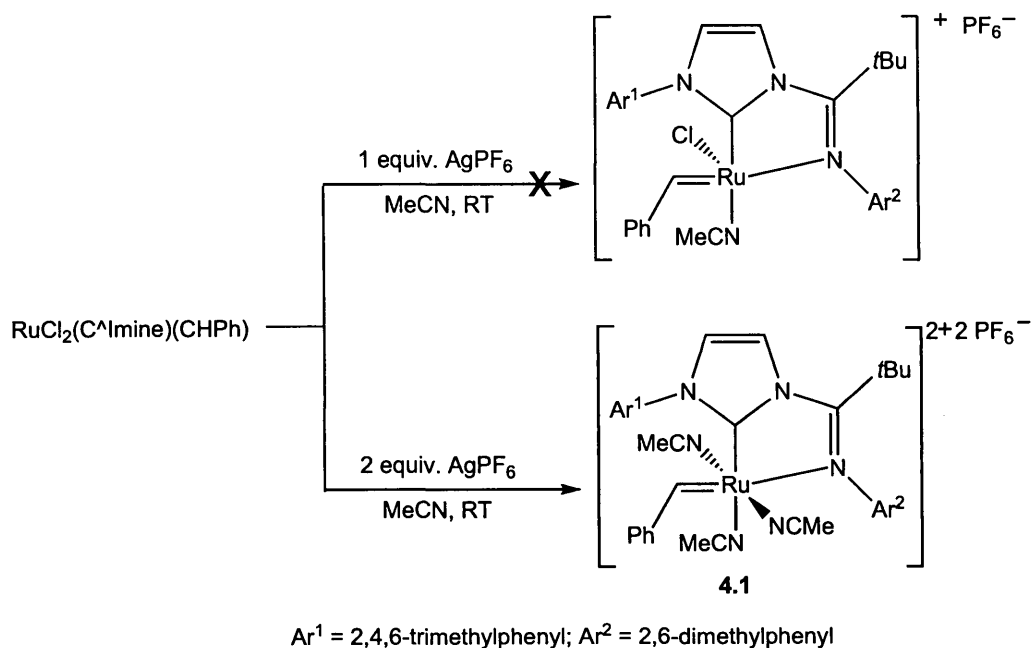
4.2 Results and Discussion

4.2.1. Synthesis and chemistry of cationic ruthenium benzylidene complex

Within the Lavoie group, an efficient synthetic route for forming a phosphine-free Grubbs-type ruthenium complex was prepared. Reacting a slight excess of C[^]Imine with Grubbs first-generation complex in toluene for 24 hours at room temperature afforded the phosphine-free RuCl₂(C[^]Imine)(CHPh)²⁸. The catalytic activity of this complex towards ring-closing metathesis of diethyl diallylmalonate and diallyl sulfide was evaluated at 70 °C using 5 mol% Ru, and monitored by ¹H NMR spectroscopy. After 1 hour, no ring-closing product, catalyst decomposition or substrate consumption was observed and the diagnostic benzylidene proton was still visible in the ¹H NMR spectrum. The

inactivity of this complex towards RCM suggests a robust chelation of the C^Imine ligand, thus impeding the initiation step via the formation of a free coordination site.

Our attention was then turned towards synthesizing the cationic derivative by abstracting one of the chloride ligands. We believed that treating $\text{RuCl}_2(\text{C}^{\text{Imine}})(\text{CHPh})$ with a halide-abstracting agent, in the presence of a weakly coordinating solvent, would yield a solvated cationic adduct. From this product, a free coordination site could be formed to initiate ring-closing metathesis via dissociation of a solvent molecule. As a result, we decided to treat $\text{RuCl}_2(\text{C}^{\text{Imine}})(\text{CHPh})$ with one equivalent of AgPF_6 in acetonitrile in an attempt to form $[\text{RuCl}(\text{C}^{\text{Imine}})(\text{MeCN})(\text{CHPh})][\text{PF}_6]$. To our surprise this led to the selective formation of one product in approximately 50% yield; addition of two equivalents of AgPF_6 led to the formation of the same product, presumably compound **4.1**, in fair yield (70%) (Scheme 4.1).



Scheme 4.1. Reaction of $\text{RuCl}_2(\text{C}^{\wedge}\text{Imine})(\text{CHPh})$ with AgPF_6 in MeCN

The solution ^1H NMR spectrum of the product showed promise, with a new resonance at δ 16.5 ppm, a characteristic region for resonances of benzyldiene protons. Likewise, the benzyldiene carbon resonance resonates far downfield at δ 334.3 ppm, similar in chemical shift to other ruthenium benzyldiene complexes. In the aliphatic region, there were 10 resonances ranging from δ 2.49 – 1.43 ppm. If the methyl groups of the ligand were spectroscopically inequivalent (similar to $\text{RuCl}_2(\text{C}^{\wedge}\text{Imine})(\text{CHPh})$), there should be 8 resonances in the aliphatic region, including two coordinated MeCN ligands. Combustion analysis of this product was not consistent with compound 4.1.

Despite the inconsistent characterization of the complex, the activity of this product towards RCM was assessed. The RCM of diethyldiallyl malonate and of diallyl sulfide was evaluated at 70 °C using 5 mol % Ru (conditions similar to other studies),^{25a} and monitored by ¹H NMR spectroscopy. To our surprise, no ring-closing product, catalyst decomposition or substrate consumption was observed and the diagnostic downfield resonances at δ 16.5 ppm was still visible in the ¹H NMR spectrum after 1 hour.

In an attempt to gain a deeper understanding of the newly formed product, and to perhaps develop structure-property relationships, our attention was turned towards growing X-ray quality crystals. X-ray quality crystals were grown from a solution NMR sample of what was thought to be compound **4.1** in CDCl₃. The product crystallized as gold needles in the P21/n space group. Surprisingly, the solid-state structure was very different from the expected product. The actual product, complex **4.2**, is a dicationic ruthenium metal centre with a distorted octahedral geometry. The complex consists of a benzyl substituted ligand, the coordinated iminic moiety of the former C[^]Imine ligand and four coordinated MeCN molecules. This unique molecule was consistent with combustion analysis (Figure 4.5).

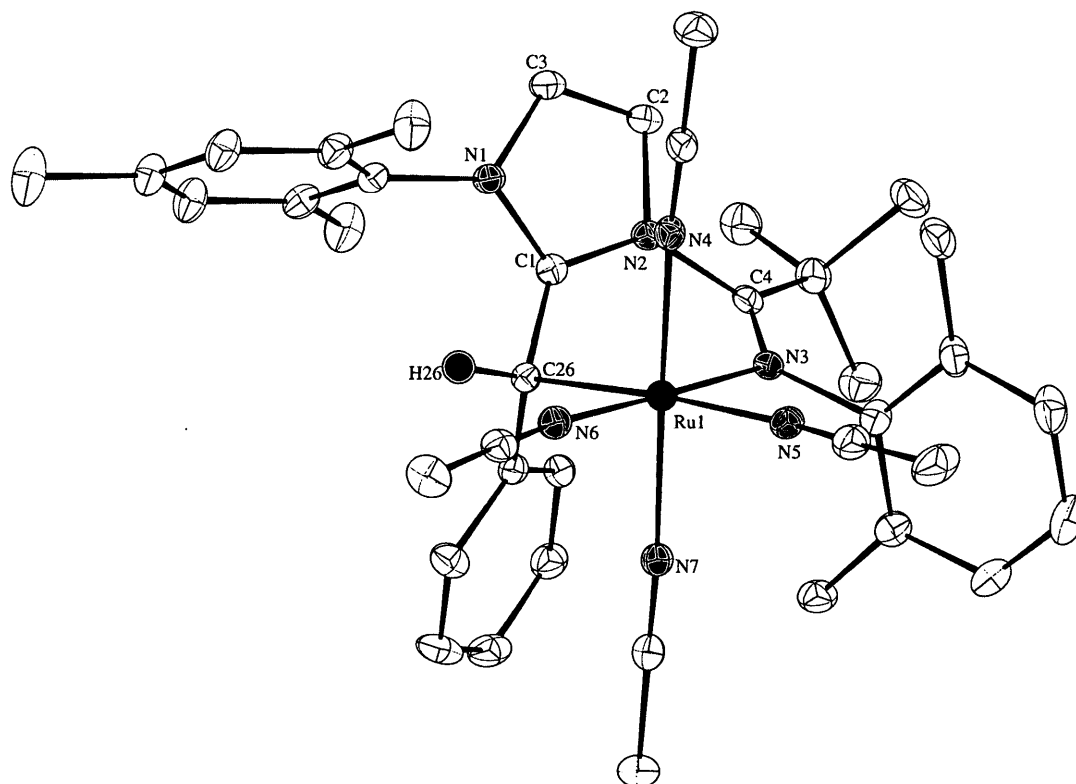


Figure 4.5. ORTEP plot (50% probability level) of 4.2. Two hexafluorophosphate anions, two chloroform- d_1 free solvent molecules and most hydrogen atoms are omitted for clarity reasons.

Most notable is the presence of an sp^3 -hybridized carbon atom (C26), with bond angles for C1–C26–C27, C1–C26–Ru1, C1–C26–Ru1, C1–C26–H26 and C27–C26–H26 determined to be 118.3(3), 98.0(2), 115.8(3), 105(3) and 113(3) $^\circ$, respectively (Table 4.1). The ruthenium-nitrogen bond lengths of the coordinated acetonitrile molecules range from 2.006(3)–2.094(4), with the longest bond length trans to the alkyl group; a likely result of a strong trans influence.

Table 4.1. Selected bond lengths and bond angles for compound 4.2

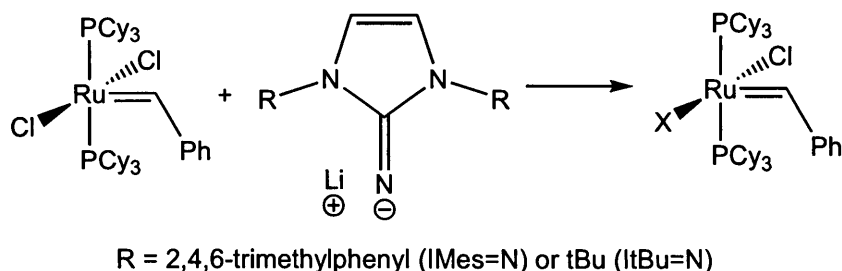
Selected Bond Lengths (Å)		Selected Bond Angles (deg)	
C(1)–C(26)	1.438(5)	C(1)–C(26)–C(27)	118.3(3)
C(1)–N(2)	1.364(5)	C(1)–C(26)–Ru(1)	98.0(2)
C(1)–N(1)	1.345(5)	C(1)–C(26)–Ru(1)	115.8(3)
C(26)–Ru(1)	2.184(4)	C(1)–C(26)–H(26)	105(3)
C(26)–C(27)	1.502(5)	C(27)–C(26)–H(26)	113(3)
N(3)–Ru(1)	2.130(3)	N(6)–Ru(1)–N(4)	90.50(14)
N(4)–Ru(1)	2.030(3)	N(6)–Ru(1)–C(26)	90.57(14)
N(5)–Ru(1)	2.094(4)	N(7)–Ru(1)–C(26)	89.30(14)
N(6)–Ru(1)	2.028(4)	N(4)–Ru(1)–N(3)	89.15(13)
N(7)–Ru(1)	2.006(3)	N(4)–Ru(1)–N(5)	87.31(13)
		N(6)–Ru(1)–N(5)	87.25(14)

The synthesis and characterization of this complex is quite remarkable and offers insight into the decomposition pathway of Grubbs-type ruthenium complexes. The decomposition pathway of Grubbs-type ruthenium catalysts has been extensively studied since the first isolation of ruthenium benzylidene complexes. Previous work into the intramolecular insertion of NHC substituents of Grubbs-type complexes has been observed experimentally²⁹ and investigated theoretically.³⁰ Despite the extensive experimental and theoretical investigations into the decomposition pathway, direct insertion of the benzylidene into a Ru-NHC bond, forming a ruthenium-benzyl complex has, to our knowledge, never been reported. It is clear that the formation of a cationic or dicationic metal centre from $\text{RuCl}_2(\text{C}^{\wedge}\text{Imine})(\text{CHPh})$ favours the migratory insertion of the NHC into the ruthenium benzylidene bond. As a result, there lies the possibility of other ruthenium alkylidene complexes undergoing decomposition via nucleophilic attack of the NHC on the benzylidene ligand for complexes with electron-poor metal centres. This new finding may help provide insight into the possible

decomposition pathway and the active species in alkene metathesis and possibly lead to tailoring ruthenium alkylidene catalysts to mitigate this nucleophilic attack, thus improving catalyst lifetime and productivity.

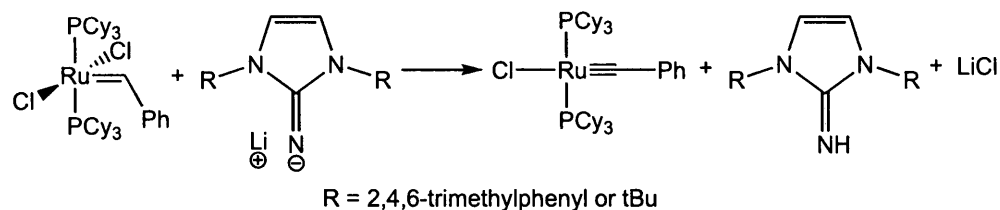
4.2.2. Synthesis and chemistry of ruthenium benzylidene complexes bearing an imidazol-2-imine ligand

Our group has become interested in incorporating the imidazol-2-imide ligand²⁶ into a Grubbs-type ruthenium metathesis catalyst. In an attempt to synthesize a new catalyst, we focused on replacing one or two halide(s) from Grubbs first-generation catalyst (GI) with an imidazol-2-imine ligand. Treating GI with one equivalent of either [IMes=N]Li or [tBu=N]Li resulted in a mixture of reaction products (Scheme 4.2).



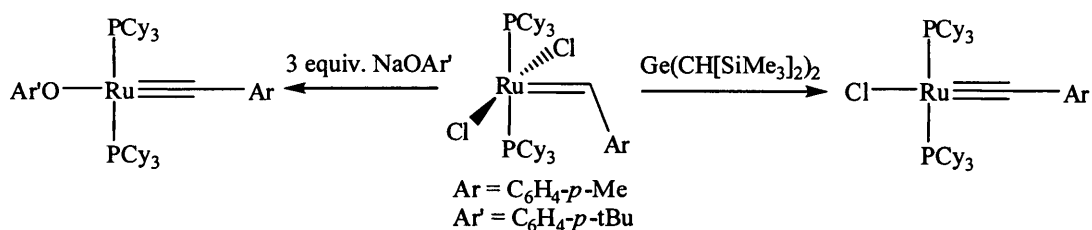
Scheme 4.2. Proposed synthetic strategy for forming RuCl(X)(PCy₃)₂(CHPh) (X = IMes=N or tBu=N)

In all cases, there was no distinct benzylidene proton observed in the ¹H NMR spectra. Also, there was protonated imidazol-2-imine present in the reaction mixtures. The presence of protonated imidazol-2-imine suggests the deprotonation of the benzylidene, which could lead to the formation of a ruthenium alkylidyne via dehydrohalogenation (Scheme 4.3).³¹



Scheme 4.3. Possible formation of a ruthenium alkylidyne complex

If the product was a ruthenium alkylidyne complex, then we would expect to see a new signal in the ^{31}P spectrum. Unfortunately, we only see free PCy_3 in the ^{31}P spectrum, thus indicating the absence of our intended benzylidene or alkylidyne product. A similar observation was recorded by Johnson with their attempts to react GI with $\text{Sn}(\text{CH}[\text{SiMe}_3]_2)_2$.^{31a}



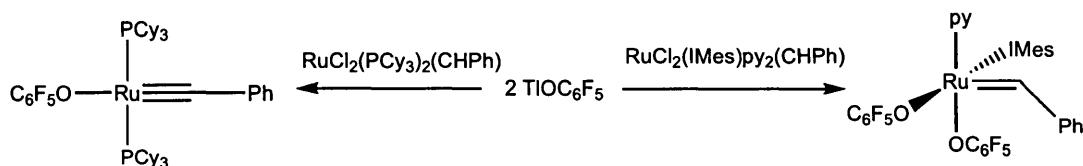
Scheme 4.4. Dehydrohalogenation of Grubbs first generation catalyst³¹

Attempts to treat GI with 2 equivalents of $[\text{IMes}=\text{N}]\text{Li}$ or $[\text{t}^i\text{Bu}=\text{N}]\text{Li}$ in hopes of synthesizing the halide-free alkylidyne complex were also unsuccessful.

At this point, we turned our attention towards treat $[\text{IMes}=\text{N}]\text{Li}$ or $[\text{t}^i\text{Bu}=\text{N}]\text{Li}$ with ruthenium benzylidene complexes bearing ancillary NHC ligands. Two ruthenium starting materials were used, $\text{RuCl}_2(\text{IMes})(\text{PCy}_3)(\text{CHPh})$ and $\text{RuCl}_2(\text{t}^i\text{Bu})(\text{PPh}_3)(\text{CHPh})$, and in both cases we see the disappearance of the benzylidene proton regardless of the stoichiometry. Unfortunately, no products in

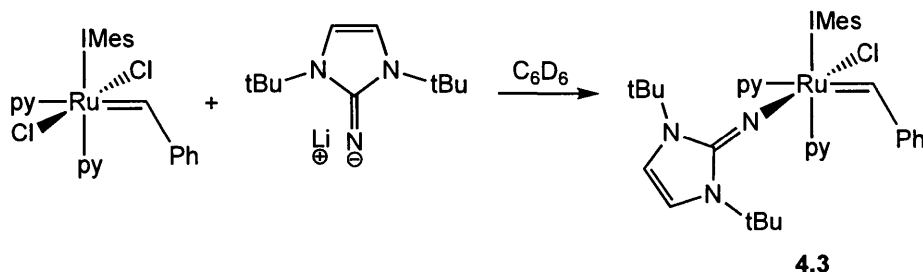
the reaction mixture could be isolated or crystallized in order to gain insight into their nature.

Despite the inability to synthesize a ruthenium benzylidene complex at this point, we decided to try using phosphine-free ruthenium benzylidene precursors. Fogg^{17b} has shown that, depending on the starting material, either the halide-free alkylidyne or substituted alkylidene can be synthesized and isolated (Scheme 4.5).



Scheme 4.5. Aryloxide selectivity based on metal precursor

Attempts to treat 2 equivalents of [IMes=N]Li or [tBu=N]Li with RuCl₂(IMes)py₂(CHPh) resulted in a mixture of reaction products and the absence of a benzylidene proton. However, adding 1 equivalent of [tBu=N]Li to RuCl₂(IMes)py₂(CHPh) in C₆D₆ resulted in the likely formation of RuCl(IMes)(tBu=N)py₂(CHPh) (**4.3**) (Scheme 4.6).

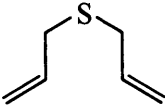
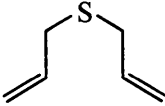
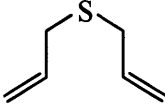
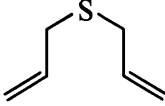
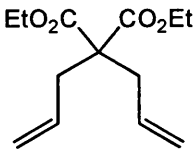
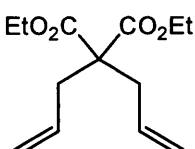


Scheme 4.6. Synthetic scheme to forming compound 4.3.

After five minutes, all the starting material was consumed and a new benzylidene proton resonance was observed downfield at δ 17.01 ppm. The aliphatic region of the ^1H NMR spectrum contained four major resonances at δ = 2.43, 2.22, 2.21 and 1.10 ppm, which correspond to the coordinated IMes and imidazol-2-imide methyl groups, respectively. The aromatic region contained from 8 resonances ranging 8.54 to 5.86 ppm, with some resonances being broad, an indication of fluxional behaviour. The reaction was monitored using NMR spectroscopy over a period of several hours. After 1.5 hours, the benzylidene proton resonance decreased by more than 80% while the broad resonances in the aliphatic region appeared. Attempts to acquire 2D HSQC, 2D HMBC and ^{13}C NMR spectra were unsuccessful due to decomposition in C_6D_6 . A variety of other NMR solvents were used (CDCl_3 , CD_2Cl_2 , CD_3CN) to acquire the desired NMR spectra and in all cases, led to relatively quick decomposition. Despite the incomplete characterization of compound **4.3**, the catalytic activity towards ring-closing metathesis was tested. The catalyst was prepared fresh in C_6D_6 , dried and redissolved in CDCl_3 prior to each catalytic run without any purification. Due to the observed decomposition of the complex at room temperature in solution, we decided to test the activity towards RCM of diallyl sulfide at room temperature. After 90 mins, no ring-closing product was observed. In light of the inactivity at room temperature, the RCM activity was tested at 70 °C. After 30 mins at 70 °C with 5 % mol catalyst, greater than 99.9% conversion of diallyl sulfide to the RCM product was observed. The activity of this complex showed promise because the

RCM activity of $\text{RuCl}_2(\text{IMes})\text{PCy}_3(\text{CHPh})$ was tested under the same conditions and yielded only 36% RCM product (Table 4.2). At lower catalyst loading (1 mol %) for complex **4.3**, we see a 48% conversion after 20 minutes at 70 °C for RCM of diallyl sulfide.

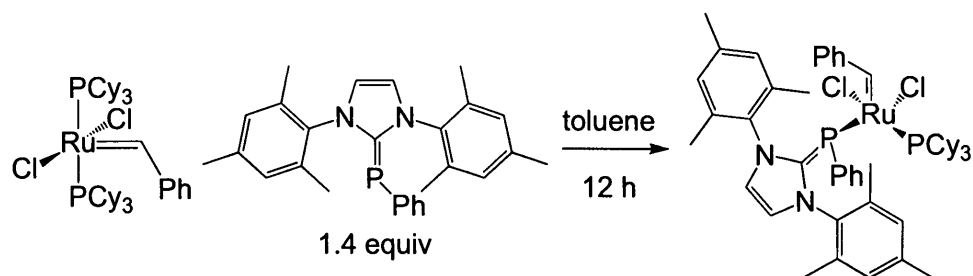
Table 4.2: Catalytic activity of ruthenium metathesis catalysts in CDCl_3

Substrate	Catalyst	mol % Ru	Conditions	% Product
	4.3	5	90 min, 23 °C	0%
	4.3	5	30 min, 70 °C	>99.9%
	4.3	1	20 min, 70 °C	48%
	$\text{RuCl}_2(\text{IMes})\text{PCy}_3(\text{CHPh})$	5	30 min, 70 °C	36%
	4.3	5	20 min, 70 °C	50%
	$\text{RuCl}_2(\text{IMes})\text{PCy}_3(\text{CHPh})$	5	20 min, 70 °C	>99.9%

On the other hand, the RCM yield with diethyl diallylmalonate for compound **4.3** was lower (50% conversion) than $\text{RuCl}_2(\text{IMes})\text{PCy}_3(\text{CHPh})$ (>99.9% conversion) after 20 minutes at 70 °C with a 5 mol % catalyst loading. The preliminary catalytic results for **4.3** are quite lower than other known ruthenium alkylidenes containing aryloxides.^{25a} These results are not surprising, considering that complex **4.3** undergoes decomposition under mild conditions and one would assume that the catalyst lifetime of this complex would be short-lived. In order to truly assess the potential catalytic application of ruthenium alkylidene complexes bearing imidazol-2-imide ancillary ligands towards olefin metathesis, we would need to synthesize and isolate more robust precatalysts.

4.2.3. Synthesis and chemistry of ruthenium benzylidene complexes bearing NHC-phosphinidene ligands

In an attempt to synthesize a Grubbs-type complex bearing the 1,3-bis(2,4,6-trimethylphenyl)imidazol-2-ylidene-phenylphosphinidene ($\text{IMes}=\text{PPh}$)^{27a} ligand as a potential catalyst for metathesis, we decided to treat GI with an excess of $\text{IMes}=\text{PPh}$ (Scheme 4.6).



Scheme 4.6. Proposed synthetic route to forming



To our surprise, the solution ^1H NMR spectrum of the product was not consistent with the desired compound. Most notable was the absence of the distinctive benzyldiene proton in the downfield range of 15 to 20 ppm. In addition, the proton signals were mainly broad singlets, suggesting fluxional behaviour. In an attempt to gain further insight into the identity of the isolated product, our attention was turned towards growing X-ray quality crystals for crystallographic analysis. Fortunately, X-ray quality crystals were isolated via slow liquid diffusion of diethyl ether into a saturated THF solution. They crystallized in the $P21/n$ space group. As expected, I did not see the desired product, but rather a decomposition product containing components of the intended target (Figure 4.6).

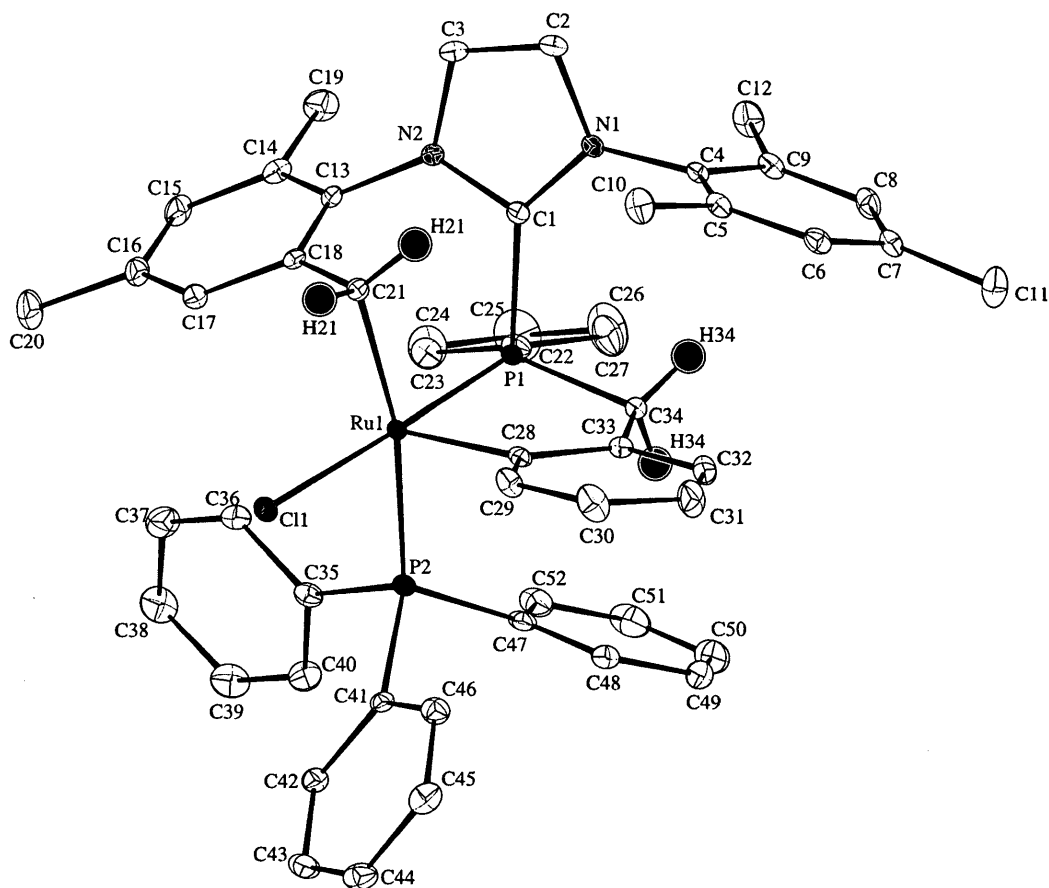


Figure 4.6. ORTEP plot (30% probability level) of 4.4.

Most hydrogens were omitted for clarity.

Table 4.3. Selected bond lengths and bond angles for compound 4.4

Selected Bond Lengths (Å)		Selected Bond Angles (deg)	
C1–N1	1.352(3)	C34–P1–C22	104.51(10)
C1–N2	1.355(3)	C34–P1–C1	107.02(10)
C1–P1	1.883(2)	C22–P1–C1	95.67(9)
Ru–Cl1	2.4899(7)	C34–P1–Ru1	107.88(7)
P1–Ru1	2.1844(6)	C28–Ru1–C21	94.09(8)
P2–Ru1	2.3464(7)	C28–Ru1–P1	80.51(6)
C28–Ru1	2.035(2)	P1–Ru1–P2	95.21(3)
C21–Ru1	2.157(2)	P2–Ru1–Cl1	86.85(3)
C22–P1	1.842(2)	P1–Ru1–Cl1	177.83(2)
C34–P1	1.839(2)	Ru1–C21–C18	89.8(1)

There are a few noteworthy observations for the X-ray structure. There are two instances in which C-H bond activation occurred. The metal centre adopts a distorted square pyramidal geometry with the apical site being occupied by C28. Interestingly, there is a five-membered metallacycle with a bite angle of $90.51(6)^\circ$ (C28–Ru1–P1). The long P1–Ru1 bond length of $2.1844(6) \text{ \AA}$ shows that there is significant single bond character for this ligand. The sp^3 carbon C34 corresponds to the former benzylidene carbon and contains two hydrogen atoms located on the density map. Lastly, we see an acute Ru1–C21–C18 bond angle of $89.8(1)^\circ$, which is considerably smaller than similar bond angles reported.^{30b,32} It is important to note that the coordination of PPh_3 is likely a result of fortuitous free PPh_3 from the starting materials. The corresponding PCy_3 decomposition product was isolated and characterized by using vigorously purified starting material. As discussed in Section 4.2.1, there have been considerable experimental²⁹ and theoretical³⁰ studies into the decomposition of Grubbs-type ruthenium catalysts and numerous examples of C-H bond activation of NHC substituents on ruthenium.^{30b,32} We believe that the decomposition of the product is initiated by the migratory insertion of the IMes=PPh ligand on the benzylidene carbon, followed by cyclometallation of the *o*-methyl group of the mesityl ring. A reductive elimination then occurs, followed by another cyclometallation and then the release of HCl (Figure 4.7).

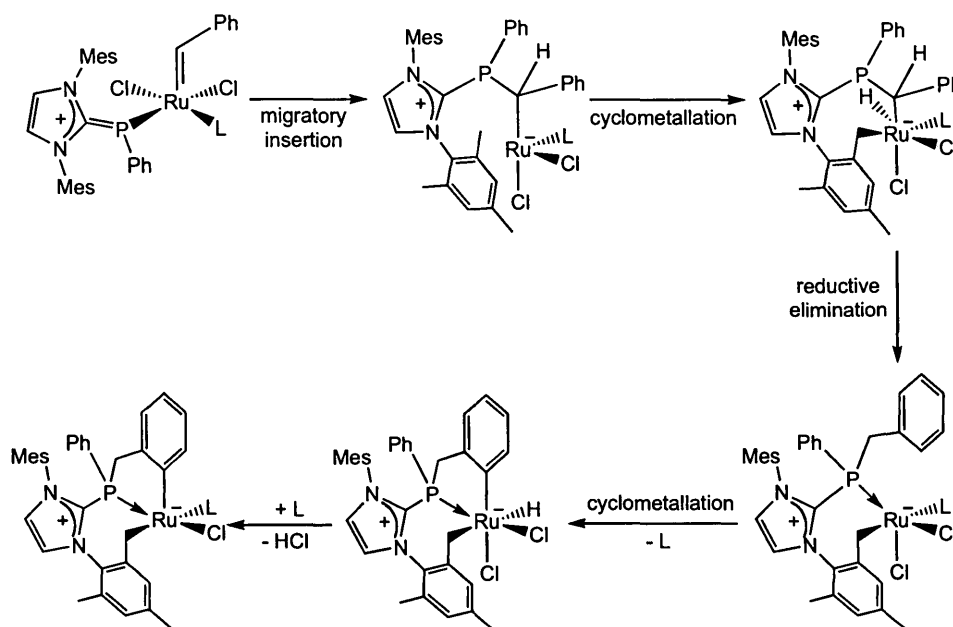
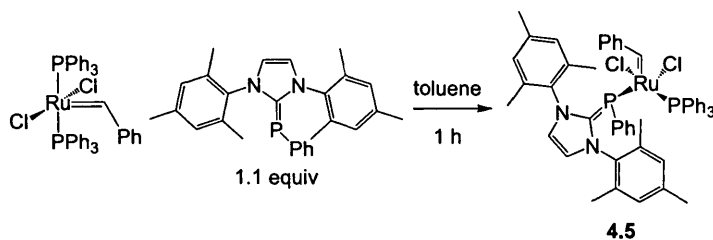


Figure 4.7. Proposed decomposition pathway of $\text{RuCl}_2(\text{IMes}=\text{PPh})(\text{PCy}_3)(\text{CHPh})$

An usual imidazolium benzylidene complex was reported recently, for which the authors suggest nucleophilic attack on the alkylidene carbon by a silver-NHC adduct.^{30d} Interestingly, treating $\text{RuCl}_2(\text{PPh}_3)_2(\text{CHPh})$ with a slight excess of $\text{IMes}=\text{PPh}$ in toluene at room temperature under nitrogen for one hour afforded a yellow-brown solution with a light brown precipitate (Scheme 4.7).



Scheme 4.7. Synthetic strategy for $\text{RuCl}_2(\text{IMes}=\text{PPh})(\text{PPh}_3)(\text{CHPh})$, 4.5

The solution was filtered, dried and recrystallized from pentane and dichloromethane to yield dark crystals of the desired compound. Solution ^1H NMR spectrum of the product was consistent with the desired compound with the benzyldiene proton resonating at δ 15.48 ppm as a doublet of doublets, a result of coupling to the two inequivalent phosphine atoms. The corresponding benzyldiene carbon resonates at δ 299.7 ppm, while the $^{31}\text{P}\{^1\text{H}\}$ spectrum contains two singlets at δ 64.8 and 37.4 ppm.

Crystals suitable for X-ray diffraction analysis were grown from slow liquid diffusion of pentane into a saturated dichloromethane solution and crystallized in the $C2/c$ space group (Figure 4.8). The crystal structure was consistent with the desired product. Its metal centre adopts a distorted square-pyramidal coordination with almost linear Cl2-Ru-P2 and Cl1-Ru-P1 bond angles of $168.06(2)^\circ$ and $158.18(2)^\circ$, respectively. The Ru-Cl2 and Ru-Cl1 bond lengths were determined to be $2.4012(6)$ and $2.3925(6)$ Å, respectively. Interestingly, we see a C1-P1 bond length of $1.847(2)$ Å, indicating significant single bond character, likely a result of electron delocalization from theazole nitrogen atoms to the phosphorus atom. The Ru-P1 and Ru-P2 bond lengths were determined to be $2.3643(7)$ and $2.3272(6)$ Å, respectively. Surprisingly, the chloride ligands adopt a cis arrangement, atypical to ruthenium alkylidene complexes without a bidentate ligand.^{10a,17b,33}

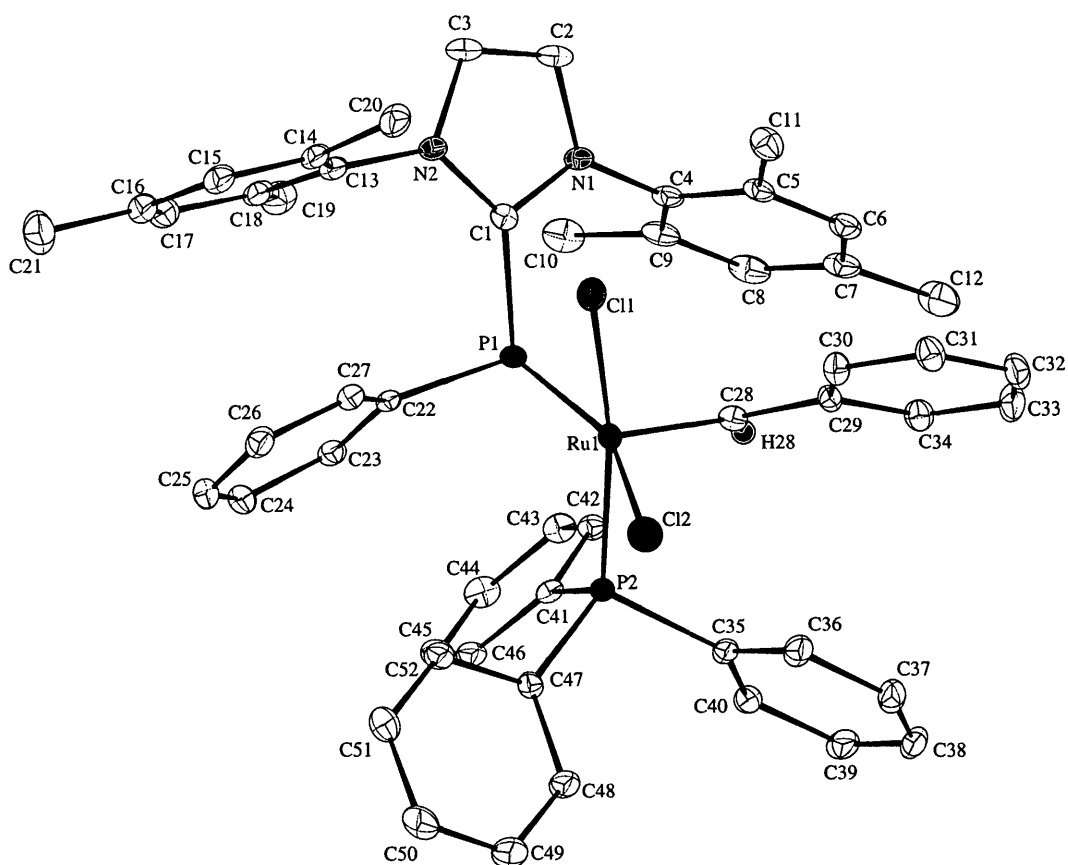


Figure 4.8. ORTEP plot (30% probability level) of 4.5. Most hydrogens and 1 molecule of dichloromethane were omitted for clarity.

Table 4.3. Selected bond lengths and angles for compounds 4.5

Selected Bond Lengths (Å)		Selected Bond Angles (deg)	
C1–N1	1.367(3)	C1–P1–Ru1	113.81(8)
C1–N2	1.361(3)	C22–P1–Ru1	98.20(8)
C1–P1	1.847(2)	C22–P1–C1	103.53(11)
Ru1–Cl1	2.3925(6)	C28–Ru1–P2	86.69(7)
Ru1–Cl2	2.4012(6)	C28–Ru1–P1	96.43(8)
P1–Ru1	2.3643(7)	P1–Ru1–P2	90.61(2)
P2–Ru1	2.3272(6)	P2–Ru1–Cl1	86.89(2)
C28–Ru1	1.841(3)		

One could argue that using a poorer electron-donating phosphine would result in the ruthenium metal centre being less electron-rich. Consequently, the metal

centre would accept more electron density from the alkylidene carbon and less π -backdonation to the carbon would result, thus making that carbon more electrophilic. In our case, it appears as though sterics, rather than electronics, played a crucial role in promoting the migratory insertion of the phosphalkene in the presence of excess reagent, thus triggering subsequent decomposition steps. The reaction between GI and IMes=PPh afforded the decomposition product **4.4**, when the tertiary phosphines in the starting material were PCy₃. On the other hand, RuCl₂(PPh₃)₂(CHPh) starting material containing sterically less demanding PPh₃, afforded the desired product (**4.5**).

Having synthesized and isolated a Grubbs-type carbene complex bearing the IMes=PPh ligand, we turned our attention towards the application of this complex towards Ring-Closing Metathesis (RCM). We decided to test the activity towards RCM of diallyl sulfide at room temperature. Surprisingly, no ring-closing product, catalyst decomposition or substrate consumption was observed and the diagnostic downfield resonances at δ 15.5 ppm was still visible in the ¹H NMR spectrum after 6 hours. In light of the inactivity at room temperature, the RCM activity was tested at 70 °C. Heating a sample of CDCl₃ solution containing diallyl sulfide and 5 mol % of catalyst to 70 °C for 1 hour resulted in no observable ring-closing and the complete conversion of complex **4.5** to a product with similar ¹H NMR chemical shifts as shown by the decomposition of the X-ray structure (**4.4**). The thermal stability of **4.5** at 70 °C was tested by heating the sample in CDCl₃ for 1 hour. Once again, the complex completely decomposed into a species with

^1H NMR resonances similar to that of **4.4**. These results, although disappointing, shows that the complex is susceptible to thermal decomposition under mild conditions. We are currently validating the decomposition mechanism of these complexes and developing NHC-phosphinidene ligand variants that would mitigate the nucleophilic attack of the alkylidene fragment.

4.3 Conclusions and Future Considerations

In an attempt to synthesize and isolate a cationic $[\text{RuCl}(\text{C}^{\wedge}\text{Imine})(\text{MeCN})(\text{CHPh})][\text{PF}_6]$ complex, we isolated an unusual decomposition product. The decomposition product was characterized and is the first example of a complex with direct insertion of the benzylidene into a Ru-NHC bond, forming a ruthenium-benzyl complex (**4.2**).

The application of imidazol-2-imide ligands as ancillary ligands on Grubbs-type ruthenium metathesis catalysts were investigated. A partially characterized ruthenium complex, $\text{RuCl}(\text{IMes})(\text{t}^{\text{Bu}}\text{=N})\text{py}(\text{CHPh})$ (**4.3**), showed promising results for the ring-closing metathesis of diallyl sulfide. Studies into the stability of these complexes are currently being conducted and the synthesis and isolation of other novel Grubbs-type metathesis catalysts are being explored.

The successful synthesis and isolation of a Grubbs-type ruthenium alkylidene complex bearing the $\text{IMes}=\text{PPh}$ was reported (**4.5**). An interesting decomposition product was also synthesized and characterized (**4.4**), providing insight into the decomposition pathway of Grubbs-type complexes. We are currently exploring the decomposition mechanism of these complexes and

developing NHC-phosphinidene ligand variants that would mitigate decomposition.

4.4 Experimental

4.4.1 General Considerations

All manipulations were performed under a dinitrogen atmosphere in a drybox or using standard Schlenk techniques. Solvents used in the preparation of air and/or moisture sensitive compounds were dried using an MBraun Solvent Purification System fitted with alumina columns and stored over molecular sieves under a positive pressure of argon. Toluene for polymerization was distilled under argon after being dried with the MBraun SPS. Deuterated solvents were degassed using three freeze-pump-thaw cycles. C_6D_6 and $CDCl_3$ were vacuum distilled from sodium and CaH_2 , respectively, and stored under dinitrogen. NMR spectra were recorded on a Bruker DRX 600 (1H at 600 MHz, ^{13}C at 150.9 MHz), Bruker AV 400 (1H at 400 MHz, ^{13}C at 100 MHz, ^{31}P at 161 MHz) or Bruker AV 300 (1H at 300 MHz, ^{13}C at 75.5 MHz, ^{31}P at 81 MHz) spectrometer and are at room temperature unless otherwise stated. The spectra were referenced internally relative to the residual protio-solvent (1H) and solvent (^{13}C) resonances and chemical shifts were reported with respect to $\delta = 0$ for tetramethylsilane. The ^{31}P spectra were referenced externally with 85% H_3PO_4 .

All metal precursors were purchased from either BDH or Sigma-Aldrich. Deuterated NMR solvents were purchased from Cambridge Isotope

Laboratories. Imidazol-2-imine²⁶ compounds and their derivatives, IMes=PPh,^{27a} RuCl₂(PCy₃)₂(CHPh),^{11b} RuCl₂(PPh₃)₂(CHPh),^{11b} RuCl₂(IMes)PCy₃(CHPh),³⁴ RuCl₂(^tBu)PPh₃(CHPh)³⁵ and RuCl₂(IMes)py₂(CHPh)^{25a} were prepared using published procedure.

4.4.2 Synthesis of [Ru(C[^]Imine)(MeCN)₄(CHPh)][PF₆]₂, 4.2

RuCl₂(C[^]Imine)(CHPh) (1) (41.7 mg, 65.6 μmol) was dissolved in a minimal amount of MeCN (5 mL). AgPF₆ (33.2 mg, 131 μmol) was added as a solid to the solution mixture. The solution was stirred for 4 h at room temperature, filtered and concentrated in vacuo. Diethyl ether was added until the product precipitated out of solution. Yield: 47 mg, 47 μmol, 72%. ¹H NMR (400 MHz, CDCl₃): δ = 16.5 (s, 1H, CHPh), 8.49 (s, 1H, NHCCN_(mesityl)), 8.13 (d, J = 7.0 Hz, 2H, *m*-CH_(2,6-xylyl)), 7.87 (t, J = 7.3 Hz, 1H, *p*-CH_(2,6-xylyl)), 7.63 (t, J = 7.8 Hz, 2H, *o*-CH_(phenyl)), 7.05 (s, 2H, *m*-CH_(mesityl)), 6.96 (m, 2H, *m*-CH_(phenyl)), 6.71 (d, J = 7.8 Hz, 1H, *p*-CH_(phenyl)), 6.63 (s, 1H, NCCHN_(mesityl)), 2.49 (br s, 3H, CH₃(MeCN)), 2.36 (s, 3H, *o*-CH₃(mesityl)), 2.18 (s, 3H, *p*-CH₃(mesityl)), 2.15 (s, 3H, *o*-CH₃(2,6-xylyl)), 2.02 (br s, 3H, CH₃(MeCN)), 1.87 (s, 3H, CH₃(MeCN)), 1.85 (s, 3H, CH₃(MeCN)), 1.59 (s, 9H, C(CH₃)₃(imine)), 1.49 (s, 3H, *o*-CH₃(2,6-xylyl)), 1.43 ppm (s, 3H, *o*-CH₃(mesityl)). ¹³C{¹H} NMR (100 MHz, CDCl₃): δ = 334.3 (CHPh), 189.8 (NCN(mesityl)), 172.3 (C=N), 151.2, 144, 139.9, 136.6 (*p*-CH_(2,6-xylyl)), 135.8, 134.8, 133.5 (*m*-CH_(2,6-xylyl)), 132.5, 130.3 (*o*-CH_(phenyl)), 129.5, 129.3 (*m*-CH_(phenyl)), 128.7 (NCCN_(mesityl)), 128.6 (C(CH₃)_(2,6-xylyl)), 128.3 (C(CH₃)_(2,6-xylyl)), 128.0 (*p*-CH_(phenyl)), 126.9, 124.58, 124.1 (*m*-CH_(mesityl)), 123.1 (NCCN_(mesityl)),

63.83, 41.1 (C(CH₃)₃(imine)), 30.1 (C(CH₃)₃(imine)), 20.74, 18.9, 18.3, 17.5, 17.2, 2.78, 1.87 ppm; elemental analysis calcd (%) for C₄₀H₄₉F₁₂N₇P₂Ru (%): C 47.15, H 4.85, N 9.62; found C 47.41, H 5.09, N 9.39.

4.4.6 Attempted synthesis of RuCl(IMes=N)(PCy₃)₂(CHPh)

[IMes=N]Li (0.032 mmol) in C₆D₆ was added to a C₆D₆ solution containing RuCl₂(PCy₃)₂(CHPh) (0.032 mmol). The solution immediately turned a dark reddish-green and was transferred to an NMR tube fitted with a rubber septum. The reaction was monitored using NMR spectroscopy over a period of several hours. During this time, the distinct alkylidene proton resonance decreases while the resonances corresponding to protonated imidazol-2-imine appears. A variety of different solvents were used including THF, pyridine and toluene and, in each case, it resulted in spectra containing a number of unidentified species and no alkylidene proton resonance.

4.4.7 Attempted synthesis of RuCl(IMes=N)(IMes)py(CHPh)

[IMes=N]Li (0.056 mmol) in C₆D₆ was added to a C₆D₆ solution containing RuCl₂(IMes)py₂(CHPh) (0.056 mmol). The solution immediately turned a dark reddish-green and was transferred to an NMR tube fitted with a rubber septum. The reaction was monitored using NMR spectroscopy over a period of several hours. During this time, the distinct alkylidene proton resonance decreases while the resonances corresponding to protonated imidazol-2-imine appears. A variety of different solvents were used including THF, pyridine and toluene and, in each case, it resulted in spectra containing

a number of unidentified species and no alkylidene proton resonance.

4.4.8 Attempted synthesis of RuCl(^tBu=N)(PCy₃)₂(CHPh)

[^tBu=N]Li (0.046 mmol) in C₆D₆ was added to a C₆D₆ solution containing RuCl₂(PCy₃)₂(CHPh) (0.046 mmol). The solution immediately turned a dark green and was transferred to an NMR tube fitted with a rubber septum. The reaction was monitored using NMR spectroscopy over a period of several hours. During this time, the distinct alkylidene proton resonance decreases while the resonances corresponding to protonated imidazol-2-imine appears. In the ³¹P spectra, there are two observed resonances corresponding to the starting material and free PCy₃. The reaction was repeated using THF and pyridine and similar spectra was obtained. Attempts to isolate the unidentified species in the reaction mixture were unsuccessful.

4.4.9 Attempted synthesis of Ru(^tBu=N)(PCy₃)₂(CPh)

[^tBu=N]Li (0.060 mmol) in C₆D₆ was added to a C₆D₆ solution containing RuCl₂(PCy₃)₂(CHPh) (0.030 mmol). The solution immediately turned a dark green and was transferred to an NMR tube fitted with a rubber septum. The reaction was monitored using NMR spectroscopy over a period of several hours. During this time, the distinct alkylidene proton resonance decreases while the resonances corresponding to protonated imidazol-2-imine appears. In the ³¹P spectra, there are two observed resonances corresponding to the starting material and free PCy₃. After 24 h, only free PCy₃ was observed in the ³¹P spectrum. The reaction was repeated using

THF and the solution was allowed to stir for 24 hours. At this time, only free PCy₃ was observed in the ³¹P NMR spectrum. In all cases, attempts to isolate the unidentified species in the reaction mixture were unsuccessful.

4.4.10 Synthesis of RuCl(IMes)(^tBu=N)py₂(CHPh), 4.3

[^tBu=N]Li (0.089 mmol) in C₆D₆ was added to a C₆D₆ solution containing RuCl₂(IMes)py₂(CHPh) (0.089 mmol). The solution immediately turned a dark green and was transferred to an NMR tube fitted with a rubber septum. After 15 minutes, all the starting material was consumed. ¹H NMR (300 MHz, CDCl₃): δ 17.09 (s, 1H), 8.54 (br s, 5H), 7.82 (br s, 2H), 7.11 (s, 3H), 6.96 (m, 5H), 6.73 (s, 2H), 6.62 (br s, 5H), 6.32 (s, 2H), 5.86 (s, 2H), 2.43 (s, 6H), 2.22 (s, 6H), 2.21 (s, 6H), 1.13 (s, 18 H).

4.4.11 Attempted Synthesis of RuCl₂(IMes=PPh)(PCy₃)(CHPh), 4.4

A toluene solution of IMes=PPh (67.1 mg, 157 μmol) was added slowly over one minute to a toluene solution (5 mL) of RuCl₂(PCy₃)₂(CHPh) (92.7 mg, 112 μmol). The solution was allowed to stir for 12 hours at room temperature. During this time, the solution turned from purple to brown with the formation of a light brown precipitate. The solution was dried under reduced pressure. The product was recrystallized from pentane and dichloromethane to yield a light brown powder (85.7 mg, 82.8%). Crystals suitable for X-ray diffraction study were grown at room temperature under nitrogen by slow liquid diffusion of diethyl ether into a saturated THF solution. ¹H NMR (400 MHz, CDCl₃): δ 11.00 (s, 1H), 8.11 (m, 2H), 7.66 (br s, 1H), 7.60 (s, 2H), 7.01 (s, 4H), 6.83 (br s, 2H), 2.57 (s, 3H),

2.18 (s, 12H), 1.76-0.90 (m, 30H). Anal. Calcd. for $C_{52}H_{67}ClN_2P_2Ru$ (%): C, 67.99; H, 7.35; N, 3.05. Found (%): C, 68.28; H, 7.53; N, 2.77.

4.4.12 Synthesis of $RuCl_2(IMes=PPh)(PPh_3)(CHPh)$, 4.5

A toluene solution of $IMes=PPh$ (30.1 mg, 73.0 μ mol) was added slowly over one minute to a toluene solution (5 mL) of $RuCl_2(PPh_3)_2(CHPh)$ (52.1 mg, 66.2 μ mol). The solution was allowed to stir for 1 hour at room temperature. During this time, the solution turned from purple to yellowish brown with the formation of a light brown precipitate. The solution was filtered and dried under reduced pressure. Recrystallization by slow liquid diffusion of pentane into a saturated dichloromethane solution at -35 °C afforded dark brown crystals (37.4 mg, 60.3%). 1H NMR (400 MHz, $CDCl_3$): δ 15.48 (dd, $J = 9.2, 8.7$ Hz, 1H, $CHPh$), 8.14 (d, $J = 7.4$ Hz, 1H), 7.62-7.44 (m, 5H), 7.08-6.65 (m, 18H), 6.56 (t, $J = 9.2, 2H$), 6.47 (br s, 2H), 6.19 (br s, 1H), 5.97 (br s, 1H), 2.54 (br s, 3H), 2.29 (br s, 3H), 2.24 (br s, 3H), 2.10 (br s, 3H), 1.60 (br s, 6H). $^{13}C\{^1H\}$ NMR (100 MHz, $CDCl_3$): δ 299.7 ($CHPh$), 169.6, 168.3, 150.93, 141.15, 21.1-20.5, 19.4-19.0, 18.5, 17.9. $^{31}P\{^1H\}$ (121 MHz, $CDCl_3$): δ 64.8 (s), 37.4 (s). Anal. Calcd. for $C_{52}H_{50}Cl_2N_2P_2Ru$ (%): C, 66.66; H, 5.38; N, 2.99. Found (%): C, 66.46; H, 5.60; N, 2.92.

Decomposition Product, 4.5a

The brown precipitate that was accumulated during the filtration step in the synthesis of 4.5 was washed thoroughly with toluene and diethyl ether. The light brown product was dried in vacuo (17.8 mg, 29.9%). 1H NMR (400 MHz, $CDCl_3$):

δ 11.09 (s, 1H), 8.11 (m, 1H), 7.33-7.18 (m), 7.01 (s, 4H), 6.83 (br s, 2H), 2.34 (s, 6H), 2.20 (s, 9H), 2.01 (br s, 2H). Anal. Calcd. for C₅₂H₄₉ClN₂P₂Ru (%): C, 69.10; H, 5.49; N, 3.11. Found (%): C, 69.10; H, 5.50; N, 2.96.

4.4.14 Ring-closing metathesis

The catalyst (0.006 mmol) was dissolved in CDCl₃ (0.5 mL). The solution was added to either an NMR tube fitted with a rubber septum or a scintillation vial fitted with a rubber septum. The neat substrate was added via syringe and the reaction vessel was either placed in a hot oil bath at 70 °C or left at room temperature. Reaction products were analyzed via solution ¹H NMR spectroscopy.

4.5 References

- 1 a) R. H. Grubbs, *Tetrahedron* **2004**, *60*, 7117; b) C. Samojlowicz, M. Bieniek and K. Grela, *Chem Rev* **2009**, *109*, 3708; c) Y. Schrodi and R. L. Pederson, *Aldrichimica Acta* **2007**, *40*, 45; d) T. M. Trnka and R. H. Grubbs, *Acc. Chem. Res.* **2001**, *34*, 18; e) G. C. Vougioukalakis and R. H. Grubbs, *Chem. Rev.* **2010**, *110*, 1746.
- 2 a) R. H. Grubbs and S. Chang, *Tetrahedron* **1998**, *54*, 4413; b) M. J. Krische, *Proc. Natl. Acad. Sci. U. S. A.* **2010**, *107*, 3279; c) J. Prunet and L. Grimaud, **2010**, pp. 287; d) G. C. Vougioukalakis and R. H. Grubbs, *Chem. Rev.* **2009**, *110*, 1746; e) A. Wojtkielewicz, *Curr. Org. Synth.* **2013**, *10*, 43; f) A. K. Chatterjee, T.-L. Choi, D. P. Sanders and R. H. Grubbs, *J. Am. Chem. Soc.*

2003, 125, 11360; g) K. C. Nicolaou, P. G. Bulger and D. Sarlah, *Angew. Chem., Int. Ed.* **2005**, 44, 4490.

3 a) M. R. Buchmeiser, *Chem. Rev.* **2000**, 100, 1565; b) W. J. Feast and E. Khosravi, *J. Fluorine Chem.* **1999**, 100, 117; c) R. H. Grubbs and E. Khosravi, **1999**, pp. 65; d) A. Hafner, d. S. P. A. van and A. Muehlebach, *Chimia* **1996**, 50, 131; e) A. Leitgeb, J. Wappel and C. Slugovc, *Polymer* **2010**, 51, 2927; f) O. Nuyken and S. D. Pask, *Polymers* **2013**, 5, 361; g) C. Pariya, K. N. Jayaprakash and A. Sarkar, *Coord. Chem. Rev.* **1998**, 168, 1; h) R. R. Schrock, *Top. Organomet. Chem.* **1998**, 1, 1.

4 a) J. M. Berlin, K. Campbell, T. Ritter, T. W. Funk, A. Chlenov and R. H. Grubbs, *Org. Lett.* **2007**, 9, 1339; b) R. H. Grubbs, S. J. Miller and G. C. Fu, *Acc. Chem. Res.* **1995**, 28, 446; c) A. J. Phillips and A. D. Abell, *Aldrichimica Acta* **1999**, 32, 75; d) S. K. Armstrong, *J. Chem. Soc., Perkin Trans. 1* **1998**, 371.

5 a) P. Atallah, K. B. Wagener and M. D. Schulz, *Macromolecules* Ahead of Print; b) T. W. Baughman and K. B. Wagener, *Adv. Polym. Sci.* **2005**, 176, 1; c) J. E. Schwendeman, A. C. Church and K. B. Wagener, *Adv. Synth. Catal.* **2002**, 344, 597.

6 a) S. J. Connon and S. Blechert, *Angew. Chem., Int. Ed.* **2003**, 42, 1900; b) G. D. Cuny and J. R. Hauske, *CHEMTECH* **1998**, 28, 25; c) C. L. Dwyer, **2006**, pp. 201; d) Y. Li, W. Zhao and X. Bai, *Jingxi Shiyou Huagong* **2007**, 24, 79; e) M. Mori, *Farumashia* **2002**, 38, 931; f) M. Schuster and S. Blechert, *Angew. Chem., Int. Ed.* **1997**, 36, 2037.

- 7 J.-L. Hérisson and Y. Chauvin, *Die Makromolekulare Chemie* **1971**, *141*, 161.
- 8 R. H. Grubbs, P. L. Burk and D. D. Carr, *J. Am. Chem. Soc.* **1975**, *97*, 3265.
- 9 a) K. Sato, *Org. Square* **2012**, *2*; b) R. R. Schrock, *Tetrahedron* **1999**, *55*, 8141; c) R. R. Schrock, *J. Mol. Catal. A: Chem.* **2004**, *213*, 21; d) R. R. Schrock, *Chem. N. Z.* **2011**, *75*, 117; e) R. R. Schrock, *Chem. Commun.* **2013**, *49*, 5529; f) R. R. Schrock and C. Czekelius, *Adv. Synth. Catal.* **2007**, *349*, 55; g) R. R. Schrock and A. H. Hoveyda, *Angew. Chem., Int. Ed.* **2003**, *42*, 4592; h) R. R. Schrock and A. H. Hoveyda, *Angew. Chem., Int. Ed.* **2003**, *42*, 4592.
- 10 a) X. Bantreil, A. Poater, C. A. Urbina-Blanco, Y. D. Bidal, L. Falivene, R. A. M. Randall, L. Cavallo, A. M. Z. Slawin and C. S. J. Cazin, *Organometallics* **2012**, *31*, 7415; b) H. Clavier and S. P. Nolan, *Chem. - Eur. J.* **2007**, *13*, 8029; c) E. Despagnet-Ayoub and T. Ritter, *Top. Organomet. Chem.* **2007**, *21*, 193; d) M. S. Sanford, J. A. Love and R. H. Grubbs, *Organometallics* **2001**, *20*, 5314.
- 11 a) P. Schwab, M. B. France, J. W. Ziller and R. H. Grubbs, *Angew. Chem., Int. Ed.* **1995**, *34*, 2039; b) P. Schwab, R. H. Grubbs and J. W. Ziller, *J. Am. Chem. Soc.* **1996**, *118*, 100.
- 12 a) L. Vieille-Petit, H. Clavier, A. Linden, S. Blumentritt, S. P. Nolan and R. Dorta, *Organometallics* **2010**, *29*, 775; b) L. Vieille-Petit, X. Luan, M. Gatti, S. Blumentritt, A. Linden, H. Clavier, S. P. Nolan and R. Dorta, *Chem. Commun.* **2009**, 3783.
- 13 K. M. Kuhn, J.-B. Bourg, C. K. Chung, S. C. Virgil and R. H. Grubbs, *J. Am. Chem. Soc.* **2009**, *131*, 5313.

- 14 V. Dragutan, I. Dragutan and A. Demonceau, *Platinum Met. Rev.* **2005**, *49*, 123.
- 15 J. Huang, E. D. Stevens, S. P. Nolan and J. L. Petersen, *J. Am. Chem. Soc.* **1999**, *121*, 2674.
- 16 a) M. S. Sanford, J. A. Love and R. H. Grubbs, *Organometallics* **2001**, *20*, 5314; b) J. A. Love, J. P. Morgan, T. M. Trnka and R. H. Grubbs, *Angew. Chem., Int. Ed.* **2002**, *41*, 4035.
- 17 a) W. Buchowicz, A. Makal and K. Wozniak, *J. Organomet. Chem.* **2009**, *694*, 3179; b) J. C. Conrad, D. Amoroso, P. Czechura, G. P. A. Yap and D. E. Fogg, *Organometallics* **2003**, *22*, 3634; c) P. S. Kumar, K. Wurst and M. R. Buchmeiser, *J. Am. Chem. Soc.* **2009**, *131*, 387; d) X. Miao, A. Blokhin, A. Pasynskii, S. Nefedov, S. Osipov, T. Roisnel, C. Bruneau and P. H. Dixneuf, *Organometallics* **2010**, *29*, 5257; e) K. Tanaka, V. P. W. Boehm, D. Chadwick, M. Roeper and D. C. Braddock, *Organometallics* **2006**, *25*, 5696; f) K. Vehlou, S. Maechling, K. Koehler and S. Blechert, *Tetrahedron Lett.* **2006**, *47*, 8617.
- 18 a) M. Ahr, C. Thieuleux, C. Coperet, B. Fenet and J.-M. Basset, *Adv. Synth. Catal.* **2007**, *349*, 1587; b) F. Boeda, H. Clavier and S. P. Nolan, *Chem. Commun.* **2008**, 2726; c) S. Gessler, S. Randl and S. Blechert, *Tetrahedron Lett.* **2000**, *41*, 9973; d) N. Ledoux, R. Drozdak, B. Allaert, A. Linden, D. V. P. Van and F. Verpoort, *Dalton Trans.* **2007**, 5201; e) S. E. Lehman, Jr. and K. B. Wagener, *Organometallics* **2005**, *24*, 1477; f) F. Nunez-Zarur, X. Solans-Monfort, L. Rodriguez-Santiago and M. Sodupe, *Organometallics* **2012**, *31*, 4203; g) H.-J.

Schanz, L. Jafarpour, E. D. Stevens and S. P. Nolan, *Organometallics* **1999**, *18*, 5187; h) V. Thiel, M. Hendann, K.-J. Wannowius and H. Plenio, *J. Am. Chem. Soc.* **2012**, *134*, 1104; i) C. A. Urbina-Blanco, A. Poater, T. Lebl, S. Manzini, A. M. Z. Slawin, L. Cavallo and S. P. Nolan, *J. Am. Chem. Soc.* **2013**, *135*, 7073.

19 S. Torker, A. Muller, R. Sigrist and P. Chen, *Organometallics* **2010**, *29*, 2735.

20 a) S. Chang, L. Jones, II, C. Wang, L. M. Henling and R. H. Grubbs, *Organometallics* **1998**, *17*, 3460; b) S. D. Drouin, H. M. Foucault, G. P. A. Yap and D. E. Fogg, *Can. J. Chem.* **2005**, *83*, 748; c) S. Monsaert, N. Ledoux, R. Drozdak and F. Verpoort, *J. Polym. Sci., Part A: Polym. Chem.* **2010**, *48*, 302; d) G. Occhipinti, H.-R. Bjorsvik, K. W. Toernroos and V. R. Jensen, *Organometallics* **2007**, *26*, 5803; e) J. S. M. Samec and R. H. Grubbs, *Chem. Commun.* **2007**, 2826; f) J.-C. Wasilke, G. Wu, X. Bu, G. Kehr and G. Erker, *Organometallics* **2005**, *24*, 4289.

21 a) J. M. Blacquiere, R. McDonald and D. E. Fogg, *Angew. Chem., Int. Ed.* **2010**, *49*, 3807; b) S. Monfette, K. D. Camm, S. I. Gorelsky and D. E. Fogg, *Organometallics* **2009**, *28*, 944; c) S. Monfette and D. E. Fogg, *Organometallics* **2006**, *25*, 1940.

22 a) M. Bieniek, R. Bujok, M. Cabaj, N. Lugan, G. Lavigne, D. Arlt and K. Grela, *J. Am. Chem. Soc.* **2006**, *128*, 13652; b) S. R. Dubberley, P. E. Romero, W. E. Piers, R. McDonald and M. Parvez, *Inorg. Chim. Acta* **2006**, *359*, 2658; c) A. Fuerstner, O. R. Thiel and C. W. Lehmann, *Organometallics* **2002**, *21*, 331; d) R. Gawin, A. Makal, K. Wozniak, M. Mauduit and K. Grela, *Angew. Chem., Int. Ed.*

2007, 46, 7206; e) A. Hejl, M. W. Day and R. H. Grubbs, *Organometallics* **2006**, 25, 6149; f) S. Kim, W. Hwang, I. S. Lim, S. H. Kim, S.-g. Lee and B. M. Kim, *Tetrahedron Lett.* **2010**, 51, 709; g) K. Zukowska, A. Szadkowska, A. E. Pazio, K. Wozniak and K. Grela, *Organometallics* **2012**, 31, 3814; h) K. Zukowska, A. Szadkowska, A. E. Pazio, K. Wozniak and K. Grela, *Organometallics* **2012**, 31, 462.

23 a) H. Jong, B. O. Patrick and M. D. Fryzuk, *Organometallics* **2011**, 30, 2333; b) C. L. Lund, M. J. Sgro and D. W. Stephan, *Organometallics* **2012**, 31, 580; c) E. Mothes, S. Sentets, M. A. Luquin, R. Mathieu, N. Lugan and G. Lavigne, *Organometallics* **2008**, 27, 1193; d) J. A. Wright, A. A. Danopoulos, W. B. Motherwell, R. J. Carroll and S. Ellwood, *J. Organomet. Chem.* **2006**, 691, 5204.

24 T. G. Larocque, A. C. Badaj, S. Dastgir and G. G. Lavoie, *Dalton Trans.* **2011**, 40, 12705.

25 a) J. C. Conrad, H. H. Parnas, J. L. Snelgrove and D. E. Fogg, *J. Am. Chem. Soc.* **2005**, 127, 11882; b) M. W. Kotyk, S. I. Gorelsky, J. C. Conrad, C. Carra and D. E. Fogg, *Organometallics* **2009**, 28, 5424; c) S. Monfette, J. M. Blacquiere, J. C. Conrad, N. J. Beach and D. E. Fogg, *NATO Sci. Ser., II* **2007**, 243, 79; d) S. Monfette, S. J. A. Duarte, S. I. Gorelsky, S. J. Dalgarno, S. E. N. dos, M. H. Araujo and D. E. Fogg, *Can. J. Chem.* **2009**, 87, 361.

26 a) M. Tamm, D. Petrovic, S. Randoll, S. Beer, T. Bannenberg, P. G. Jones and J. Grunenberg, *Org. Biomol. Chem.* **2007**, 5, 523; b) M. Tamm, S. Randoll,

E. Herdtweck, N. Kleigrew, G. Kehr, G. Erker and B. Rieger, *Dalton Trans.* **2006**, 459.

27 a) A. J. Arduengo, III, J. C. Calabrese, A. H. Cowley, H. V. R. Dias, J. R. Goerlich, W. J. Marshall and B. Riegel, *Inorg. Chem.* **1997**, *36*, 2151; b) O. Back, M. Henry-Ellinger, C. D. Martin, D. Martin and G. Bertrand, *Angew. Chem., Int. Ed.* **2013**, *52*, 2939.

28 A. Badaj and G. G. Lavoie, *unpublished work* **2013**.

29 a) B. R. Galan, K. P. Kalbarczyk, S. Szczepankiewicz, J. B. Keister and S. T. Diver, *Org. Lett.* **2007**, *9*, 1203; b) B. R. Galan, M. Pitak, M. Gembicky, J. B. Keister and S. T. Diver, *J. Am. Chem. Soc.* **2009**, *131*, 6822; c) F. Grisi, A. Mariconda, C. Costabile, V. Bertolasi and P. Longo, *Organometallics* **2009**, *28*, 4988; d) M. B. Herbert, Y. Lan, B. K. Keitz, P. Liu, K. Endo, M. W. Day, K. N. Houk and R. H. Grubbs, *J. Am. Chem. Soc.* **2012**, *134*, 7861; e) E. M. Leitao, S. R. Dubberley, W. E. Piers, Q. Wu and R. McDonald, *Chem. - Eur. J.* **2008**, *14*, 11565; f) T. M. Trnka, J. P. Morgan, M. S. Sanford, T. E. Wilhelm, M. Scholl, T.-L. Choi, S. Ding, M. W. Day and R. H. Grubbs, *J. Am. Chem. Soc.* **2003**, *125*, 2546. g) S. M. Hansen, F. Rominger, M. Metz and P. Hofmann, *Chem. - Eur. J.* **1999**, *5*, 557; h) H. Tsurugi, T. Ohno, T. Kanayama, R. A. Arteaga-Muller and K. Mashima, *Organometallics* **2009**, *28*, 1950.

30 a) J. Mathew, N. Koga and C. H. Suresh, *Organometallics* **2008**, *27*, 4666; b) A. Poater and L. Cavallo, *J. Mol. Catal. A: Chem.* **2010**, *324*, 75; c) A. Poater and

- L. Cavallo, *Theor. Chem. Acc.* **2012**, *131*, 1; d) G. Occhipinti, V. R. Jensen, K. W. Tornroos, N. A. Froeystein and H.-R. Bjoersvik, *Tetrahedron* **2009**, *65*, 7186.
- 31 a) S. R. Caskey, M. H. Stewart, Y. J. Ahn, M. J. A. Johnson and J. W. Kampf, *Organometallics* **2005**, *24*, 6074; b) S. R. Caskey, M. H. Stewart, Y. J. Ahn, M. J. A. Johnson, J. L. C. Rowsell and J. W. Kampf, *Organometallics* **2007**, *26*, 1912.
- 32 a) K. Abdur-Rashid, T. Fedorkiw, A. J. Lough and R. H. Morris, *Organometallics* **2004**, *23*, 86; b) M. J. Chilvers, R. F. R. Jazzar, M. F. Mahon and M. K. Whittlesey, *Adv. Synth. Catal.* **2003**, *345*, 1111.
- 33 a) X. Bantreil, T. E. Schmid, R. A. M. Randall, A. M. Z. Slawin and C. S. J. Cazin, *Chem. Commun.* **2010**, *46*, 7115; b) C. E. Diesendruck, E. Tzur, A. Ben-Asuly, I. Goldberg, B. F. Straub and N. G. Lemcoff, *Inorg. Chem.* **2009**, *48*, 10819; c) S. Pruehs, C. W. Lehmann and A. Fuerstner, *Organometallics* **2004**, *23*, 280; d) T. Ung, A. Hejl, R. H. Grubbs and Y. Schrodi, *Organometallics* **2004**, *23*, 5399.
- 34 K. Zhang, M. A. Lackey, J. Cui and G. N. Tew, *J. Am. Chem. Soc.* **2011**, *133*, 4140.
- 35 T. Weskamp, F. J. Kohl and W. A. Herrmann, *J. Organomet. Chem.* **1999**, *582*, 362.

Chapter 5 Conclusions and Future Work

The focus of this work was aimed at utilizing the unique reactivity of *N*-heterocyclic carbenes to develop novel, robust catalysts to mediate organic transformations. As overviewed in Chapter 1, the synthesis and coordination of NHCs has revolutionized the field of synthetic organometallic chemistry and homogenous catalysis. In addition, the reactivity of NHCs towards azides, chalcogens and pnictinidenes has resulted in unique classes of ligands with varying steric and electronic properties.

The reactivity of the aryl-substituted acyclic imino-*N*-heterocyclic carbene towards Group 4 and 6 transition metals was presented in Chapter 2. The catalytic activities of these complexes towards ethylene polymerization were explored. The zirconium and titanium complexes activities showed promise and warranted further tailoring of their coordination sphere. In an attempt to enhance the catalytic activity of the titanium complexes, we decided to synthesize titanium-C[^]imine complexes containing either two phenoxide ligands or one catecholate ligand. Unfortunately, the catalytic activities of these two complexes were lower than the corresponding titanium tetrachloride.

The reactivity of NHCs towards azides to form imidazole-2-imines presented the opportunity to synthesize a new monoanionic bidentate ligand with an imidazol-2-imine fragment incorporated into the ligand scaffold. The synthesis and coordination of this novel ligand class was explored in Chapter 3. Bis(ethenolate) and (cyclopentadienyl)(ethenolate) metal dichloride complexes

were successfully prepared and fully characterized. We see enhanced activity when there is a decrease in the electron-donating capabilities of the ligand through the inductive effect of a more electronegative atom in the ligand scaffold. As a result, future work could include exploring different substitution patterns on the ligand, testing the activity of these complexes towards ethylene polymerization, and developing structure-property relationships.

Chapter 4 of this thesis was a multifaceted approach to leverage our knowledge of NHCs and of their reactivity by developing new catalytically active ruthenium benzylidene complex. We first looked at synthesizing a cationic $[\text{RuCl}(\text{C}^{\wedge}\text{Imine})(\text{MeCN})(\text{CHPh})][\text{PF}_6]$ complex, but instead isolated an unusual decomposition product. Upon characterization, we discovered the first example of a complex with direct insertion of the benzylidene into a Ru-NHC bond, forming a ruthenium-benzyl complex. This structure offers insight into the potential decomposition pathway of ruthenium alkylidene catalysts and this information would be relevant to future catalyst design.

Investigations into the incorporation of the electron-rich imidazol-2-imide ligand with ruthenium benzylidene complexes were also presented in Chapter 4. A partially characterized ruthenium complex, $\text{RuCl}(\text{IMes})(\text{t}^{\text{Bu}}\text{N}=\text{N})\text{py}(\text{CHPh})$ showed promising results for the ring-closing metathesis of diallyl sulfide when freshly prepared. Future work could include utilizing imidazole-2-imine variants with less sterically demanding substituents and less electron-rich imides in hopes of synthesizing and isolating stable ruthenium benzylidene complexes.

Lastly, the successful synthesis and isolation of the first Grubbs-type ruthenium alkylidene complex bearing IMes=PPh was reported. An interesting decomposition product was also isolated and fully characterized. Interestingly, we see an unusual decomposition product upon coordination of the IMes=PPh ligand. Future work could include using less sterically demanding carbene-phosphinidene ligands to mitigate the nucleophilic attack on the benzylidene since we believe sterics, rather than electronics, plays a crucial role in promoting the migratory insertion of the phosphalkene, thus triggering the subsequent decomposition steps. If the trigger for decomposition could be determined, then perhaps a ligand variant could be utilized to mitigate decomposition and the catalytic activity of these complexes could be explored.

Supplementary Material

Table 6.1. Crystal data and structure refinement for compound 4.2.	138
Table 6.2. Atomic coordinates and equivalent isotropic displacement parameters for 4.2.	140
Table 6.3. Bond lengths and angles for 4.2.	144
Table 6.4. Anisotropic displacement parameters for 4.2.	160
Table 6.6. Crystal data and structure refinement for compound 4.4.	166
Table 6.7. Atomic coordinates and equivalent isotropic displacement parameters for compound 4.4.	168
Table 6.8. Bond lengths and angles for compound 4.4.	171
Table 6.9. Anisotropic displacement parameters for compound 4.4.	179
Table 6.11. Crystal data and structure refinement for compound 4.5.	185
Table 6.12. Atomic coordinates and equivalent isotropic displacement parameters for compound 4.5.	187
Table 6.13. Bond lengths and angles for compound 4.5.	190
Table 6.14. Anisotropic displacement parameters for compound 4.5.	199

Table 6.1. Crystal data and structure refinement for compound 4.2.

Identification code	d1397	
Empirical formula	C ₄₂ H ₅₁ Cl ₆ F ₁₂ N ₇ P ₂ Ru	
Formula weight	1257.61	
Temperature	150(2) K	
Wavelength	0.71073 Å	
Crystal system	Monoclinic	
Space group	P 21/n	
Unit cell dimensions	a = 16.913(3) Å	a = 90°.
	b = 15.631(2) Å	b = 95.168(3)°.
	c = 20.393(3) Å	g = 90°.
Volume	5369.4(14) Å ³	
Z	4	
Density (calculated)	1.554 Mg/m ³	
Absorption coefficient	0.730 mm ⁻¹	
F(000)	2540	
Crystal size	0.230 x 0.110 x 0.040 mm ³	
Theta range for data collection	1.50 to 27.57°.	
Index ranges	-21 ≤ h ≤ 21, -20 ≤ k ≤ 20, -23 ≤ l ≤ 26	
Reflections collected	47744	
Independent reflections	12360 [R(int) = 0.0488]	
Completeness to theta = 27.57°	99.6 %	

Absorption correction	Semi-empirical from equivalents
Max. and min. transmission	0.7456 and 0.6597
Refinement method	Full-matrix least-squares on F ²
Data / restraints / parameters	12360 / 0 / 643
Goodness-of-fit on F ²	1.029
Final R indices [I > 2σ(I)]	R1 = 0.0596, wR2 = 0.1534
R indices (all data)	R1 = 0.0858, wR2 = 0.1691
Largest diff. peak and hole	1.856 and -1.539 e.Å ⁻³

Table 6.2. Atomic coordinates ($\times 10^4$) and equivalent isotropic displacement parameters ($\text{\AA}^2 \times 10^3$) for 4.2. $U(\text{eq})$ is defined as one third of the trace of the orthogonalized U_{ij} tensor.

	x	y	z	$U(\text{eq})$
C(1)	798(2)	3251(2)	1318(2)	24(1)
C(1S)	6492(3)	-52(3)	785(2)	40(1)
C(2)	-128(3)	2931(3)	496(2)	32(1)
C(2S)	8652(3)	6715(4)	1965(3)	51(1)
C(3)	513(3)	3201(3)	227(2)	32(1)
C(4)	-474(2)	2592(3)	1639(2)	28(1)
C(5)	-1363(2)	2829(3)	1522(2)	34(1)
C(6)	-1729(3)	2977(4)	2177(2)	44(1)
C(7)	-1834(3)	2107(3)	1153(2)	43(1)
C(8)	-1497(3)	3678(3)	1134(2)	43(1)
C(9)	-536(3)	1502(3)	2471(2)	32(1)
C(10)	-630(3)	1672(3)	3132(2)	35(1)
C(11)	-904(3)	1007(3)	3510(2)	45(1)
C(12)	-1081(3)	211(4)	3247(3)	53(1)

C(13)	-1011(3)	66(3)	2591(3)	49(1)
C(14)	-731(3)	700(3)	2185(2)	37(1)
C(15)	-608(3)	464(3)	1486(2)	43(1)
C(16)	-501(3)	2535(3)	3449(2)	36(1)
C(17)	1805(2)	3881(3)	641(2)	28(1)
C(18)	1785(3)	4773(3)	699(2)	33(1)
C(19)	2471(3)	5225(3)	604(2)	40(1)
C(20)	3160(3)	4818(3)	450(2)	40(1)
C(21)	3157(3)	3943(3)	390(2)	38(1)
C(22)	2487(3)	3453(3)	483(2)	34(1)
C(23)	1029(3)	5228(3)	856(3)	46(1)
C(24)	3909(3)	5322(4)	364(3)	60(2)
C(25)	2518(3)	2492(3)	422(3)	47(1)
C(26)	1255(2)	3266(2)	1947(2)	23(1)
C(27)	1024(2)	3892(2)	2455(2)	26(1)
C(28)	275(2)	4243(3)	2473(2)	29(1)
C(29)	86(3)	4790(3)	2977(2)	37(1)
C(30)	664(3)	5008(3)	3472(2)	42(1)
C(31)	1417(3)	4691(3)	3451(2)	45(1)
C(32)	1606(3)	4147(3)	2948(2)	35(1)
C(33)	2997(3)	1704(3)	2411(2)	31(1)
C(34)	3844(3)	1584(3)	2559(3)	44(1)

C(35)	1078(3)	-46(3)	2674(2)	39(1)
C(36)	1066(4)	-926(3)	2900(3)	59(2)
C(37)	1368(3)	2402(3)	3697(2)	33(1)
C(38)	1481(3)	2659(4)	4383(2)	49(1)
C(39)	1080(3)	1167(3)	755(2)	31(1)
C(40)	1054(3)	773(3)	102(2)	44(1)
CI(1S)	7119(1)	451(1)	266(1)	51(1)
CI(2S)	5871(1)	-794(1)	351(1)	54(1)
CI(3S)	7069(1)	-560(1)	1429(1)	67(1)
CI(4S)	9306(1)	6109(1)	1524(1)	57(1)
CI(5S)	7949(1)	6032(2)	2261(2)	125(1)
CI(6S)	8255(2)	7560(2)	1513(1)	136(1)
F(1)	5129(2)	3443(3)	830(3)	112(2)
F(2)	5199(3)	2124(6)	408(3)	185(4)
F(3)	6250(2)	2729(3)	916(2)	86(1)
F(4)	5625(3)	1639(3)	1410(3)	127(2)
F(5)	5566(3)	2930(3)	1792(2)	93(1)
F(6)	4470(2)	2365(3)	1216(2)	88(1)
F(7)	1965(2)	8907(3)	767(2)	83(1)
F(8)	1560(3)	7566(3)	567(2)	93(1)
F(9)	1682(2)	8061(2)	1583(2)	64(1)
F(10)	490(3)	7778(4)	1031(2)	118(2)

F(11)	908(3)	9185(3)	1248(2)	106(2)
F(12)	769(2)	8671(2)	235(2)	68(1)
N(1)	1086(2)	3412(2)	737(2)	26(1)
N(2)	34(2)	2982(2)	1181(2)	27(1)
N(3)	-114(2)	2095(2)	2066(2)	26(1)
N(4)	1106(2)	1481(2)	1256(2)	28(1)
N(5)	1074(2)	636(2)	2490(2)	31(1)
N(6)	2336(2)	1787(2)	2302(2)	28(1)
N(7)	1241(2)	2230(2)	3154(2)	29(1)
P(1)	1204(1)	8372(1)	927(1)	39(1)
P(2)	5377(1)	2537(1)	1082(1)	48(1)
Ru(1)	1138(1)	1916(1)	2196(1)	25(1)

Table 6.3. Bond lengths [Å] and angles [°] for 4.2.

C(1)-N(1)	1.345(5)
C(1)-N(2)	1.364(5)
C(1)-C(26)	1.438(5)
C(1S)-Cl(1S)	1.750(5)
C(1S)-Cl(2S)	1.752(5)
C(1S)-Cl(3S)	1.754(5)
C(1S)-H(1S)	0.9800
C(2)-C(3)	1.328(6)
C(2)-N(2)	1.401(5)
C(2)-H(2)	0.9300
C(2S)-Cl(6S)	1.712(6)
C(2S)-Cl(5S)	1.745(6)
C(2S)-Cl(4S)	1.764(6)
C(2S)-H(2S)	0.9800
C(3)-N(1)	1.394(5)
C(3)-H(3)	0.9300
C(4)-N(3)	1.279(5)
C(4)-N(2)	1.457(5)
C(4)-C(5)	1.547(6)
C(5)-C(7)	1.538(6)

C(5)-C(6)	1.539(6)
C(5)-C(8)	1.551(7)
C(6)-H(6A)	0.9600
C(6)-H(6B)	0.9600
C(6)-H(6C)	0.9600
C(7)-H(7A)	0.9600
C(7)-H(7B)	0.9600
C(7)-H(7C)	0.9600
C(8)-H(8A)	0.9600
C(8)-H(8B)	0.9600
C(8)-H(8C)	0.9600
C(9)-C(10)	1.398(6)
C(9)-C(14)	1.408(6)
C(9)-N(3)	1.468(5)
C(10)-C(11)	1.396(6)
C(10)-C(16)	1.503(6)
C(11)-C(12)	1.377(8)
C(11)-H(11)	0.9300
C(12)-C(13)	1.374(8)
C(12)-H(12)	0.9300
C(13)-C(14)	1.400(7)
C(13)-H(13)	0.9300

C(14)-C(15)	1.505(6)
C(15)-H(15A)	0.9600
C(15)-H(15B)	0.9600
C(15)-H(15C)	0.9600
C(16)-H(16A)	0.9600
C(16)-H(16B)	0.9600
C(16)-H(16C)	0.9600
C(17)-C(22)	1.397(6)
C(17)-C(18)	1.399(6)
C(17)-N(1)	1.449(5)
C(18)-C(19)	1.386(6)
C(18)-C(23)	1.522(6)
C(19)-C(20)	1.388(7)
C(19)-H(19)	0.9300
C(20)-C(21)	1.374(7)
C(20)-C(24)	1.515(7)
C(21)-C(22)	1.394(6)
C(21)-H(21)	0.9300
C(22)-C(25)	1.508(6)
C(23)-H(23A)	0.9600
C(23)-H(23B)	0.9600
C(23)-H(23C)	0.9600

C(24)-H(24A)	0.9600
C(24)-H(24B)	0.9600
C(24)-H(24C)	0.9600
C(25)-H(25A)	0.9600
C(25)-H(25B)	0.9600
C(25)-H(25C)	0.9600
C(26)-C(27)	1.502(5)
C(26)-Ru(1)	2.184(4)
C(26)-H(26)	1.02(5)
C(27)-C(28)	1.384(6)
C(27)-C(32)	1.401(6)
C(28)-C(29)	1.395(6)
C(28)-H(28)	0.9300
C(29)-C(30)	1.383(7)
C(29)-H(29)	0.9300
C(30)-C(31)	1.371(7)
C(30)-H(30)	0.9300
C(31)-C(32)	1.391(6)
C(31)-H(31)	0.9300
C(32)-H(32)	0.9300
C(33)-N(6)	1.127(5)
C(33)-C(34)	1.449(6)

C(34)-H(34A)	0.9600
C(34)-H(34B)	0.9600
C(34)-H(34C)	0.9600
C(35)-N(5)	1.130(6)
C(35)-C(36)	1.452(7)
C(36)-H(36A)	0.9600
C(36)-H(36B)	0.9600
C(36)-H(36C)	0.9600
C(37)-N(7)	1.141(5)
C(37)-C(38)	1.452(6)
C(38)-H(38A)	0.9600
C(38)-H(38B)	0.9600
C(38)-H(38C)	0.9600
C(39)-N(4)	1.131(5)
C(39)-C(40)	1.464(6)
C(40)-H(40A)	0.9600
C(40)-H(40B)	0.9600
C(40)-H(40C)	0.9600
F(1)-P(2)	1.551(5)
F(2)-P(2)	1.523(5)
F(3)-P(2)	1.572(4)
F(4)-P(2)	1.596(5)

F(5)-P(2)	1.579(4)
F(6)-P(2)	1.605(4)
F(7)-P(1)	1.592(4)
F(8)-P(1)	1.604(4)
F(9)-P(1)	1.576(3)
F(10)-P(1)	1.553(4)
F(11)-P(1)	1.534(4)
F(12)-P(1)	1.602(3)
N(3)-Ru(1)	2.130(3)
N(4)-Ru(1)	2.030(3)
N(5)-Ru(1)	2.094(4)
N(6)-Ru(1)	2.028(4)
N(7)-Ru(1)	2.006(3)
N(1)-C(1)-N(2)	106.9(3)
N(1)-C(1)-C(26)	125.1(4)
N(2)-C(1)-C(26)	127.7(3)
Cl(1S)-C(1S)-Cl(2S)	111.1(3)
Cl(1S)-C(1S)-Cl(3S)	109.3(3)
Cl(2S)-C(1S)-Cl(3S)	110.3(3)
Cl(1S)-C(1S)-H(1S)	108.7
Cl(2S)-C(1S)-H(1S)	108.7

Cl(3S)-C(1S)-H(1S)	108.7
C(3)-C(2)-N(2)	107.5(4)
C(3)-C(2)-H(2)	126.2
N(2)-C(2)-H(2)	126.2
Cl(6S)-C(2S)-Cl(5S)	114.3(4)
Cl(6S)-C(2S)-Cl(4S)	111.9(3)
Cl(5S)-C(2S)-Cl(4S)	109.0(3)
Cl(6S)-C(2S)-H(2S)	107.1
Cl(5S)-C(2S)-H(2S)	107.1
Cl(4S)-C(2S)-H(2S)	107.1
C(2)-C(3)-N(1)	107.8(4)
C(2)-C(3)-H(3)	126.1
N(1)-C(3)-H(3)	126.1
N(3)-C(4)-N(2)	114.8(3)
N(3)-C(4)-C(5)	130.2(4)
N(2)-C(4)-C(5)	115.0(3)
C(7)-C(5)-C(6)	107.8(4)
C(7)-C(5)-C(4)	110.7(4)
C(6)-C(5)-C(4)	111.3(4)
C(7)-C(5)-C(8)	109.4(4)
C(6)-C(5)-C(8)	105.2(4)
C(4)-C(5)-C(8)	112.2(4)

C(5)-C(6)-H(6A)	109.5
C(5)-C(6)-H(6B)	109.5
H(6A)-C(6)-H(6B)	109.5
C(5)-C(6)-H(6C)	109.5
H(6A)-C(6)-H(6C)	109.5
H(6B)-C(6)-H(6C)	109.5
C(5)-C(7)-H(7A)	109.5
C(5)-C(7)-H(7B)	109.5
H(7A)-C(7)-H(7B)	109.5
C(5)-C(7)-H(7C)	109.5
H(7A)-C(7)-H(7C)	109.5
H(7B)-C(7)-H(7C)	109.5
C(5)-C(8)-H(8A)	109.5
C(5)-C(8)-H(8B)	109.5
H(8A)-C(8)-H(8B)	109.5
C(5)-C(8)-H(8C)	109.5
H(8A)-C(8)-H(8C)	109.5
H(8B)-C(8)-H(8C)	109.5
C(10)-C(9)-C(14)	121.7(4)
C(10)-C(9)-N(3)	121.7(4)
C(14)-C(9)-N(3)	115.9(4)
C(11)-C(10)-C(9)	117.6(4)

C(11)-C(10)-C(16)	118.2(4)
C(9)-C(10)-C(16)	124.1(4)
C(12)-C(11)-C(10)	122.0(5)
C(12)-C(11)-H(11)	119.0
C(10)-C(11)-H(11)	119.0
C(13)-C(12)-C(11)	119.5(5)
C(13)-C(12)-H(12)	120.2
C(11)-C(12)-H(12)	120.2
C(12)-C(13)-C(14)	121.5(5)
C(12)-C(13)-H(13)	119.3
C(14)-C(13)-H(13)	119.3
C(13)-C(14)-C(9)	117.7(4)
C(13)-C(14)-C(15)	117.9(4)
C(9)-C(14)-C(15)	124.2(4)
C(14)-C(15)-H(15A)	109.5
C(14)-C(15)-H(15B)	109.5
H(15A)-C(15)-H(15B)	109.5
C(14)-C(15)-H(15C)	109.5
H(15A)-C(15)-H(15C)	109.5
H(15B)-C(15)-H(15C)	109.5
C(10)-C(16)-H(16A)	109.5
C(10)-C(16)-H(16B)	109.5

H(16A)-C(16)-H(16B)	109.5
C(10)-C(16)-H(16C)	109.5
H(16A)-C(16)-H(16C)	109.5
H(16B)-C(16)-H(16C)	109.5
C(22)-C(17)-C(18)	121.6(4)
C(22)-C(17)-N(1)	120.6(4)
C(18)-C(17)-N(1)	117.8(4)
C(19)-C(18)-C(17)	118.0(4)
C(19)-C(18)-C(23)	121.4(4)
C(17)-C(18)-C(23)	120.6(4)
C(18)-C(19)-C(20)	121.8(4)
C(18)-C(19)-H(19)	119.1
C(20)-C(19)-H(19)	119.1
C(21)-C(20)-C(19)	118.7(4)
C(21)-C(20)-C(24)	120.2(4)
C(19)-C(20)-C(24)	121.0(4)
C(20)-C(21)-C(22)	122.1(4)
C(20)-C(21)-H(21)	118.9
C(22)-C(21)-H(21)	118.9
C(21)-C(22)-C(17)	117.7(4)
C(21)-C(22)-C(25)	120.1(4)
C(17)-C(22)-C(25)	122.2(4)

C(18)-C(23)-H(23A)	109.5
C(18)-C(23)-H(23B)	109.5
H(23A)-C(23)-H(23B)	109.5
C(18)-C(23)-H(23C)	109.5
H(23A)-C(23)-H(23C)	109.5
H(23B)-C(23)-H(23C)	109.5
C(20)-C(24)-H(24A)	109.5
C(20)-C(24)-H(24B)	109.5
H(24A)-C(24)-H(24B)	109.5
C(20)-C(24)-H(24C)	109.5
H(24A)-C(24)-H(24C)	109.5
H(24B)-C(24)-H(24C)	109.5
C(22)-C(25)-H(25A)	109.5
C(22)-C(25)-H(25B)	109.5
H(25A)-C(25)-H(25B)	109.5
C(22)-C(25)-H(25C)	109.5
H(25A)-C(25)-H(25C)	109.5
H(25B)-C(25)-H(25C)	109.5
C(1)-C(26)-C(27)	118.3(3)
C(1)-C(26)-Ru(1)	98.0(2)
C(27)-C(26)-Ru(1)	115.8(3)
C(1)-C(26)-H(26)	105(3)

C(27)-C(26)-H(26)	113(3)
Ru(1)-C(26)-H(26)	105(3)
C(28)-C(27)-C(32)	117.0(4)
C(28)-C(27)-C(26)	125.0(4)
C(32)-C(27)-C(26)	118.1(4)
C(27)-C(28)-C(29)	122.2(4)
C(27)-C(28)-H(28)	118.9
C(29)-C(28)-H(28)	118.9
C(30)-C(29)-C(28)	119.7(4)
C(30)-C(29)-H(29)	120.1
C(28)-C(29)-H(29)	120.1
C(31)-C(30)-C(29)	119.0(4)
C(31)-C(30)-H(30)	120.5
C(29)-C(30)-H(30)	120.5
C(30)-C(31)-C(32)	121.3(4)
C(30)-C(31)-H(31)	119.3
C(32)-C(31)-H(31)	119.3
C(31)-C(32)-C(27)	120.7(4)
C(31)-C(32)-H(32)	119.7
C(27)-C(32)-H(32)	119.7
N(6)-C(33)-C(34)	179.0(5)
C(33)-C(34)-H(34A)	109.5

C(33)-C(34)-H(34B)	109.5
H(34A)-C(34)-H(34B)	109.5
C(33)-C(34)-H(34C)	109.5
H(34A)-C(34)-H(34C)	109.5
H(34B)-C(34)-H(34C)	109.5
N(5)-C(35)-C(36)	178.6(6)
C(35)-C(36)-H(36A)	109.5
C(35)-C(36)-H(36B)	109.5
H(36A)-C(36)-H(36B)	109.5
C(35)-C(36)-H(36C)	109.5
H(36A)-C(36)-H(36C)	109.5
H(36B)-C(36)-H(36C)	109.5
N(7)-C(37)-C(38)	175.9(5)
C(37)-C(38)-H(38A)	109.5
C(37)-C(38)-H(38B)	109.5
H(38A)-C(38)-H(38B)	109.5
C(37)-C(38)-H(38C)	109.5
H(38A)-C(38)-H(38C)	109.5
H(38B)-C(38)-H(38C)	109.5
N(4)-C(39)-C(40)	179.0(5)
C(39)-C(40)-H(40A)	109.5
C(39)-C(40)-H(40B)	109.5

H(40A)-C(40)-H(40B)	109.5
C(39)-C(40)-H(40C)	109.5
H(40A)-C(40)-H(40C)	109.5
H(40B)-C(40)-H(40C)	109.5
C(1)-N(1)-C(3)	109.2(3)
C(1)-N(1)-C(17)	126.0(3)
C(3)-N(1)-C(17)	123.7(3)
C(1)-N(2)-C(2)	108.5(3)
C(1)-N(2)-C(4)	126.8(3)
C(2)-N(2)-C(4)	122.9(3)
C(4)-N(3)-C(9)	122.8(3)
C(4)-N(3)-Ru(1)	124.8(3)
C(9)-N(3)-Ru(1)	112.1(3)
C(39)-N(4)-Ru(1)	173.7(3)
C(35)-N(5)-Ru(1)	175.9(4)
C(33)-N(6)-Ru(1)	174.7(3)
C(37)-N(7)-Ru(1)	174.1(4)
F(11)-P(1)-F(10)	98.6(3)
F(11)-P(1)-F(9)	93.3(2)
F(10)-P(1)-F(9)	92.6(2)
F(11)-P(1)-F(7)	87.4(3)
F(10)-P(1)-F(7)	173.8(3)

F(9)-P(1)-F(7)	88.55(18)
F(11)-P(1)-F(12)	89.6(2)
F(10)-P(1)-F(12)	89.6(2)
F(9)-P(1)-F(12)	176.1(2)
F(7)-P(1)-F(12)	88.9(2)
F(11)-P(1)-F(8)	175.8(3)
F(10)-P(1)-F(8)	85.4(3)
F(9)-P(1)-F(8)	87.8(2)
F(7)-P(1)-F(8)	88.6(3)
F(12)-P(1)-F(8)	89.2(2)
F(2)-P(2)-F(1)	93.5(4)
F(2)-P(2)-F(3)	90.0(3)
F(1)-P(2)-F(3)	89.2(3)
F(2)-P(2)-F(5)	177.8(4)
F(1)-P(2)-F(5)	88.6(3)
F(3)-P(2)-F(5)	90.4(3)
F(2)-P(2)-F(4)	91.7(4)
F(1)-P(2)-F(4)	174.5(3)
F(3)-P(2)-F(4)	92.4(3)
F(5)-P(2)-F(4)	86.1(3)
F(2)-P(2)-F(6)	88.2(3)
F(1)-P(2)-F(6)	88.5(2)

F(3)-P(2)-F(6)	177.1(3)
F(5)-P(2)-F(6)	91.5(3)
F(4)-P(2)-F(6)	90.0(3)
N(7)-Ru(1)-N(6)	85.56(14)
N(7)-Ru(1)-N(4)	173.68(14)
N(6)-Ru(1)-N(4)	90.50(14)
N(7)-Ru(1)-N(5)	87.57(13)
N(6)-Ru(1)-N(5)	87.25(14)
N(4)-Ru(1)-N(5)	87.31(13)
N(7)-Ru(1)-N(3)	94.98(13)
N(6)-Ru(1)-N(3)	177.84(13)
N(4)-Ru(1)-N(3)	89.15(13)
N(5)-Ru(1)-N(3)	94.86(13)
N(7)-Ru(1)-C(26)	89.30(14)
N(6)-Ru(1)-C(26)	90.57(14)
N(4)-Ru(1)-C(26)	95.68(14)
N(5)-Ru(1)-C(26)	176.31(14)
N(3)-Ru(1)-C(26)	87.35(13)

Symmetry transformations used to generate equivalent atoms:

Table 6.4. Anisotropic displacement parameters ($\text{\AA}^2 \times 10^3$) for 4.2. The anisotropic displacement factor exponent takes the form: $-2p^2 [h^2 a^*{}^2 U^{11} + \dots + 2 h k a^* b^* U^{12}]$

	U ¹¹	U ²²	U ³³	U ²³	U ¹³	U ¹²
C(1)	26(2)	23(2)	24(2)	0(1)	3(2)	2(2)
C(1S)	45(3)	39(2)	35(2)	5(2)	9(2)	8(2)
C(2)	34(2)	38(2)	22(2)	-4(2)	1(2)	-4(2)
C(2S)	54(3)	52(3)	48(3)	3(2)	8(2)	7(2)
C(3)	35(2)	41(2)	21(2)	-1(2)	1(2)	-1(2)
C(4)	29(2)	31(2)	24(2)	-10(2)	4(2)	-8(2)
C(5)	25(2)	45(3)	33(2)	-4(2)	3(2)	-2(2)
C(6)	32(2)	59(3)	41(3)	-5(2)	9(2)	4(2)
C(7)	30(2)	57(3)	43(3)	-11(2)	-3(2)	-8(2)
C(8)	32(2)	51(3)	46(3)	-2(2)	2(2)	4(2)
C(9)	33(2)	29(2)	35(2)	1(2)	9(2)	-2(2)
C(10)	35(2)	38(2)	32(2)	0(2)	7(2)	1(2)
C(11)	53(3)	53(3)	33(2)	8(2)	13(2)	-4(2)
C(12)	54(3)	46(3)	60(3)	15(3)	17(3)	-10(2)

C(13)	49(3)	34(3)	64(3)	-4(2)	10(2)	-13(2)
C(14)	32(2)	32(2)	47(3)	-5(2)	8(2)	-10(2)
C(15)	44(3)	39(3)	47(3)	-16(2)	8(2)	-12(2)
C(16)	39(2)	42(3)	29(2)	-6(2)	7(2)	1(2)
C(17)	32(2)	29(2)	22(2)	2(2)	5(2)	-3(2)
C(18)	38(2)	32(2)	29(2)	8(2)	6(2)	5(2)
C(19)	44(3)	28(2)	50(3)	8(2)	14(2)	-1(2)
C(20)	38(2)	38(2)	44(3)	6(2)	12(2)	-7(2)
C(21)	36(2)	37(2)	43(2)	3(2)	16(2)	2(2)
C(22)	36(2)	36(2)	32(2)	1(2)	9(2)	-1(2)
C(23)	46(3)	32(2)	61(3)	6(2)	15(2)	7(2)
C(24)	49(3)	46(3)	88(4)	8(3)	28(3)	-9(2)
C(25)	44(3)	34(2)	65(3)	-9(2)	24(2)	-2(2)
C(26)	25(2)	23(2)	22(2)	1(1)	2(1)	-1(1)
C(27)	35(2)	19(2)	23(2)	3(2)	2(2)	-3(2)
C(28)	35(2)	25(2)	27(2)	-2(2)	4(2)	-5(2)
C(29)	46(3)	32(2)	33(2)	-2(2)	10(2)	-1(2)
C(30)	73(3)	27(2)	27(2)	-2(2)	9(2)	2(2)
C(31)	75(4)	29(2)	28(2)	-2(2)	-17(2)	-1(2)
C(32)	42(2)	28(2)	34(2)	0(2)	-7(2)	2(2)
C(33)	38(2)	27(2)	30(2)	-5(2)	5(2)	2(2)
C(34)	34(2)	48(3)	49(3)	-8(2)	0(2)	10(2)

C(35)	51(3)	33(2)	32(2)	-4(2)	9(2)	-3(2)
C(36)	107(5)	31(3)	42(3)	8(2)	18(3)	-5(3)
C(37)	37(2)	30(2)	32(2)	2(2)	4(2)	-6(2)
C(38)	61(3)	58(3)	28(2)	-5(2)	4(2)	-13(3)
C(39)	37(2)	25(2)	32(2)	-6(2)	9(2)	-6(2)
C(40)	58(3)	41(3)	34(2)	-12(2)	7(2)	-1(2)
CI(1S)	63(1)	45(1)	45(1)	12(1)	10(1)	-6(1)
CI(2S)	57(1)	53(1)	50(1)	7(1)	1(1)	-6(1)
CI(3S)	65(1)	82(1)	51(1)	31(1)	-11(1)	-9(1)
CI(4S)	52(1)	61(1)	59(1)	14(1)	15(1)	13(1)
CI(5S)	83(1)	106(2)	200(3)	3(2)	80(2)	-4(1)
CI(6S)	208(3)	115(2)	89(2)	40(1)	39(2)	104(2)
F(1)	67(3)	108(4)	157(4)	83(3)	-12(3)	-13(2)
F(2)	115(4)	348(10)	98(4)	-137(5)	52(3)	-105(5)
F(3)	50(2)	133(4)	76(3)	-8(3)	12(2)	-3(2)
F(4)	143(5)	46(2)	191(6)	6(3)	17(4)	24(3)
F(5)	140(4)	84(3)	57(2)	-15(2)	12(2)	22(3)
F(6)	73(3)	84(3)	115(3)	21(2)	46(2)	-11(2)
F(7)	72(2)	105(3)	70(2)	37(2)	-9(2)	-34(2)
F(8)	101(3)	85(3)	86(3)	-32(2)	-33(2)	34(2)
F(9)	71(2)	71(2)	43(2)	21(2)	-19(2)	-24(2)
F(10)	82(3)	162(5)	103(3)	76(3)	-32(2)	-74(3)

F(11)	157(4)	95(3)	65(2)	-32(2)	5(3)	51(3)
F(12)	91(3)	43(2)	63(2)	7(2)	-36(2)	-4(2)
N(1)	26(2)	30(2)	22(2)	0(1)	2(1)	0(1)
N(2)	26(2)	32(2)	23(2)	-4(1)	4(1)	-2(1)
N(3)	29(2)	26(2)	22(2)	-4(1)	4(1)	-5(1)
N(4)	32(2)	22(2)	32(2)	-2(1)	7(1)	-2(1)
N(5)	38(2)	28(2)	27(2)	-2(1)	7(1)	-1(2)
N(6)	34(2)	23(2)	28(2)	0(1)	4(1)	2(1)
N(7)	35(2)	24(2)	28(2)	1(1)	3(1)	-2(1)
P(1)	46(1)	34(1)	35(1)	0(1)	-7(1)	-5(1)
P(2)	58(1)	42(1)	49(1)	-5(1)	22(1)	-2(1)
Ru(1)	29(1)	22(1)	24(1)	-2(1)	4(1)	-1(1)

Table 6.5. Hydrogen coordinates (x 104) and isotropic displacement parameters (Å²x 103) for 4.2.

	x	y	z	U(eq)
H(1S)	6162	384	973	48
H(2)	-598	2743	271	38
H(2S)	8965	6955	2349	61
H(3)	570	3243	-221	39
H(6A)	-2268	3165	2090	66
H(6B)	-1429	3406	2428	66
H(6C)	-1717	2452	2423	66
H(7A)	-1835	1610	1429	65
H(7B)	-1591	1969	759	65
H(7C)	-2370	2292	1039	65
H(8A)	-1406	3586	682	65
H(8B)	-1136	4104	1321	65
H(8C)	-2033	3869	1159	65
H(11)	-969	1106	3952	55

H(12)	-1247	-225	3513	63
H(13)	-1153	-465	2411	58
H(15A)	-151	101	1482	65
H(15B)	-528	974	1238	65
H(15C)	-1068	167	1292	65
H(16A)	-1004	2806	3484	55
H(16B)	-185	2882	3185	55
H(16C)	-230	2467	3880	55
H(19)	2469	5818	645	48
H(21)	3616	3668	283	45
H(23A)	1123	5833	881	68
H(23B)	874	5026	1270	68
H(23C)	614	5111	515	68
H(24A)	4327	4936	273	89
H(24B)	4063	5635	760	89
H(24C)	3811	5715	3	89
H(25A)	3016	2327	267	70
H(25B)	2091	2301	115	70
H(25C)	2468	2237	844	70
H(28)	-116	4109	2139	35
H(29)	-425	5007	2979	44
H(30)	543	5364	3815	50

H(31)	1810	4842	3780	54
H(32)	2124	3951	2939	42
H(34A)	4014	1865	2966	66
H(34B)	4121	1823	2211	66
H(34C)	3959	984	2598	66
H(36A)	601	-1019	3128	88
H(36B)	1532	-1037	3192	88
H(36C)	1056	-1305	2529	88
H(38A)	1142	3136	4454	73
H(38B)	2025	2820	4490	73
H(38C)	1351	2190	4657	73
H(40A)	826	1169	-222	66
H(40B)	735	265	95	66
H(40C)	1582	628	5	66
H(26)	1830(30)	3330(30)	1840(20)	40(13)

Table 6.6. Crystal data and structure refinement for compound 4.4.

Identification code	d1324
Empirical formula	C ₅₃ H ₅₂ Cl ₄ N ₂ P ₂ Ru
Formula weight	1021.78
Temperature	150(1) K

Wavelength	0.71073 Å	
Crystal system	monoclinic	
Space group	C 2/c	
Unit cell dimensions	a = 39.366(4) Å	α = 90°.
	b = 10.3992(11) Å	β = 104.747(2)°.
	c = 24.505(3) Å	γ = 90°.
Volume	9701.5(18) Å ³	
Z	8	
Density (calculated)	1.399 Mg/m ³	
Absorption coefficient	0.648 mm ⁻¹	
F(000)	4208	
Crystal size	0.36 x 0.22 x 0.20 mm ³	
Theta range for data collection	1.07 to 27.52°.	
Index ranges	-50 ≤ h ≤ 51, -13 ≤ k ≤ 13, -31 ≤ l ≤ 31	
Reflections collected	42646	
Independent reflections	11151 [R(int) = 0.0520]	
Completeness to theta = 27.52°	99.7 %	
Refinement method	Full-matrix least-squares on F ²	
Data / restraints / parameters	11151 / 0 / 569	
Goodness-of-fit on F ²	1.019	
Final R indices [I > 2σ(I)]	R1 = 0.0367, wR2 = 0.0736	

R indices (all data)

R1 = 0.0579, wR2 = 0.0834

Largest diff. peak and hole

0.589 and -0.555 e.Å⁻³

Table 6.7. Atomic coordinates (x 10⁴) and equivalent isotropic displacement parameters (Å²x 10³) for compound 4.4. U(eq) is defined as one third of the trace of the orthogonalized U^{ij} tensor.

	x	y	z	U(eq)
C(1)	1800(1)	3994(2)	2471(1)	21(1)
C(1S)	949(1)	8740(4)	2356(2)	72(1)
C(2)	2373(1)	4551(3)	2768(1)	33(1)
C(3)	2272(1)	4136(3)	3217(1)	35(1)
C(4)	2083(1)	4926(2)	1755(1)	24(1)
C(5)	2240(1)	4158(2)	1423(1)	24(1)
C(6)	2241(1)	4616(3)	891(1)	28(1)
C(7)	2100(1)	5807(3)	694(1)	33(1)
C(8)	1951(1)	6547(3)	1046(1)	34(1)
C(9)	1943(1)	6144(2)	1583(1)	29(1)
C(10)	1792(1)	6998(2)	1957(1)	37(1)

C(11)	2411(1)	2894(3)	1629(1)	33(1)
C(12)	2124(1)	6269(3)	124(1)	47(1)
C(13)	1721(1)	3410(3)	3431(1)	25(1)
C(14)	1747(1)	2154(3)	3633(1)	27(1)
C(15)	1546(1)	1829(3)	4004(1)	31(1)
C(16)	1337(1)	2720(3)	4189(1)	35(1)
C(17)	1338(1)	3979(3)	4001(1)	34(1)
C(18)	1527(1)	4357(3)	3623(1)	28(1)
C(19)	1527(1)	5732(3)	3431(1)	37(1)
C(20)	1983(1)	1180(3)	3462(1)	35(1)
C(21)	1122(1)	2332(4)	4593(1)	52(1)
C(22)	1057(1)	3617(2)	2370(1)	19(1)
C(23)	803(1)	4549(3)	2381(1)	25(1)
C(24)	533(1)	4306(3)	2636(1)	34(1)
C(25)	513(1)	3134(3)	2891(1)	36(1)
C(26)	762(1)	2202(3)	2886(1)	31(1)
C(27)	1030(1)	2425(2)	2624(1)	23(1)
C(28)	1495(1)	2796(2)	832(1)	21(1)
C(29)	1699(1)	2039(2)	522(1)	21(1)
C(30)	1817(1)	782(2)	674(1)	27(1)
C(31)	2002(1)	122(3)	351(1)	31(1)
C(32)	2063(1)	663(3)	-128(1)	35(1)

C(33)	1943(1)	1884(3)	-290(1)	39(1)
C(34)	1764(1)	2565(3)	34(1)	29(1)
C(35)	735(1)	3142(2)	35(1)	22(1)
C(36)	849(1)	2083(3)	-219(1)	30(1)
C(37)	835(1)	2097(3)	-792(1)	36(1)
C(38)	707(1)	3159(3)	-1116(1)	39(1)
C(39)	592(1)	4214(3)	-872(1)	36(1)
C(40)	603(1)	4209(3)	-299(1)	27(1)
C(41)	664(1)	4779(2)	921(1)	18(1)
C(42)	918(1)	5698(2)	897(1)	22(1)
C(43)	855(1)	6993(2)	959(1)	27(1)
C(44)	539(1)	7384(2)	1055(1)	30(1)
C(45)	288(1)	6487(2)	1092(1)	30(1)
C(46)	349(1)	5182(2)	1022(1)	24(1)
C(47)	367(1)	2228(2)	836(1)	20(1)
C(48)	103(1)	1915(3)	364(1)	33(1)
C(49)	-182(1)	1186(3)	415(1)	45(1)
C(50)	-208(1)	779(3)	936(1)	40(1)
C(51)	50(1)	1108(3)	1415(1)	35(1)
C(52)	334(1)	1830(2)	1365(1)	27(1)
CI(1)	1030(1)	149(1)	982(1)	31(1)
CI(1S)	526(1)	8562(1)	2453(1)	78(1)

Cl(2)	1712(1)	961(1)	2006(1)	28(1)
Cl(2S)	1263(1)	8941(1)	2995(1)	65(1)
N(1)	2083(1)	4476(2)	2311(1)	23(1)
N(2)	1919(1)	3791(2)	3036(1)	25(1)
P(1)	1370(1)	4001(1)	1947(1)	18(1)
P(2)	761(1)	3106(1)	796(1)	17(1)
Ru(1)	1270(1)	2176(1)	1352(1)	17(1)

Table 6.8. Bond lengths [Å] and angles [°] for compound 4.4.

C(1)-N(2)	1.361(3)
C(1)-N(1)	1.367(3)
C(1)-P(1)	1.847(2)
C(1S)-Cl(2S)	1.745(4)
C(1S)-Cl(1S)	1.751(4)
C(2)-C(3)	1.332(4)
C(2)-N(1)	1.383(3)
C(3)-N(2)	1.394(3)
C(4)-C(5)	1.394(4)
C(4)-C(9)	1.402(3)
C(4)-N(1)	1.439(3)
C(5)-C(6)	1.389(4)

C(5)-C(11)	1.503(3)
C(6)-C(7)	1.393(4)
C(7)-C(8)	1.390(4)
C(7)-C(12)	1.503(4)
C(8)-C(9)	1.390(4)
C(9)-C(10)	1.503(4)
C(13)-C(14)	1.391(4)
C(13)-C(18)	1.398(4)
C(13)-N(2)	1.445(3)
C(14)-C(15)	1.391(4)
C(14)-C(20)	1.504(4)
C(15)-C(16)	1.390(4)
C(16)-C(17)	1.389(4)
C(16)-C(21)	1.510(4)
C(17)-C(18)	1.386(4)
C(18)-C(19)	1.505(4)
C(22)-C(23)	1.398(3)
C(22)-C(27)	1.404(3)
C(22)-P(1)	1.843(3)
C(23)-C(24)	1.390(4)
C(24)-C(25)	1.380(4)
C(25)-C(26)	1.381(4)

C(26)-C(27)	1.387(4)
C(28)-C(29)	1.469(3)
C(28)-Ru(1)	1.841(3)
C(29)-C(34)	1.396(4)
C(29)-C(30)	1.406(3)
C(30)-C(31)	1.385(4)
C(31)-C(32)	1.378(4)
C(32)-C(33)	1.378(4)
C(33)-C(34)	1.383(4)
C(35)-C(36)	1.394(4)
C(35)-C(40)	1.398(4)
C(35)-P(2)	1.840(3)
C(36)-C(37)	1.389(4)
C(37)-C(38)	1.379(4)
C(38)-C(39)	1.381(4)
C(39)-C(40)	1.395(4)
C(41)-C(46)	1.389(3)
C(41)-C(42)	1.394(3)
C(41)-P(2)	1.824(2)
C(42)-C(43)	1.384(3)
C(43)-C(44)	1.384(4)
C(44)-C(45)	1.379(4)

C(45)-C(46)	1.397(3)
C(47)-C(48)	1.383(3)
C(47)-C(52)	1.396(4)
C(47)-P(2)	1.827(2)
C(48)-C(49)	1.385(4)
C(49)-C(50)	1.373(4)
C(50)-C(51)	1.384(4)
C(51)-C(52)	1.381(3)
Cl(1)-Ru(1)	2.3925(6)
Cl(2)-Ru(1)	2.4012(6)
P(1)-Ru(1)	2.3643(7)
P(2)-Ru(1)	2.3272(6)
N(2)-C(1)-N(1)	104.77(19)
N(2)-C(1)-P(1)	136.43(19)
N(1)-C(1)-P(1)	118.01(18)
Cl(2S)-C(1S)-Cl(1S)	111.8(2)
C(3)-C(2)-N(1)	107.0(2)
C(2)-C(3)-N(2)	107.7(2)
C(5)-C(4)-C(9)	122.7(3)
C(5)-C(4)-N(1)	118.2(2)
C(9)-C(4)-N(1)	119.0(2)

C(6)-C(5)-C(4)	117.4(2)
C(6)-C(5)-C(11)	120.5(2)
C(4)-C(5)-C(11)	122.1(2)
C(5)-C(6)-C(7)	122.2(3)
C(8)-C(7)-C(6)	118.1(3)
C(8)-C(7)-C(12)	122.4(3)
C(6)-C(7)-C(12)	119.5(3)
C(9)-C(8)-C(7)	122.4(3)
C(8)-C(9)-C(4)	117.1(3)
C(8)-C(9)-C(10)	120.5(2)
C(4)-C(9)-C(10)	122.5(3)
C(14)-C(13)-C(18)	122.6(3)
C(14)-C(13)-N(2)	119.5(2)
C(18)-C(13)-N(2)	117.8(2)
C(15)-C(14)-C(13)	117.3(2)
C(15)-C(14)-C(20)	120.8(3)
C(13)-C(14)-C(20)	121.9(2)
C(16)-C(15)-C(14)	122.3(3)
C(17)-C(16)-C(15)	117.9(3)
C(17)-C(16)-C(21)	121.3(3)
C(15)-C(16)-C(21)	120.8(3)
C(18)-C(17)-C(16)	122.5(3)

C(17)-C(18)-C(13)	117.2(3)
C(17)-C(18)-C(19)	121.3(3)
C(13)-C(18)-C(19)	121.5(3)
C(23)-C(22)-C(27)	117.9(2)
C(23)-C(22)-P(1)	116.32(19)
C(27)-C(22)-P(1)	125.37(18)
C(24)-C(23)-C(22)	121.1(3)
C(25)-C(24)-C(23)	120.2(3)
C(24)-C(25)-C(26)	119.6(3)
C(25)-C(26)-C(27)	120.8(3)
C(26)-C(27)-C(22)	120.4(2)
C(29)-C(28)-Ru(1)	126.40(18)
C(34)-C(29)-C(30)	118.1(2)
C(34)-C(29)-C(28)	118.5(2)
C(30)-C(29)-C(28)	123.3(2)
C(31)-C(30)-C(29)	119.8(3)
C(32)-C(31)-C(30)	121.0(3)
C(33)-C(32)-C(31)	120.0(3)
C(32)-C(33)-C(34)	119.7(3)
C(33)-C(34)-C(29)	121.5(3)
C(36)-C(35)-C(40)	118.6(2)
C(36)-C(35)-P(2)	119.7(2)

C(40)-C(35)-P(2)	121.6(2)
C(37)-C(36)-C(35)	120.6(3)
C(38)-C(37)-C(36)	120.3(3)
C(37)-C(38)-C(39)	120.0(3)
C(38)-C(39)-C(40)	120.2(3)
C(39)-C(40)-C(35)	120.3(3)
C(46)-C(41)-C(42)	118.8(2)
C(46)-C(41)-P(2)	123.56(18)
C(42)-C(41)-P(2)	117.60(18)
C(43)-C(42)-C(41)	120.8(2)
C(44)-C(43)-C(42)	119.8(2)
C(45)-C(44)-C(43)	120.1(2)
C(44)-C(45)-C(46)	120.1(2)
C(41)-C(46)-C(45)	120.3(2)
C(48)-C(47)-C(52)	118.7(2)
C(48)-C(47)-P(2)	122.7(2)
C(52)-C(47)-P(2)	118.54(18)
C(47)-C(48)-C(49)	120.4(3)
C(50)-C(49)-C(48)	120.3(3)
C(49)-C(50)-C(51)	120.1(3)
C(52)-C(51)-C(50)	119.6(3)
C(51)-C(52)-C(47)	120.8(2)

C(1)-N(1)-C(2)	110.6(2)
C(1)-N(1)-C(4)	125.82(19)
C(2)-N(1)-C(4)	123.5(2)
C(1)-N(2)-C(3)	109.9(2)
C(1)-N(2)-C(13)	128.3(2)
C(3)-N(2)-C(13)	121.5(2)
C(22)-P(1)-C(1)	103.53(11)
C(22)-P(1)-Ru(1)	98.20(8)
C(1)-P(1)-Ru(1)	113.81(8)
C(41)-P(2)-C(47)	104.46(11)
C(41)-P(2)-C(35)	101.00(11)
C(47)-P(2)-C(35)	103.68(11)
C(41)-P(2)-Ru(1)	118.95(7)
C(47)-P(2)-Ru(1)	112.19(8)
C(35)-P(2)-Ru(1)	114.79(8)
C(28)-Ru(1)-P(2)	86.69(7)
C(28)-Ru(1)-P(1)	96.43(8)
P(2)-Ru(1)-P(1)	90.61(2)
C(28)-Ru(1)-Cl(1)	105.05(8)
P(2)-Ru(1)-Cl(1)	86.89(2)
P(1)-Ru(1)-Cl(1)	158.18(2)
C(28)-Ru(1)-Cl(2)	104.61(7)

P(2)-Ru(1)-Cl(2)	168.06(2)
P(1)-Ru(1)-Cl(2)	91.89(2)
Cl(1)-Ru(1)-Cl(2)	86.45(2)

Symmetry transformations used to generate equivalent atoms:

Table 6.9. Anisotropic displacement parameters ($\text{\AA}^2 \times 10^3$) for compound

4.4. The anisotropic displacement factor exponent takes the form: $-2p^2[h^2a^*2U_{11} + \dots + 2hk a^* b^* U_{12}]$

	U_{11}	U_{22}	U_{33}	U_{23}	U_{13}	U_{12}
C(1)	20(1)	18(1)	25(2)	-1(1)	5(1)	1(1)
C(1S)	127(4)	52(2)	42(2)	-4(2)	34(2)	-25(2)
C(2)	17(1)	41(2)	34(2)	-2(1)	-4(1)	-2(1)
C(3)	20(1)	48(2)	31(2)	-1(2)	-5(1)	-1(1)
C(4)	16(1)	26(1)	27(2)	2(1)	1(1)	-7(1)
C(5)	15(1)	27(1)	30(2)	5(1)	3(1)	-7(1)
C(6)	18(1)	35(1)	31(2)	4(1)	4(1)	-7(1)
C(7)	19(1)	42(2)	35(2)	14(1)	0(1)	-9(1)

C(8)	23(1)	26(1)	48(2)	13(1)	1(1)	-6(1)
C(9)	18(1)	23(1)	42(2)	4(1)	0(1)	-8(1)
C(10)	35(1)	21(1)	52(2)	-4(1)	5(1)	-3(1)
C(11)	29(1)	31(1)	38(2)	6(1)	11(1)	5(1)
C(12)	36(2)	57(2)	48(2)	24(2)	8(2)	-4(2)
C(13)	20(1)	34(1)	18(1)	-2(1)	-1(1)	4(1)
C(14)	24(1)	38(2)	16(1)	-1(1)	-1(1)	6(1)
C(15)	30(1)	38(2)	22(2)	4(1)	1(1)	5(1)
C(16)	29(1)	51(2)	23(2)	0(1)	4(1)	7(1)
C(17)	27(1)	44(2)	29(2)	-8(1)	4(1)	10(1)
C(18)	25(1)	35(1)	19(2)	-3(1)	-2(1)	6(1)
C(19)	39(2)	32(2)	36(2)	-8(1)	3(1)	3(1)
C(20)	36(2)	44(2)	23(2)	7(1)	5(1)	15(1)
C(21)	50(2)	71(2)	43(2)	7(2)	24(2)	6(2)
C(22)	17(1)	22(1)	16(1)	-4(1)	1(1)	-2(1)
C(23)	23(1)	29(1)	21(2)	-6(1)	2(1)	0(1)
C(24)	23(1)	48(2)	30(2)	-8(1)	7(1)	5(1)
C(25)	27(1)	57(2)	26(2)	-6(2)	12(1)	-8(1)
C(26)	35(1)	37(2)	21(2)	1(1)	7(1)	-8(1)
C(27)	23(1)	26(1)	19(1)	-2(1)	2(1)	-1(1)
C(28)	19(1)	17(1)	25(2)	1(1)	4(1)	-1(1)
C(29)	20(1)	23(1)	23(1)	-3(1)	9(1)	-3(1)

C(30)	32(1)	26(1)	27(2)	-2(1)	13(1)	-1(1)
C(31)	33(1)	26(1)	36(2)	-4(1)	14(1)	1(1)
C(32)	33(1)	41(2)	38(2)	-12(1)	21(1)	-4(1)
C(33)	43(2)	50(2)	29(2)	1(2)	20(1)	-6(1)
C(34)	28(1)	32(1)	29(2)	4(1)	10(1)	-4(1)
C(35)	21(1)	27(1)	18(1)	-3(1)	5(1)	-11(1)
C(36)	33(1)	31(1)	25(2)	-6(1)	9(1)	-11(1)
C(37)	36(1)	45(2)	30(2)	-15(2)	15(1)	-17(1)
C(38)	37(2)	62(2)	18(2)	-6(2)	8(1)	-21(2)
C(39)	31(1)	51(2)	23(2)	8(1)	3(1)	-14(1)
C(40)	24(1)	34(1)	23(2)	2(1)	6(1)	-6(1)
C(41)	22(1)	16(1)	16(1)	1(1)	0(1)	-1(1)
C(42)	21(1)	21(1)	23(1)	0(1)	3(1)	-2(1)
C(43)	30(1)	20(1)	29(2)	1(1)	4(1)	-4(1)
C(44)	34(1)	19(1)	34(2)	-2(1)	2(1)	4(1)
C(45)	24(1)	28(1)	36(2)	-4(1)	4(1)	4(1)
C(46)	20(1)	25(1)	25(2)	-3(1)	2(1)	-3(1)
C(47)	20(1)	18(1)	23(1)	-3(1)	7(1)	-4(1)
C(48)	28(1)	47(2)	24(2)	-2(1)	5(1)	-16(1)
C(49)	33(2)	63(2)	37(2)	-14(2)	6(1)	-26(2)
C(50)	30(1)	43(2)	50(2)	-7(2)	14(1)	-21(1)
C(51)	34(1)	37(2)	37(2)	5(1)	16(1)	-8(1)

C(52)	23(1)	31(1)	26(2)	0(1)	5(1)	-9(1)
Cl(1)	38(1)	14(1)	41(1)	-4(1)	12(1)	-7(1)
Cl(1S)	102(1)	73(1)	56(1)	9(1)	15(1)	12(1)
Cl(2)	32(1)	26(1)	26(1)	6(1)	9(1)	10(1)
Cl(2S)	105(1)	43(1)	50(1)	7(1)	23(1)	-7(1)
N(1)	18(1)	25(1)	23(1)	1(1)	0(1)	-3(1)
N(2)	20(1)	33(1)	20(1)	1(1)	1(1)	2(1)
P(1)	16(1)	16(1)	20(1)	-1(1)	2(1)	0(1)
P(2)	18(1)	15(1)	18(1)	-2(1)	4(1)	-5(1)
Ru(1)	19(1)	13(1)	19(1)	0(1)	7(1)	-1(1)

Table 6.10. Hydrogen coordinates (x 104) and isotropic displacement parameters (Å²x 103) for compound 4.4.

	x	y	z	U(eq)
H(1S1)	1007	7986	2164	86
H(1S2)	953	9481	2117	86
H(3)	2596	4837	2764	39
H(2)	2412	4085	3584	42
H(6)	2340	4110	658	34
H(8)	1854	7340	917	40
H(10A)	1787	7870	1826	56
H(10B)	1935	6948	2337	56
H(10C)	1558	6723	1946	56
H(11A)	2452	2418	1316	49
H(11B)	2259	2408	1802	49
H(11C)	2630	3047	1900	49
H(12A)	1959	6955	0	71
H(12B)	2070	5573	-141	71

H(12C)	2357	6576	149	71
H(15)	1552	986	4134	37
H(17)	1206	4592	4133	41
H(19A)	1408	6259	3646	55
H(19B)	1407	5789	3038	55
H(19C)	1764	6025	3486	55
H(20A)	1920	1095	3059	52
H(20B)	1956	365	3631	52
H(20C)	2222	1459	3588	52
H(21A)	877	2352	4401	78
H(21B)	1167	2919	4906	78
H(21C)	1187	1477	4729	78
H(23)	816	5346	2214	30
H(24)	364	4934	2635	40
H(25)	333	2973	3065	43
H(26)	750	1416	3061	37
H(27)	1192	1780	2617	28
H(30)	1772	395	990	33
H(31)	2086	-700	460	37
H(32)	2185	204	-342	42
H(33)	1981	2248	-615	46
H(34)	1686	3393	-75	35

H(36)	935	1362	-4	35
H(37)	912	1386	-957	43
H(38)	698	3164	-1499	46
H(39)	506	4931	-1091	43
H(40)	522	4917	-137	32
H(42)	1132	5437	838	26
H(43)	1025	7598	937	32
H(44)	496	8254	1095	36
H(45)	78	6751	1163	36
H(46)	178	4580	1043	29
H(48)	116	2195	10	40
H(49)	-357	970	94	54
H(50)	-398	281	967	48
H(51)	31	844	1769	42
H(52)	507	2053	1687	32
H(28)	1455(6)	3650(30)	686(11)	25(7)

Table 6.11. Crystal data and structure refinement for compound 4.5.

Identification code	d12283
Empirical formula	C52 H49 Cl N2 P2 Ru
Formula weight	900.39

Temperature	150(1) K	
Wavelength	0.71073 Å	
Crystal system	monoclinic	
Space group	P 21/n	
Unit cell dimensions	a = 11.796(3) Å	$\alpha = 90^\circ$.
	b = 18.979(5) Å	$\beta = 99.625(7)^\circ$.
	c = 20.473(5) Å	$\gamma = 90^\circ$.
Volume	4519(2) Å ³	
Z	4	
Density (calculated)	1.323 Mg/m ³	
Absorption coefficient	0.514 mm ⁻¹	
F(000)	1864	
Crystal size	0.19 x 0.05 x 0.02 mm ³	
Theta range for data collection	1.47 to 27.42°.	
Index ranges	-15<=h<=15, -24<=k<=14, -26<=l<=26	
Reflections collected	40082	
Independent reflections	10285 [R(int) = 0.0505]	
Completeness to theta = 27.42°	99.9 %	
Refinement method	Full-matrix least-squares on F ²	
Data / restraints / parameters	10285 / 0 / 523	
Goodness-of-fit on F ²	1.011	

Final R indices [$I > 2\sigma(I)$]	R1 = 0.0331, wR2 = 0.0675
R indices (all data)	R1 = 0.0506, wR2 = 0.0736
Largest diff. peak and hole	0.554 and -0.359 e.Å ⁻³

Table 6.12. Atomic coordinates ($\times 10^4$) and equivalent isotropic displacement parameters ($\text{Å}^2 \times 10^3$) for compound 4.5. $U(\text{eq})$ is defined as one third of the trace of the orthogonalized U^{ij} tensor.

	x	y	z	$U(\text{eq})$
C(1)	5336(2)	723(1)	3082(1)	15(1)
C(2)	5888(2)	-178(1)	3770(1)	24(1)
C(3)	6477(2)	-231(1)	3263(1)	23(1)
C(4)	4479(2)	675(1)	4123(1)	16(1)
C(5)	4942(2)	1194(1)	4568(1)	19(1)
C(6)	4209(2)	1492(1)	4961(1)	21(1)
C(7)	3069(2)	1282(1)	4917(1)	23(1)
C(8)	2675(2)	727(1)	4495(1)	24(1)
C(9)	3370(2)	404(1)	4092(1)	21(1)
C(10)	6164(2)	1448(1)	4622(1)	28(1)

C(11)	2289(3)	1641(1)	5326(1)	39(1)
C(12)	2942(2)	-212(1)	3656(1)	31(1)
C(13)	6660(2)	520(1)	2273(1)	17(1)
C(14)	6515(2)	76(1)	1728(1)	22(1)
C(15)	7078(2)	266(1)	1202(1)	26(1)
C(16)	7744(2)	869(1)	1223(1)	26(1)
C(17)	7852(2)	1307(1)	1778(1)	21(1)
C(18)	7322(2)	1147(1)	2330(1)	16(1)
C(19)	5784(2)	-580(1)	1692(1)	31(1)
C(20)	8380(3)	1051(1)	660(1)	40(1)
C(21)	7388(2)	1624(1)	2898(1)	16(1)
C(22)	3642(2)	1015(1)	2014(1)	21(1)
C(23)	3895(2)	860(1)	1389(1)	26(1)
C(24)	3112(3)	488(2)	932(2)	42(1)
C(25)	2078(3)	268(2)	1095(2)	57(1)
C(26)	1815(3)	421(2)	1714(2)	55(1)
C(27)	2585(2)	798(1)	2171(1)	36(1)
C(28)	5625(2)	2721(1)	3188(1)	17(1)
C(29)	6387(2)	3210(1)	3545(1)	24(1)
C(30)	6140(3)	3551(1)	4106(1)	34(1)
C(31)	5113(3)	3418(1)	4335(1)	36(1)
C(32)	4357(2)	2922(1)	4009(1)	28(1)

C(33)	4611(2)	2564(1)	3453(1)	20(1)
C(34)	3831(2)	1985(1)	3129(1)	18(1)
C(35)	4650(2)	2627(1)	745(1)	20(1)
C(36)	5409(2)	2106(1)	602(1)	24(1)
C(37)	5384(2)	1874(1)	-45(1)	34(1)
C(38)	4623(3)	2166(1)	-560(1)	37(1)
C(39)	3859(2)	2679(1)	-426(1)	35(1)
C(40)	3865(2)	2905(1)	219(1)	27(1)
C(41)	5038(2)	3871(1)	1570(1)	18(1)
C(42)	5065(2)	4244(1)	986(1)	22(1)
C(43)	5308(2)	4967(1)	1009(1)	27(1)
C(44)	5502(2)	5323(1)	1602(1)	29(1)
C(45)	5509(2)	4954(1)	2188(1)	29(1)
C(46)	5289(2)	4232(1)	2174(1)	24(1)
C(47)	3180(2)	2945(1)	1698(1)	24(1)
C(48)	2838(2)	3365(1)	2192(1)	31(1)
C(49)	1705(3)	3340(1)	2313(2)	44(1)
C(50)	904(3)	2900(2)	1946(2)	54(1)
C(51)	1231(2)	2483(2)	1460(2)	46(1)
C(52)	2364(2)	2499(1)	1338(1)	32(1)
CI(1)	7539(1)	3059(1)	2128(1)	20(1)
N(1)	5187(2)	414(1)	3657(1)	17(1)

N(2)	6136(2)	330(1)	2843(1)	17(1)
P(1)	4699(1)	1514(1)	2601(1)	14(1)
P(2)	4722(1)	2915(1)	1610(1)	16(1)
Ru(1)	6003(1)	2243(1)	2361(1)	13(1)

Table 6.13. Bond lengths [Å] and angles [°] for compound 4.5.

C(1)-N(1)	1.352(3)
C(1)-N(2)	1.355(3)
C(1)-P(1)	1.883(2)
C(2)-C(3)	1.346(3)
C(2)-N(1)	1.391(3)
C(3)-N(2)	1.384(3)
C(4)-C(5)	1.391(3)
C(4)-C(9)	1.397(3)
C(4)-N(1)	1.456(3)
C(5)-C(6)	1.396(3)
C(5)-C(10)	1.506(3)
C(6)-C(7)	1.391(3)
C(7)-C(8)	1.392(3)
C(7)-C(11)	1.507(3)
C(8)-C(9)	1.398(3)

C(9)-C(12)	1.506(3)
C(13)-C(14)	1.386(3)
C(13)-C(18)	1.418(3)
C(13)-N(2)	1.454(3)
C(14)-C(15)	1.404(3)
C(14)-C(19)	1.510(3)
C(15)-C(16)	1.385(3)
C(16)-C(17)	1.396(3)
C(16)-C(20)	1.517(3)
C(17)-C(18)	1.414(3)
C(18)-C(21)	1.466(3)
C(21)-Ru(1)	2.157(2)
C(22)-C(23)	1.393(3)
C(22)-C(27)	1.400(3)
C(22)-P(1)	1.842(2)
C(23)-C(24)	1.391(4)
C(24)-C(25)	1.382(4)
C(25)-C(26)	1.385(4)
C(26)-C(27)	1.389(4)
C(28)-C(29)	1.408(3)
C(28)-C(33)	1.426(3)
C(28)-Ru(1)	2.035(2)

C(29)-C(30)	1.391(3)
C(30)-C(31)	1.393(4)
C(31)-C(32)	1.387(4)
C(32)-C(33)	1.400(3)
C(33)-C(34)	1.514(3)
C(34)-P(1)	1.839(2)
C(35)-C(36)	1.397(3)
C(35)-C(40)	1.400(3)
C(35)-P(2)	1.841(2)
C(36)-C(37)	1.392(3)
C(37)-C(38)	1.381(4)
C(38)-C(39)	1.385(4)
C(39)-C(40)	1.388(3)
C(41)-C(42)	1.394(3)
C(41)-C(46)	1.400(3)
C(41)-P(2)	1.857(2)
C(42)-C(43)	1.401(3)
C(43)-C(44)	1.375(4)
C(44)-C(45)	1.389(3)
C(45)-C(46)	1.394(3)
C(47)-C(52)	1.397(4)
C(47)-C(48)	1.399(3)

C(47)-P(2)	1.859(2)
C(48)-C(49)	1.400(4)
C(49)-C(50)	1.384(5)
C(50)-C(51)	1.377(5)
C(51)-C(52)	1.400(4)
Cl(1)-Ru(1)	2.4899(7)
P(1)-Ru(1)	2.1844(6)
P(2)-Ru(1)	2.3464(7)

N(1)-C(1)-N(2)	105.98(17)
N(1)-C(1)-P(1)	134.54(15)
N(2)-C(1)-P(1)	119.48(15)
C(3)-C(2)-N(1)	107.51(19)
C(2)-C(3)-N(2)	106.70(18)
C(5)-C(4)-C(9)	123.53(19)
C(5)-C(4)-N(1)	117.67(19)
C(9)-C(4)-N(1)	118.78(19)
C(4)-C(5)-C(6)	116.9(2)
C(4)-C(5)-C(10)	122.79(19)
C(6)-C(5)-C(10)	120.3(2)
C(7)-C(6)-C(5)	122.1(2)
C(6)-C(7)-C(8)	118.4(2)

C(6)-C(7)-C(11)	120.5(2)
C(8)-C(7)-C(11)	121.1(2)
C(7)-C(8)-C(9)	122.0(2)
C(4)-C(9)-C(8)	116.7(2)
C(4)-C(9)-C(12)	122.0(2)
C(8)-C(9)-C(12)	121.3(2)
C(14)-C(13)-C(18)	124.64(19)
C(14)-C(13)-N(2)	118.97(18)
C(18)-C(13)-N(2)	116.36(18)
C(13)-C(14)-C(15)	116.9(2)
C(13)-C(14)-C(19)	122.2(2)
C(15)-C(14)-C(19)	120.9(2)
C(16)-C(15)-C(14)	121.7(2)
C(15)-C(16)-C(17)	119.5(2)
C(15)-C(16)-C(20)	121.0(2)
C(17)-C(16)-C(20)	119.5(2)
C(16)-C(17)-C(18)	122.0(2)
C(17)-C(18)-C(13)	115.21(19)
C(17)-C(18)-C(21)	122.00(18)
C(13)-C(18)-C(21)	122.65(18)
C(18)-C(21)-Ru(1)	89.79(13)
C(23)-C(22)-C(27)	119.0(2)

C(23)-C(22)-P(1)	118.82(17)
C(27)-C(22)-P(1)	122.16(19)
C(24)-C(23)-C(22)	120.3(2)
C(25)-C(24)-C(23)	120.3(3)
C(24)-C(25)-C(26)	119.9(3)
C(25)-C(26)-C(27)	120.2(3)
C(26)-C(27)-C(22)	120.2(3)
C(29)-C(28)-C(33)	116.40(19)
C(29)-C(28)-Ru(1)	121.03(16)
C(33)-C(28)-Ru(1)	122.53(16)
C(30)-C(29)-C(28)	122.0(2)
C(29)-C(30)-C(31)	120.5(2)
C(32)-C(31)-C(30)	119.1(2)
C(31)-C(32)-C(33)	120.8(2)
C(32)-C(33)-C(28)	121.0(2)
C(32)-C(33)-C(34)	120.8(2)
C(28)-C(33)-C(34)	118.18(18)
C(33)-C(34)-P(1)	104.67(14)
C(36)-C(35)-C(40)	118.1(2)
C(36)-C(35)-P(2)	118.86(18)
C(40)-C(35)-P(2)	123.02(17)
C(37)-C(36)-C(35)	120.6(2)

C(38)-C(37)-C(36)	120.5(2)
C(37)-C(38)-C(39)	119.5(2)
C(38)-C(39)-C(40)	120.3(2)
C(39)-C(40)-C(35)	120.8(2)
C(42)-C(41)-C(46)	118.48(19)
C(42)-C(41)-P(2)	124.54(17)
C(46)-C(41)-P(2)	116.97(16)
C(41)-C(42)-C(43)	120.2(2)
C(44)-C(43)-C(42)	120.9(2)
C(43)-C(44)-C(45)	119.4(2)
C(44)-C(45)-C(46)	120.2(2)
C(45)-C(46)-C(41)	120.7(2)
C(52)-C(47)-C(48)	118.1(2)
C(52)-C(47)-P(2)	121.96(19)
C(48)-C(47)-P(2)	119.5(2)
C(47)-C(48)-C(49)	120.5(3)
C(50)-C(49)-C(48)	120.7(3)
C(51)-C(50)-C(49)	119.4(3)
C(50)-C(51)-C(52)	120.5(3)
C(47)-C(52)-C(51)	120.8(3)
C(1)-N(1)-C(2)	109.52(17)
C(1)-N(1)-C(4)	126.63(17)

C(2)-N(1)-C(4)	123.70(17)
C(1)-N(2)-C(3)	110.28(17)
C(1)-N(2)-C(13)	124.57(16)
C(3)-N(2)-C(13)	124.76(17)
C(34)-P(1)-C(22)	104.51(10)
C(34)-P(1)-C(1)	107.02(10)
C(22)-P(1)-C(1)	95.67(9)
C(34)-P(1)-Ru(1)	107.88(7)
C(22)-P(1)-Ru(1)	127.16(7)
C(1)-P(1)-Ru(1)	112.78(7)
C(35)-P(2)-C(41)	103.06(9)
C(35)-P(2)-C(47)	102.37(11)
C(41)-P(2)-C(47)	100.45(9)
C(35)-P(2)-Ru(1)	112.97(7)
C(41)-P(2)-Ru(1)	116.63(8)
C(47)-P(2)-Ru(1)	119.07(7)
C(28)-Ru(1)-C(21)	94.09(8)
C(28)-Ru(1)-P(1)	80.51(6)
C(21)-Ru(1)-P(1)	92.48(6)
C(28)-Ru(1)-P(2)	95.52(6)
C(21)-Ru(1)-P(2)	168.55(6)
P(1)-Ru(1)-P(2)	95.21(3)

C(28)-Ru(1)-Cl(1)	98.62(6)
C(21)-Ru(1)-Cl(1)	85.59(6)
P(1)-Ru(1)-Cl(1)	177.83(2)
P(2)-Ru(1)-Cl(1)	86.85(3)

Symmetry transformations used to generate equivalent atoms:

Table 6.14. Anisotropic displacement parameters ($\text{\AA}^2 \times 10^3$) for compound

4.5. The anisotropic displacement factor exponent takes the form: $-2p^2[$

$h^2a^2U^{11} + \dots + 2hkab^*U^{12}]$

	U ¹¹	U ²²	U ³³	U ²³	U ¹³	U ¹²
C(1)	15(1)	12(1)	16(1)	-1(1)	2(1)	-3(1)
C(2)	28(1)	19(1)	27(1)	9(1)	7(1)	5(1)
C(3)	26(1)	15(1)	28(1)	4(1)	5(1)	6(1)
C(4)	19(1)	17(1)	14(1)	5(1)	4(1)	1(1)
C(5)	18(1)	21(1)	17(1)	5(1)	2(1)	-3(1)
C(6)	28(1)	21(1)	13(1)	1(1)	2(1)	-2(1)
C(7)	28(1)	24(1)	18(1)	5(1)	9(1)	1(1)
C(8)	18(1)	29(1)	25(1)	4(1)	6(1)	-6(1)
C(9)	24(1)	20(1)	19(1)	3(1)	5(1)	-5(1)
C(10)	21(1)	34(1)	28(2)	-3(1)	3(1)	-9(1)
C(11)	36(2)	49(2)	38(2)	-7(1)	20(1)	-1(1)
C(12)	33(2)	28(1)	33(2)	-6(1)	9(1)	-12(1)
C(13)	17(1)	17(1)	17(1)	1(1)	5(1)	6(1)
C(14)	23(1)	19(1)	24(1)	-2(1)	2(1)	5(1)

C(15)	32(2)	29(1)	18(1)	-7(1)	5(1)	7(1)
C(16)	27(1)	33(1)	18(1)	3(1)	7(1)	9(1)
C(17)	19(1)	22(1)	23(1)	4(1)	5(1)	3(1)
C(18)	13(1)	18(1)	18(1)	3(1)	2(1)	6(1)
C(19)	40(2)	22(1)	30(2)	-7(1)	4(1)	-1(1)
C(20)	45(2)	52(2)	28(2)	0(1)	20(1)	5(1)
C(21)	13(1)	18(1)	17(1)	2(1)	2(1)	1(1)
C(22)	19(1)	20(1)	22(1)	5(1)	-2(1)	-3(1)
C(23)	24(1)	28(1)	24(1)	1(1)	-1(1)	-4(1)
C(24)	43(2)	51(2)	30(2)	-11(1)	-2(1)	-8(1)
C(25)	46(2)	72(2)	47(2)	-17(2)	-10(2)	-28(2)
C(26)	33(2)	79(2)	52(2)	-7(2)	3(2)	-31(2)
C(27)	28(2)	47(2)	32(2)	3(1)	6(1)	-14(1)
C(28)	22(1)	15(1)	14(1)	4(1)	4(1)	1(1)
C(29)	28(1)	25(1)	19(1)	0(1)	6(1)	-6(1)
C(30)	48(2)	31(1)	23(1)	-8(1)	10(1)	-13(1)
C(31)	56(2)	29(1)	30(2)	-10(1)	24(2)	-4(1)
C(32)	37(2)	22(1)	31(2)	2(1)	20(1)	2(1)
C(33)	24(1)	16(1)	21(1)	4(1)	8(1)	4(1)
C(35)	20(1)	17(1)	21(1)	2(1)	1(1)	-4(1)
C(36)	25(1)	21(1)	25(1)	4(1)	1(1)	2(1)
C(37)	45(2)	27(1)	32(2)	-4(1)	8(1)	5(1)

C(38)	50(2)	36(1)	21(1)	-7(1)	0(1)	-4(1)
C(39)	38(2)	40(1)	22(1)	2(1)	-9(1)	1(1)
C(40)	22(1)	31(1)	26(1)	1(1)	-3(1)	2(1)
C(41)	14(1)	16(1)	24(1)	4(1)	3(1)	3(1)
C(42)	19(1)	21(1)	25(1)	4(1)	5(1)	3(1)
C(43)	24(1)	24(1)	33(2)	12(1)	4(1)	0(1)
C(44)	22(1)	19(1)	44(2)	3(1)	2(1)	-2(1)
C(45)	25(1)	26(1)	34(2)	-7(1)	1(1)	-1(1)
C(46)	22(1)	24(1)	24(1)	3(1)	1(1)	0(1)
C(47)	18(1)	23(1)	32(1)	16(1)	4(1)	4(1)
C(48)	29(2)	28(1)	38(2)	16(1)	13(1)	10(1)
C(49)	37(2)	42(1)	61(2)	25(1)	29(2)	18(1)
C(50)	24(2)	58(2)	86(3)	39(2)	24(2)	11(1)
C(51)	20(2)	52(2)	63(2)	27(2)	-1(2)	-5(1)
C(52)	20(1)	36(1)	40(2)	16(1)	0(1)	0(1)
Cl(1)	19(1)	19(1)	25(1)	4(1)	8(1)	-2(1)
N(1)	18(1)	16(1)	18(1)	4(1)	5(1)	0(1)
N(2)	19(1)	14(1)	18(1)	1(1)	5(1)	2(1)
P(1)	14(1)	14(1)	15(1)	2(1)	3(1)	0(1)
P(2)	15(1)	16(1)	18(1)	4(1)	3(1)	1(1)
Ru(1)	13(1)	14(1)	13(1)	2(1)	3(1)	0(1)